Dynamic and Differential-Algebraic Modeling, Analysis and Simulation of a Bioreactor-Extractor by equilibrium models for the Production of Biodiesel

Juan Bernardo Restrepo Betancourt

Universidad Nacional de Colombia - Sede Manizales

Facultad de Ingeniería y Arquitectura

Departamento de Ingenieria Electrica, Electrónica y Computación

Maestría en Ingeniería - Automatización Industrial

Manizales, Colombia

2009

Análisis Modelado y Simulación Dinámica y Algebraico-Diferencial de un Biorreactor-Extractor por Modelos de Equilibrio para la Producción de Biodiesel

Juan Bernardo Restrepo Betancourt
Chemical Engineer

Tesis presentada en cumplimiento a los requerimientos
para optar por el título de
Magíster en Automatización Industrial

Director
Gerard Olivar Tost

Universidad Nacional de Colombia - Sede Manizales
Facultad de Ingeniería y Arquitectura
Departamento de Ingenieria Electrica, Electrónica y Computación
Maestría en Ingeniería - Automatización Industrial
Manizales, Colombia
2009

To mi father, who has always been an inspiration

Acknowledgments

Dynamical modeling and analysis are elusive topics for a Chemical Engineer in Colombia, this section is dedicated to all people who have contributed in my pursuit of Chemical Engineering Dynamic modeling, design and analysis principles and that had made me a better person along the way.

In first place the realization of this work was possible due to my Father and Mother efforts of always giving me the best education and their constant struggle to make me and my sister better persons, I owe them everything that I am and that I will be.

First time I heard about Dynamics and Lyapunov theory was during the "IV Jornada Técnica de Ingeniería Química" on November 26 of 2004, this day changed my way to see the world and my way to understand Chemical Engineering, thanks to the organizers of this event and special thanks to Dr. Hernan Dario Alvarez for his conference and for his exceptional labor as teacher, guide and mentor to many generations of students who are as grateful as I am. Thanks to Rafael Muñoz who allowed me to attend to his control course and gave me his friendship and guide.

I would not be able to put all this mathematical and technical concepts together unless for an excellent formation, thanks to my former mathematics teachers: Omar Evelio Ospina,Luis Alvaro Salazar and Juan Carlos Riaño (Math I), Luz Marina Velásquez (Math II and III), German Barco Gomez (Math IV) and finally to Bernardo Acevedo and again to Omar Evelio Ospiana (Math V). Also thanks to my former teachers in Chemical Engineering: Alvaro Gomez Peña, Oscar Hernan Giraldo, Luis Fernando Cortés, Carlos Ariel Cardona, Ramiro Betancourt G, Jose Nelson Rojas, Nelson Gonzales and Luis Fernando Gutierrez M.

To fabiola Angulo, Eduardo Cano and Camilo Younes, who are excellent teachers and human beings, thanks to them for believing in me.

To Dr. John Charles Butcher,Dr. Daniel Wise, Dr. Ernst Hairer and Dr. Linda Peztold for their constant feedback about my work and for their help, also for all the books they have sent me, they were a great help, without them I

would not be able to accomplish all my goals in this work.

To Juan Daniel Melo and his radio show Efecto Doppler for many hours of sonic freedom.

Finally thanks to the most important persons in the realization of this work and in my academic life, Gerard Olivar Tost and Carlos Ariel Cardona, who have unconditionally believed in me and my potential, and have encouraged and supported me during my short academic career, giving me not only their knowledge and experience but their friendship.

Contents

List of Figures

List of Tables

Resumen

El presente trabajo comprende el modelamiento análisis y simulación de dinámica de un proceso de reacción extracción auto inducida para la producción de biodiesel mediante el uso de enzimas con el fin de de realizar una análisis previo del comportamiento tanto de arranque como dinámico de operación del mismo. El desarrollo del el trabajo se hace en 6 capitulos con el fin de abarcar los diferentes problemas tanto numérico como conceptuales que el problema de modelamiento y simulación algebraico diferencial presenta.

Capítulo 1

Este capítulo es una investigación en el estado del arte sobre la producción de biodiesel donde se exponen las diferentes tecnologías empleadas para la obtención de este, se exponen los pros y los contras de cada una y se explora brevemente el uso de procesos intensificados como solución a los diferentes problemas que presenta la producción tanto enzimática como convencional.

Capítulo 2

Este capítulo contiene una breve introducción al modelamiento de sistemas heterogéneos tanto por modelos de equilibrio como por modelos de transferencia de masa, donde finalmente se selecciona y desarrolla el modelo algebraico diferencial de un reactor extractor para la producción de biodiesel usando enzimas inmovilizadas, en donde se plantea un modelo tanto para la fase de arranque como todas las simplificaciones y asunciones para el correcto desarrollo del modelo algebraico diferencial para la fase de operación del biorreactor.

Capítulo 3

El capitulo expone la teoría básica sobre ecuaciones algebraico diferenciales haciendo énfasis en la teoría de estabilidad de los integradores numéricos y en los integradores del tipo Runge-Kutta para la integración de ecuaciones algebraicos diferenciales, donde se trata el recientemente aplicado concepto de orden efectivo para el desarrollo de métodos de Runge-Kutta singularmente implícitos de orden efectivo, que poseen características de estabilidad y precisión superiores a los métodos convencionales para la integración de ecuaciones algebraico diferenciales o DAEs; también se trata el aspecto de la implementación numérica de estos, así como el control del tamaño de paso y la estimación del error de truncamiento.

Capítulo 4

Este capítulo comprende la realización de experimentos numéricos tanto con diferentes sistemas de ecuaciones algebraico diferenciales comunes en la literatura como con el modelo del biorreactor-extractor, mostrando las ventajas y desventajas de la integración numérica usando los métodos de Runge-Kutta singularmente implícitos de orden efectivo.

Capítulo 5

En el desarrollo de este capítulo se muestran tanto los análisis de bifurcación en un solo parámetro como el análisis de la superficie operación del equipo demostrando la utilidad de este tipo de análisis para moldear la respuesta del sistema a una respuesta deseada con el uso de análisis simples.

Capítulo 6

Se presentan las conclusiones generales del trabajo y algunas observaciones del autor.

Abstract

In this work nonlinear dynamics and topology are combined to conceptually design a reactor-extractor for the production of biodiesel. In this case a dynamic and differential algebraic piecewise model based on globally stable equilibrium thermodynamics is developed, creating a dynamical conceptual design strategy that can be generalized for the design and stability analysis of combined extraction and reaction processes.

The nonlinear dynamics and the behavior of the bioreactor-extractor model in the starting procedure are analyzed in order to select the best starting conditions and strategy. Simulation and nonlinear analysis techniques are numerically implemented and improved in order to attain the most accurate and numerically stable results result. A rigorous search for multiplicity of steady-states is done and bifurcation analysis search for undesired and desired behaviors in codimension 1 is performed in order to shape the desired response of the reactor due to simple analysis.

Motivation

Petroleum is the largest single source of energy consumed by the world's population, exceeding coal, natural gas, nuclear, hydro and renewables [5], its increasing global demand, and concerns about oil supply and energy security have motivated many countries to promote research and production of alternative fuels.

Colombia itself has promoted the production of bio-ethanol by the law 693 of 2001, stimulating its production from sugar cane and the addition of it to gasoline for vehicular use (5% Mixture). It is expected that a new law regulating and promoting the use of biodiesel will be approved and implemented in the future years.

Colombia as a mainly agricultural country and having excellent perspective for the production of biodiesel, should be prepared to make a change from agricultural country to agroindustrial country, in order to take advantage of the big opportunities the new born bio-fuels markets is bringing. This is the reason why, many investigation groups in the world and specifically in colombia, started to work on biodiesel and bioethanol production from different sources and using different technologies. All of this with the purpose of finding the best way of production and the best way to take advantage of natural resources in a clean way. Many of this studies locally and worldwide have been done experimentaly, leaving behind theoretical research, specially all concerning to biodiesel and reactive-extraction. For this reason it is important to continue working in the creation of shortcut methods based on scientific principles to conceptually design complex reaction-separation equipment and previously assess the potential benefits this kind of process could bring.

Chapter 1

Biodiesel

Biodiesel can be produced from several sources and by several processes each one with its own advantages and disadvantages. The scarcity of conventional fossil fuels, growing emissions of combustion generated pollutants, and their increasing cost, will make biomass sources more attractive [8]. Original Dr. Rudolph Diesel's engine was meant to run on Vegetable Oils but economic factors associated with the production of gasoline for "spark-ignition engines" made petroleum diesel or petrodiesel more available at the time, but since the early 1980's, the use of vegetable oils as an alternative renewable fuel competing with petroleum was proposed. The main advantages of vegetable oils are portability, availability, renewability, high heat content, low sulfur content, lower aromatic content and biodegradability, all of them environmentally friendly characteristics.

In order to understand Biodiesel production advantages and disadvantages, is necessary to first understand what biodiesel is, where does it come from, the different ways of producing it and its proccess flowcharts, also understand the possibilities and opportunities of the intensified process application to improve biodiesel production in a continuous and very competitive way. This chapter addresses this topics as an state of the art review to contextualize the nonexpert reader with the complexity issues of biodiesel production.

1.1 Biodiesel Definition

Biodiesel refers to a diesel-equivalent, processed fuel derived from biological sources. Biodiesel is the name for a variety of ester-based oxygenated fuels form renewable biological source. It can be made from processed organic oils and fats. Chemically Biodiesel is defined as monoalkyl esters of long chain fatty acids derived from renewable bio-lipids. Biodiesel is

typically produced through the reaction of vegetal oil or animal fats with methanol or ethanol in presence of a catalyst to yield methyl or ethyl esters (Biodiesel) and glycerine.
In general terms, biodiesel may be defined as a domestic renewable fuel for diesel engines derived from natural oils like soybean, sunflower,castor, palm ...etc. In technical terms (ASTM D 6751) biodiesel is a diesel engine fuel comprised of monoalkyl esters of long chain fatty acids derived from vegetable oils or animal fats, designated B100 and meeting the requirements of ASTM D 6751.

Table 1.1: Biodiesel ASTM D 6751 Standard Properties from [5]

Common name	Biodiesel (Biodiesel)
Common Chemical name	Fatty acid (m)ethyl ester
Chemical formula Range	$C_{14} - C_{24}$ methyl esters or $C_{15-25}H_{28-48}O_2$
Kinematic viscosity Range (mm^2/s at 313 K)	3.3-5.2
Density range (Kg/m^3 at 288 K)	860-894
Boiling point range (K)	$>$475
Flash point range	430-455
Distillation range	470-600
Vapor pressure (mm Hg, at 295 K)	$<$5
Solubility in water	Insoluble in water
Physical appearance	light to dark yellow clear liquid
Odor	light musty/Soapy odor
Biodegradability	more than Petrodiesel
Reactivity	Stable, but avoid strong oxidizing agents

1.2 Oil/Fat Sources for Biodiesel

Oils and fats are mainly formed by triglycerides, triglycerides are formed from a single molecule of glycerol, combined with three fatty acids replacing each of the OH groups. The use of a triglyceride feedstock for biodiesel production depends on regional availability and economics. Rape seed oil is the most widely used feedstock in Europe; soybean mainly used in the United States and palm oil is used in tropical regions. The main difference between this sources is the fatty acid (replacing OH groups of the glycerol molecule) composition. The most abundant

acids are palmitic, stearic, oleic and linoleic acids. The main properties of an oil/fat depend on the chemical structures of its fatty acids. In this regard, a frequent problem with biodiesel is its stability to oxidation. In linseed, sunflower and soybean oils the high content of linoleic acid confers low stability to oxidation as result of the presence of two double bonds [9].

Table 1.2: Main fatty acids constituent of the most common oil/fat sources for biodiesel production

Oil/fat source	Palmitic Acid (C16:0)	Stearic Acid (C18:0)	Oleic Acid (C18:1)	Linoleic Acid (C18:2)	Problems
Soybean Oil	8	4	28	53	Oxidation Stability
Palm Oil	42	5	41	10	Low Temperature
Rape Seed oil	4	1	60	20	–
Sunflower Oil	6	4	28	61	Oxidation Stability
Jatropha oil	13	7	45	34	Low Temperature

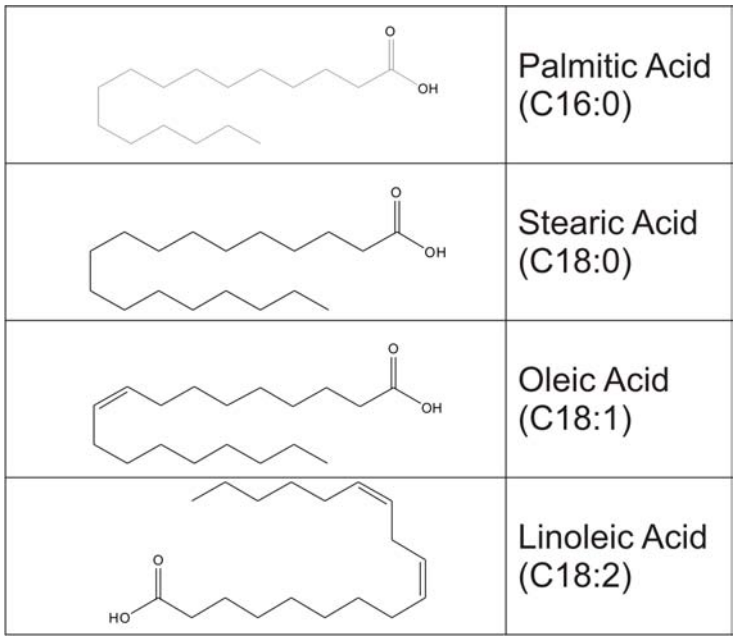

Figure 1.1: Chemical structure of the most common fatty acids occurring in oils and fats

The Oxidation of unsaturated compounds proceeds at different rates depending on the number and position of the double bonds. The CH_2 groups in allylic positions relative to the double bonds in the fatty acid chain are those susceptible to oxidation. By comparison fat oil and

animals fat contains high percentages of saturated fatty acids that are responsible of the poor low temperature properties (i.e. high cloud point and pour point values). This constitutes a problem in cold regions during winter. From these considerations and and data in the table 1.2 it can be concluded that the properties of fuels are likely to be dependent on the oil used in its preparation, and that is not a perfect single source oil, in fact a mixture of biodiesels from different sources seems to be the more appropriate to use.

1.3 Biodiesel Production

To transform fats and vegetable oils (mainly triglycerides) into long chain fatty acid esters (biodiesel), they should react with an alcohol generally methanol or ethanol, in presence of a catalyst to produce esters and glycerine, this process is known as transesterification and its the base of industrial production of biodiesel. this process is normally a sequence of three consecutive steps which are reversible reactions. In the first step from triglyceride diglyceride is obtained, from this diglyceride monoglyceride is obtained in the second step, and as final step glycerine is obtained from the monoglyceride:

$$\mathrm{Triglycerides(TG)} + \mathrm{R'OH} \rightleftharpoons \mathrm{Diglycerides(DG)} + \mathrm{R'COOR_1} \tag{1.1}$$

$$\mathrm{Diglycerides(DG)} + \mathrm{R'OH} \rightleftharpoons \mathrm{Monoglycerides(MG)} + \mathrm{R'COOHR_2} \tag{1.2}$$

$$\mathrm{Monoglycerides(MG)} + \mathrm{R'OH} \rightleftharpoons \mathrm{Glycerine(GL)} + \mathrm{R'COOR_3} \tag{1.3}$$

Giving the overall reaction:

$$\begin{array}{lcccl}
\mathrm{CH_2-OOC-R_1} & & & & \mathrm{R_1-COO-R'} \quad \mathrm{CH_2-OH} \\
| & & \xrightarrow{\text{Catalyst}} & & | \\
\mathrm{CH-OOC-R_2} & + \quad \mathrm{3R'OH} & \rightleftarrows & & \mathrm{R_2-COO-R'} \quad + \quad \mathrm{CH-OH} \\
| & & & & | \\
\mathrm{CH_2-OOC-R_1} & & & & \mathrm{R_3-COO-R'} \quad \mathrm{CH_2-OH} \\
\\
\text{Glycerides} & \text{Alcohol} & & \text{Esters} & \text{Glycerine}
\end{array} \tag{1.4}$$

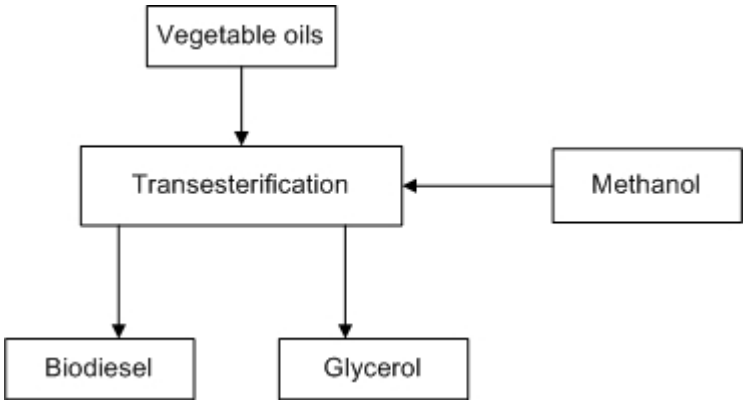

Figure 1.2: Biodiesel Production sequence by transesterification

The conventional flowchart for biodiesel production as any other chemical industrial process, comprises 3 main stages with material and energy recycles between each of them: the pretreatment stage, reaction stage, and the separation stage. In the first step raw materials are processed (i.e. palm, rapeseed, sunflowers) to obtain vegetable oils, in the second step the transesterification reaction in presence of a catalyst occurs to produce a mixture of biodiesel and glycerol, which is separated in the third step. The most important step is the reaction, where the different technologies and catalyst are used to obtain different kinds of biodiesel with different degrees of efficiency. There are three different types of catalyst for biodiesel production: alkali, acid and enzymatic(lipases). There is also supercritical alcohol transesterification which could be carried on with any of the catalysts types listed above, or without catalyst.

1.3.1 Alkali Catalyst Transesterification

For a basic catalyst, either sodium hydroxide (NaOH) or Potassium hydroxide (KOH) should be used with methanol or ethanol as well as any kind of oils, refine, crude or waste (i.e frying). In this process it is better to produce the Alcoxy before the reaction to obtain a better global efficiency. The Alcoxy reaction is:

$$\mathrm{R-CH_2OH + NaOH \rightarrow H_2O + R-CH_2ONa} \tag{1.5}$$

The alcohol oil molar ratio that should be used varies from 1:1 to 6:1. However 6:1 is the most used ratio giving an important conversion for the alkali catalyst without using a great amount of alcohol. The amount of catalyst that should be added to the reactor varies from 0.5% to 1%

w/w. The last but not least important variable is the reaction temperature, depending on the different type of catalyst optimal temperature varies from 25 to 120 C. [10]

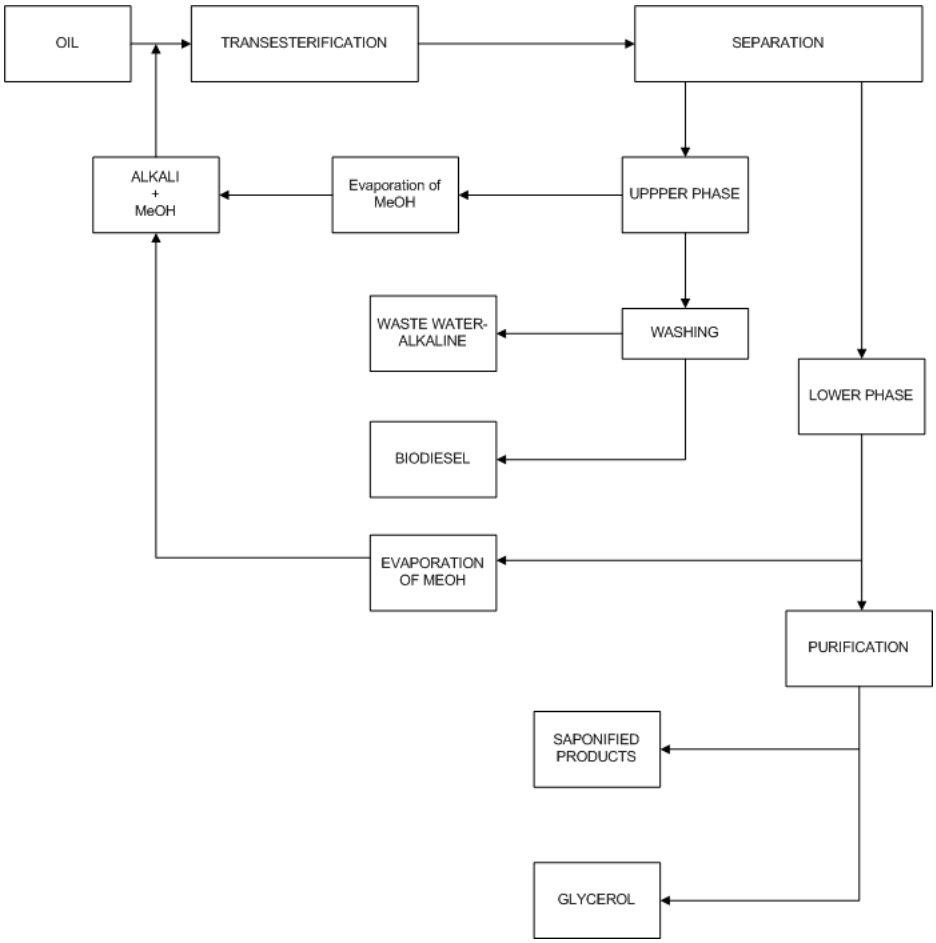

Figure 1.3: Production of biodiesel by alkali process

In Figure 1.3 a conventional industrial alkali catalyzed batch process is described, this is the only process that is carried out in an industrial scale. It is cost effective and highly efficient. But problems arise in the downstream operations including separation of the catalyst and unreacted methanol from biodiesel. The removal of catalyst involves many complications and biodiesel requires repeated washing to attain the necessary purity [11]. It can be seen that saponification as a secondary undesired reaction may contaminate the products, that is mainly because the catalyst (NaOH or KOH) is not selective, and is one of the reactants of the saponification

Figure 1.4: Conventional pilot scale plant for the production of biodiesel at Biotechnology plant in the Universidad Nacional de Colombia sede Manizales

reaction:

$$\begin{array}{llllll}
CH_2 - OOC - R_1 & & & R_1 - COO - Na & & CH_2 - OH \\
| & & & & & | \\
CH - OOC - R_2 & + \quad NaOH & \longrightarrow & R_2 - COO - Na & + & CH - OH \\
| & & & & & | \\
CH_2 - OOC - R_1 & & & R_3 - COO - Na & & CH_2 - OH \\
 & & & & & \\
\text{Glycerides} & \quad \text{Base} & & \text{Soap} & & \text{Glycerine}
\end{array} \tag{1.6}$$

An important aspect of the figure 1.3 is that the transesterification reaction products are immiscible, so two liquid phases are formed during the reaction stage and they should be separated after, an upper phase (low density) containing mainly biodiesel and the lower phase (high density) containing mainly glycerol, both phases containing non-reacted ethanol which have to be evaporated and then recycled, and also catalyst that have to be washed and recycled or disposed.

1.3.2 Acid Catalyst Transesterification

This way of producing is the second conventional way of making biodiesel. The main idea is to use triglycerides and alcohol but instead of a base to use an acid, the most common used are

sulfuric and sulphonic acid [6, 9, 10]. This type of catalyst gives very high yield in esters but the reaction is very slow taking almost one day to finish (batch Operation) [8].
As in the Alkali reaction an excess of alcohol is used, so better conversions of the triglycerides are attained, but recovering glycerol becomes more difficult and that is why optimal relation between alcohol and oil should be determined experimentally considering each process as a new problem.
The possible operation condition is: usually molar ratio 30:1 (alcholol:oil). The type of alcohol and the oils, is the same that can be used on an alkali catalyst reaction.
The typical amount of catalyst that is supposed to be added to the reactor varies from 0.5 to 1 mol%.
The temperature range varies from 55 to 80 C. This process is very effective specially when the oil used has a high free fatty acids composition. [10]
In this process there are also two immiscible phases produced during the reaction and also catalyst and alcohol should be separated from them, but due to the high ratio of alcohol to oil, separation is even more difficult and expensive.

1.3.3 Supercritical Catalytic and Non-Catalytic Transesterification

Although this is a new topic, is becoming more relevant. The transesterification of triglycerides by super critical alcohols (methanol, ethanol,propanol and butanol) has proved to be the most promising process [6, 8, 10, 12]. The basic idea of supercritical treatment is a relationship between pressure and temperature upon thermophysical properties of the solvent such as viscosity, specific weight, and polarity.

Catalytic transesterification

The most important variables affecting methyl and ethyl ester yields during supercritical transesterification are molar ratio of alcohol to vegetable oil and reaction temperature, typical values for molar ratio are 1:6-1:40 (oil:alcohol) and critical temperatures of several alcohols can be seen in Table 1.3, also a typical scheme for the production of biodiesel can be seen in Figure 1.5, where (1) is the Autoclave where the reaction takes place; (2) an electrical furnace to heat the Autocalve; (3) a temperature control monitor to ensure the desired temperature;(4) Pressure control monitor to ensure critical or supercritical pressure;(5) Product exit valve; (6)

Table 1.3: Critical Temperatures and pressures of various alcohols relevant to biodiesel production

Alcohol	Critical Temperature (K)	Critical pressure (MPa)
Methanol	512.2	8.1
Ethanol	516.2	6.4
1-Propanol	537.2	5.1
1-Butanol	560.2	4.9

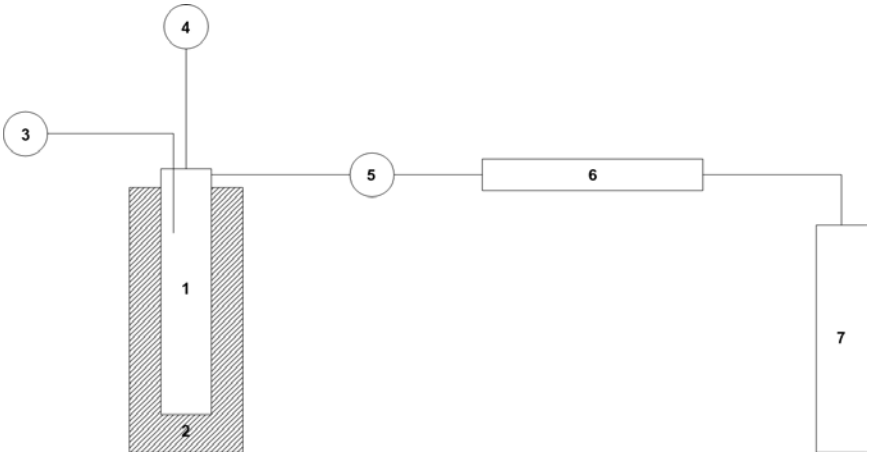

Figure 1.5: Supercritical methanol transesterification system

Condenser; (7) Product collecting vessel.

Non-Catalytic transesterification

A non-catalytic biodiesel production route has been developed in [13] that allows a simple process and high yield because of simultaneous transesterification of triglycerides and methyl esterification of fatty acids.

The parameters affecting the methyl esters formations are reaction temperature, pressure, molar ratio, water content and free fatty acid content. It is evident that at subcritical state of alcohol, reaction rate is very low and gradually increases as either pressure or temperature rise. It has been observed that increasing the reaction temperature specially to supercritical conditions, has

Table 1.4: Comparison between catalytic Methanol process and and supercritical methanol (SCM) method for biodiesel vegetable oil tranesterification from [6]

	Catalytic Methanol Process	SCM method
Methylating agent	Methanol	Methanol
Catalyst	Alkali	None
Reaction temperature (K)	303-338	523-573
Reaction pressure (Mpa)	.1	10-25
Reaction time (min)	60-360	7-15
Methyl ester yield (%w)	96	98

a favorable influence of the yield of ester conversion [13]. The yield of alkyl esters is increased increasing the molar ratio of oil to alcohol.

Water content is an important factor in the conventional catalytic transesterification, free fatty acids and water cause soap formation (alkali catalyst) that consumes catalyst and reduced its effectiveness, however the presence of water affects positively the formation of methyl esters in supercritical methanol non catalytic method [8].

1.3.4 Enzymatic Transesterification

Enzymatic production is possible using both extracellular and intracellular lipases, the main advantage of lipase use is their extreme specificity to an special reaction, i.e a lipase would only catalyze reactions with lipids like transesterification and no other undesired reactions would occur. The enzyme is immobilized and used which eliminates downstream operations like separation and recycling. Hence in all works reported in literature either immobilized (extracellular) enzymes or immobilized whole cells (intracellular enzymes) are used for catalysis. Both the process are reported to be highly efficient compared to using free enzymes.

Most of the work realized about enzymatic transesterification is experimental and at a laboratory scale, there are few theoretical works but most of them are about free and immobilized lipase kinetics [3, 14, 15] which also have an experimental component.

Biodiesel production using lipases was first described by Mittlebach [16], who showed that the lipase from *Pseudomonas fluorescences* was superior to those from *Candida sp* and *Mucor miehi* for sunflower oil alcoholysis. The alcoholysis was carried out both in presence of sol-

vent (petroleum ether) and in solvent free conditions, using five homologous alcohols with or without the addition of water. Since then subsequent studies have focused on different lipases, different triglycerides feedstocks, different alcohols and different experimental conditions such as temperature, water content, stoichiometric ratio between reagents, enzyme concentration, solvent used etc.

Solvent Versus Solvent-Free Process

Miscibility between methanol and triglycerides is poor, thus the presence of a solvent helps to form of a monophasic system. However, the use of solvent has some disadvantages such as its storage before use and specially its removal and disposal after the process, both which generate environmental problems. Several authors have treated the production of biodiesel by the solvent and solvent-free approach [3, 9, 14–18] but the general conclusion is that in spite of the benefits brought by the use of a solvent, the separation is difficult and expensive enough in an industrial scale to make it a viable choice.

Water Content

Water content in biocatalysis in non-conventional media (non-aqueous) is a very important parameter since it strongly affects enzymatic activities. There are conflicting reports on the effect of water content in the synthesis of biodiesel. Some authors state that ester yield increases if high amounts of water are present in the system [19], whilst others claim the contrary [20]. This apparent contradiction might be explained by considering that the effect of water in these systems depend on the enzyme, the support and the medium (solvent or solvent-free). As a general consideration, high water content should decrease ester yield since undesirable triglycerides hydrolysis occurs. Although water is involved in several enzyme denaturalization processes, a certain ammount of water must be present to 'lubricate' polypeptide chains and keep an enzyme in its active conformation . In this regard, water content is better expressed in water activity since only the use of this thermodynamic parameter allows a real comparison of the effects of water among different enzymes in the same medium. Unfortunately the majority of papers reporting studies on the effect of water cite water concentration instead of water activity.

Lipase Inhibitions

Both reagents and products of alcoholysis reaction and some substances contained in the feedstock can inhibit lipases. Inhibition is one of the most important aspect in the production of biodiesel and Enzyme transesterification reactor design, this is mainly because inhibition factors has to be taken into account in the formulation of a a correct kinetic expression [14].

Methanol inhibition: Methanol is poorly miscible with oil/fat and tend to inactive enzymes.

Glycerol inhibition: Glycerol has negative effect on FAME (Fatty Acid Methyl Esters) by some enzymes.

Phospholipids inhibition: The gum present in crude soybean oil inhibits some lipases since this negative effect was not observed with degummed oil. The main components of gum are phospholipids[1], the inhibition observed may be due to phospholipid bound to the immobilized preparation that interfere with the enzyme substrate interaction.

Inhibition during continuous operation: Glycerol is formed during the alcoholysis of tryglicerides as seen in equation (1.4) on page 5. If this reaction is performed in a packed-bed reactor glycerol tends to adsorb onto the hydrophilic support instead of being withdrawn by the flow. this adsorption inhibits enzyme activity [9].

[1] Phospholipids are a class of lipids and are a major component of all biological membranes. All phospholipids contain a diglyceride, a phosphate group, and a simple organic molecule such as choline.

Table 1.5: Type of inhibition and Possible remediation for discontinuous and continuous enzymatic production of biodiesel

Type of Process	Lipase	Inhibitor	Possible remediation	Reference
Discontinuous (Batch)	*Candida antartica*	Methanol	Three step addition of methanol	[21]
	Candida antartica	Methanol	adition of 10wt% of Silica Gel	[22]
	Candida antartica	Methanol	Pre-treatment in 2-butanol or tertbutanol	[23]
	Candida antartica	Phospholipids	Oil degumming	[24]
	Candida antartica	Phospholipids	Lipase pre-treatment	[25]
	Candida antartica	Phospholipids	Simultaneous dewaxing and degumming	[26]
	Thermomyces Lanuginosa	Methanol	Three step addition of methanol	[27]
		Glycerol	Enzyme wasing with isopropanol	
Continuous (Packed-Bed Reactors)	*Rizhomucor miehei*	Glycerol	Adition of Silica gel; Use of hexane and acetone; Rinsing the Catalyst	[28]
	Candida Antartica	Methanol	Three step flow reaction	[24]
	Candida Antartica	Glycerol	Use of Dialysis membrane	[29]

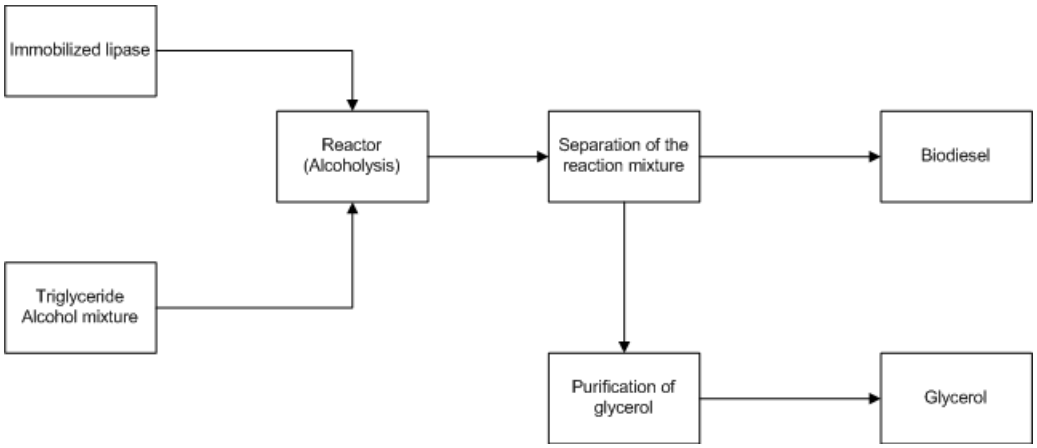

Figure 1.6: Flow diagram of biodiesel production by lipases

1.4 Intensification of Biodiesel Production

The standards make sure that the following important factors in biodiesel fuel production process by transesterification are satisfied:

1. Complete transesterification reaction
2. Removal of catalyst
3. removal of alcohol
4. removal of glycerol
5. complete esterifications of free fatty acids

As seen in figures 1.3,1.2 and 1.6 a successful transesterification produces two liquid phases: ester and crude glycerol. The entire mixture settles and glycerol is left on the bottom and biodiesel is left on top. Crude glycerol, the heavier liquid will collect at the bottom after several hours of settling. Phase separation can be observed within 10 min and can be complete within 2 hours after stirring has stopped. complete settling can be taken as long as 18 h. After settling is complete the glycerol is drained and the ester layer remains [6]. This kind of separation process is performed after the reaction takes place and is a discontinuous(batch) operation, for this reason it requires intermediate storage and very long settling times. After the two phases are separated specialized washing processes to remove the catalyst (if alkali or acid where

used) and to evaporate and recover the non-reacted methanol should be performed. In this sense immobilized lipase and solid catalyst approach are better because no catalyst removal should be done, although solid catalysts and immobilized lipase are susceptible to deactivation by the adsorption of the glycerol onto the catalyst support.

To overcome problems like inhibition in enzymatic reactors and solid catalyst deactivation, to avoid unnecessary long downstream separation procedures and to improve the reaction efficiency even over equilibrium's conversion, some authors have intensified biodiesel production by combining the reaction and separation in the same equipment (process Integration) by means of membrane reactors [1, 30–34] or by reactor extractors [2, 35, 36], the effect of both procedures are basically the same, a concentration field redistribution is achieved by the reaction and separation processes taking place simultaneously in the same vessel, this is specially useful for equilibrium reactions like transesterification, as it has been observed in reactive distillation [2, 36–40] where the equilibrium conversion barrier is widely surpassed, which means more rentability due to less time and energy is used and also a reduction of the necessary equipment to accomplish the same task [39].

1.4.1 Membrane Reactor

It is known that methanol is only slightly miscible in oil and that temperature has only a slight effect on this miscibility. For all practical purposes, it could be said that the two phases are immiscible. On the other hand, FAME is entirely miscible in methanol over a broad range of temperatures. At normal reaction temperatures (e.g. 60 C), FAME and methanol are miscible. The immiscibility of oil and methanol is at the root of the mass transfer issues for biodiesel production. However, in the operation of a membrane reactor, the formation of a two-phase (emulsified) system is exactly what is necessary. Thus, the transesterification of Triglicerides to FAME is ideally suited to operation in a membrane reactor.

The principle of membrane reactor operation is depicted in Figure 1.7. due to the immiscibility of oil and methanol,and due to various surface forces, the oil will exist in the form of an emulsion; i.e. droplets suspended in methanol. One can thus envisage the transesterification occurring at the surface of the oil droplets. In the presence of a permeable membrane, the oil droplets are too large to pass through the pores of the membrane. On the other hand, the FAME is soluble in the methanol and, due to its small molecular size, will pass through the

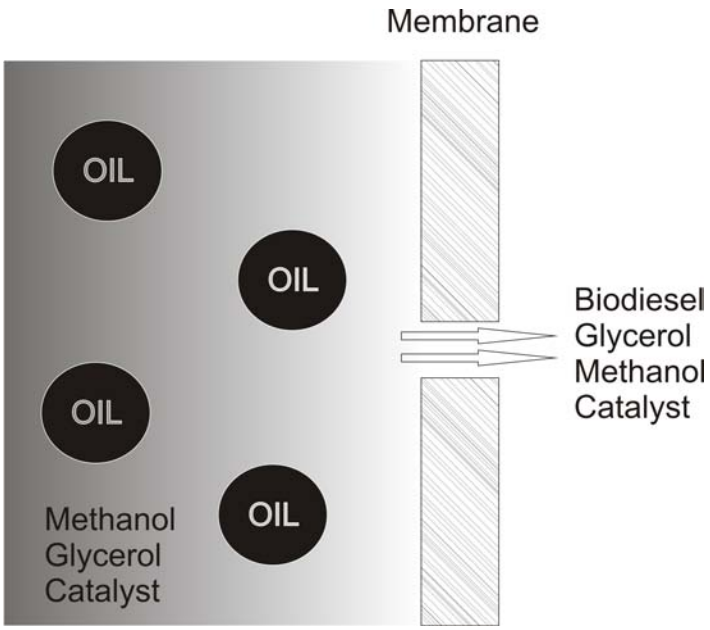

Figure 1.7: Separation of oil and FAME by a separative membrane adapted from [1]

membrane pores along with the methanol, glycerol and catalyst [1]. This *in situ* withdrawn of products accelerates the direct transesterification reaction improving reaction efficiency, also if a immobilized lipase is used, the withdrawn of glycerol prevents the inhibition by glycerol and by continuous reactor operation.

1.4.2 Reactor-Extractor

Reaction-extraction is a special case of the reaction and separation integration, combining a chemical transformation (reaction) with a liquid-liquid extraction.

Liquid-Liquid extraction objective is to separate the components of a liquid mixture by using an immiscible liquid that forms a two phase system. Separation is achieved because the desired liquid mixture components are distributed between the two different phases, selectivity is achieved due to the special chemical affinity of some of the mixture components with one of the liquid phases formed.

Biodiesel reaction is a special case of reaction-extraction processes because there is no need to add a solvent to form a second liquid phase, the second liquid phase is formed by the immiscibility of the reactants and the products and is called auto-inducted [2], this special type reactive extraction can also be seen in butyl-acetate, amyl-acetate and ethyl-acetate production [35].

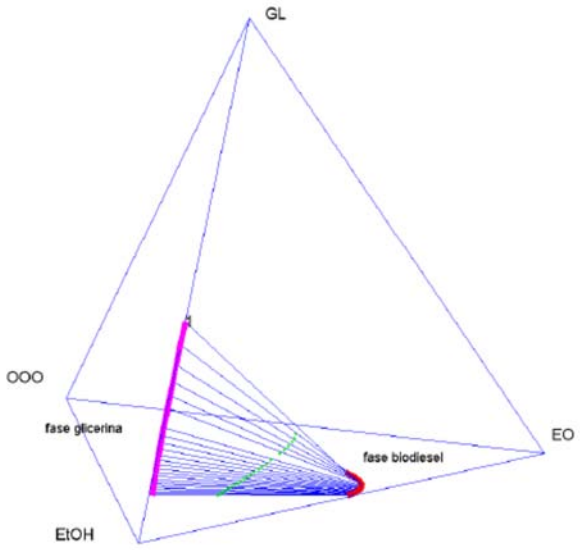

Figure 1.8: Reactive liquid-liquid equilibrium of triolein (OOO), ethanol (EtOH), glycerol (GL) and biodiesel (EO) from [2]

Figure 1.8 is a simultaneous chemical and physical equilibrium diagram, it clearly shows for biodiesel transesterification reaction that two phases are formed, biodiesel rich phase (red) and glycerol rich phase (magenta). As it can be seen methanol is miscible in both phases having high concentration on glycerol rich phase and moderate concentration in biodiesel rich phase, this prevents inhibition. It can be seen also that there are only traces of triolein in the glycerol rich phase, this mean the reaction only takes place in biodiesel rich phase. In the reaction phase two reactants are present but only one product is, this is called concentration field redistribution and it is what makes this process much more effective than a conventional batch process.
Evident advantages of reaction-extraction technology over membrane technology are economic: membrane technology is as expensive as effective and need constant maintenance of the membrane as also periodic replacement of the used membrane, while reaction extraction technology equipment is less expensive and doesn't need any special maintenance.

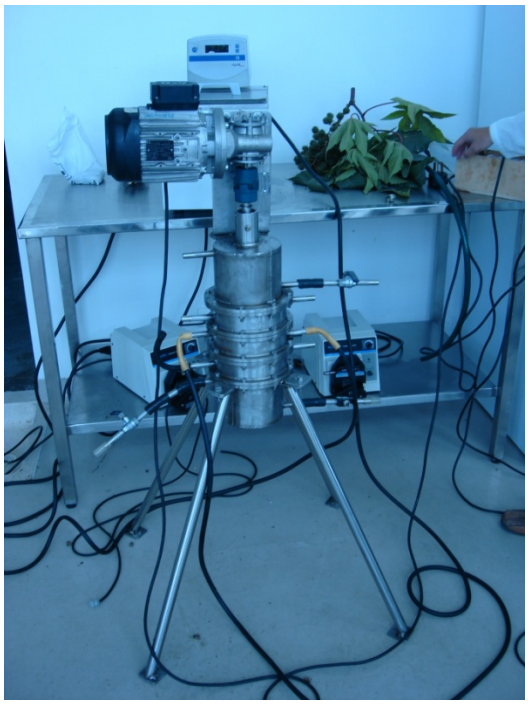

Figure 1.9: Reactive-extraction pilot scale equipment for the production of biodiesel at Biotechnology plant in the Universidad Nacional de Colombia sede Manizales, developed during PhD. Thesis of Luis Fernando Gutierrez M. [2]

1.5 Conclusions and Perspectives

Conventional biodiesel production is cost effective and efficient, alkali and acid catalyst are industrially implementable and they have been widely studied by many authors, this makes them the most immediately available options for industrial implementation, nevertheless they are not the most promising options. Immobilized Enzyme catalyst, and supercritical transesterification are indeed most promising options, specially if applied to intensified process schemes as membrane or reaction-extraction, this is mainly because of the high conversion rates attained and their capability of continuous operation combined with the *in situ* separation can widely reduce costs and operation times, also increase the productivity even over the chemical equilibrium conversion.

Design principles widely used in distillation and reactive distillation [35, 37, 38, 41], like the concentration field redistribution are applicable to different technologies like reaction-extraction and membrane rectors, giving to the investigator more theoretical understanding of what is happening inside the process and what to do to make the process even better, a clear example of this is Luis Fernando Gutierrez M. PhD. Thesis [2], which is an application of shortcut methods with topologically aided design [37, 42–45] to improve well known processes.

Biodiesel production perspectives in colombia are a great opportunity to develop national industry and agriculture, situating colombia between the 5 countries with more biodiesel production potential [5].

Even with today's high oil prices biofuels cost more than conventional fuels. The biofuel economy will grow rapidly during the XXI century, shaped by some of the same forces that shaped hydrocarbon economy and its refineries over the past century [46].

Chapter 2

Dynamical Piecewise Differential-Algebraic Bioreactor-Extractor Conceptual Design Model

Mathematics may be defined as the subject
in which we never know what we are talking
about,nor whether what we are saying is true.
Bertrand Russell, Mysticism and Logic

As seen in the previous chapter enzymatic catalysis is extremely selective and the reported ester yields are high. Enzyme catalysis for Biodiesel production is very promising but it has clear inconveniences as inhibition and continuous process operation, some of this inconveniences have been previously solved as seen in Table 1.5 at page 14, one of the most important references in this table is [29], who has used a dialysis membrane that in spite of being extremely expensive is an irrefutable evidence that simultaneous reaction and separation processes are a solution to many of the inhibitions and continuous operation problems occurring in enzyme catalyzed Biodiesel production. The design of simultaneous processes is complicated, many parameters have to be supposed and successively adjusted in order to obtain a good design, even if a MINLP (Mixed Integer Nonlinear Programming) optimization algorithm is used to deal with the complexity of the problem, possibilities of making a globally optimal design are scarce due to the high computational power needed and the availability of it for most researchers to solve complex combinatorial problems as this. A most simple and systematic approach must be used as an starting point for the design of integrated processes , the conceptual design approach is appropriate and has proved to be efficient in the most complex processes as distillation [42–44]

(azeotropic, conventional and extractive) and reactive distillation [36–40]. This approach has even been proved to be optimal using MINLP [45].

Conceptual design is very useful to previously assess a process in order to know how would integration benefit the performance of it.

Enzymatic Biodiesel production is the perfect candidate for the bioreactor-extractor process: as enzymes are relatively expensive [10], immobilization is necessary[1], with immobilized enzymes the continuous process is possible but long settling times in decanters to separate Biodiesel (upper phase) and glycerol (lower phase) prevent the process to be fully continuous, also Enzyme's activity by its is inhibited by glycerol and methanol excess in the reacting mixture, so a continuous withdraw of glycerol while the reaction is taking place would at least theoretically prevent enzyme inhibition and would make possible a continuous operation. Evidence of this can be observed in the experimental alkali catalyzed reaction extraction process reported in [2], who used a non-dynamical and topology aided reaction extraction conceptual design model to develop the equipment used in his experiment (Figure 1.9).

2.1 Reaction and Separation False Dichotomy

For a chemical reaction to take place some conditions must be fulfilled, such as constant stirring, an specific temperature, pressure and in special cases a catalyst. For phase splitting to take place also some special conditions must be fulfilled: pressure, temperature and in the cases of liquid phase splitting, low or no stirring and long settling times. This apparently contradictory and mutually exclusive stirring and no-stirring condition for reaction and liquid phase splitting respectively is indeed false, and this has been proved in several reaction-extraction examples where successfully constant stirred reactions and simultaneous extraction with or without solvent (auto-inducted) have been carried on. Examples of this are lactic acid production with different solvents [47], Reactive extraction of N-acetylneuraminic acid [48, 49], Biodiesel alkali catalyzed simultaneous reaction and extraction [2] and some antibiotics production [50, 51].

In a theoretical simultaneous simplified reaction and extraction model, the first assumption that should be made is that the stirring is high enough for the reaction to take place at good rates but low enough for the phase split to take place, the assumption is made because in a short-cut model(not using CFD) it isn't possible to determine optimal stirring velocity accurately, also

[1] Reason why no free enzyme literature is cited or free enzyme processes are described in this work

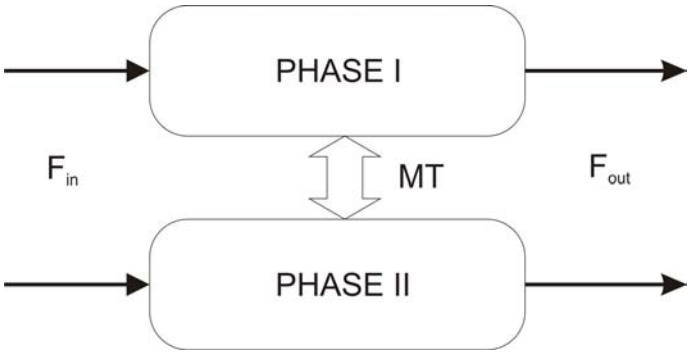

Figure 2.1: Mass Transfer model scheme for a two phase system

in some models stirring it is not taken into account.

2.2 Heterogeneous Process Modeling: Assumptions and Simplifications

Most real chemical and biochemical systems are heterogeneous. This means that the system is formed of more than one phase, with strong interaction between the various phases. Heterogeneous reacting and non reacting systems are complex to model specially for design, and some simplifications have to be done in order make the model adequate for a preliminary design. there are two approaches to model heterogeneous reacting and non-reacting systems, the thermodynamic equilibrium and the Mass Transfer:

2.2.1 Two Liquid Phase Mass Transfer Modeling

Figure 2.1 shows how is modeled a two phase system. Each phase is modeled as an independent subsystem that only interacts with the other phase by outgoing and incoming component mass transport. A dynamic molar balance for the $i-th$ component in a reacting phase one is performed:

$$\frac{N_i^{TI}}{dt} = N_{(in)i}^I - N_{(out)i}^I \pm MT_i \pm V^I \cdot \nu_i^I \tag{2.1}$$

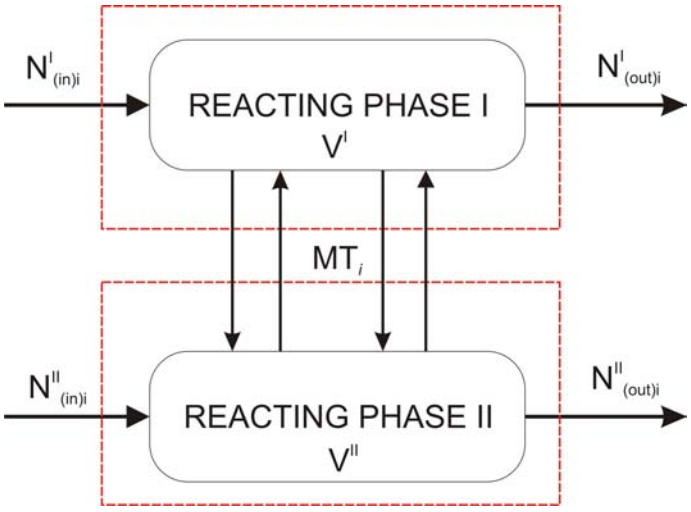

Figure 2.2: Reactive mass transfer model scheme for a two phase system

And also for the reacting phase two:

$$\frac{N_i^{TII}}{dt} = N_{(in)i}^{II} - N_{(out)i}^{II} \pm MT_i \pm V^{II} \cdot \nu_i^{II} \tag{2.2}$$

Where N^{TI} and N^{TII} are the molar accumulation (mol) of the $i-th$ component in phases I and II respectively, $N_{(in)i}^{I}$ and $N_{(in)i}^{II}$ are the input molar flows (mol/time) to phases I and II respectively, $N_{(out)i}^{I}$ and $N_{(out)i}^{II}$ are the output molar flows (mol/time) of phase I and II respectively, MT_i is the mass transfer flux (mol/s) of the $i-th$ component between the phases, V^I and V^{II} are the phase I and II respective volumes, ν_i^I and ν_i^{II} are the $i-th$ component conversion rate by the chemical reaction taking place in each phase(mol/time*volume).

Figure 2.2 shows the scheme used to develop the mass balances for the $i-th$ component.

First conceptual design modeling problem arises form the MT_i term, which for the $i-th$ component is expressed in terms of $\overline{C_i}$, that is the molar composition(mol/volume) of component i on the interface and C_i that is the current molar composition of component i in the bulk of the liquid phase[2]:

$$MT_i = a_m \cdot K_{L_i} \cdot (C_i - \overline{C_i}) \tag{2.3}$$

[2]The number of the liquid phase is omitted because the same flux equation applies for both phases

Where a_m is the total for mass transfer area between the two phases and K_{L_i} is the liquid mass transfer coefficient (length/time). Finding the correct $\overline{C_i}$ implies a priori experimental data or to suppose that the interphase is at equilibrium (a state where no further mass transfer is possible) and perform a thermodynamic equilibrium calculation (to be accurate experimental data is needed but not necessary due to group contribution methods [52]). The proper estimation of a_m depends on the reactor geometry and in some cases on the stirring velocity and the impeller type, so to properly design using this particular model implies supposing a geometry and adjust it successively until certain desired conditions are fulfilled. The mass transfer coefficient K_{Li} also depends on many variables specially in all related to the interface, so specific analytical, empiric and semi empiric correlations must be used in order to predict this coefficient [53–56]. In conclusion mass transfer reactor modeling is adequate to predict the behavior of liquid-liquid contact equipment with or without reaction, but for a first design it requires a priori knowledge of the equipment geometry and sizing, also requires to select impellers and nozzles[3] (if needed) and know or at least presume if the agitation speed selected is low enough to form a continuous phase system or high enough to form disperse phases [4].

2.2.2 Two Liquid Phase Equilibrium Model

For a system in which the contact between the two phases is long and/or the rate of mass transfer is very high, the concentrations of the different components in the two phases reach a state of equilibrium (a state where no further mass transfer is possible). The equilibrium relations relate the molar percent (x_i) in the two, three or more phases, such that for example,

$$\overline{x_i} = f(x_i) \tag{2.4}$$

Where the relation between $\overline{x_i}$ and x_i is called equilibrium relation and is an algebraic equation. Equilibrium thermodynamics has been widely studied and there are hundreds of journals and books treating this topic. Equilibrium relations have proven to be remarkably accurate to model distillation (reactive and conventional) and extraction columns [36, 52, 53, 56],it has also been proved to be an excellent conceptual design approach [2, 42–45, 57].

[3] Impellers and Nozzles affect the total mass transfer area a_m

[4] Different empirical correlations are needed to model continuous and disperse phase systems [55]

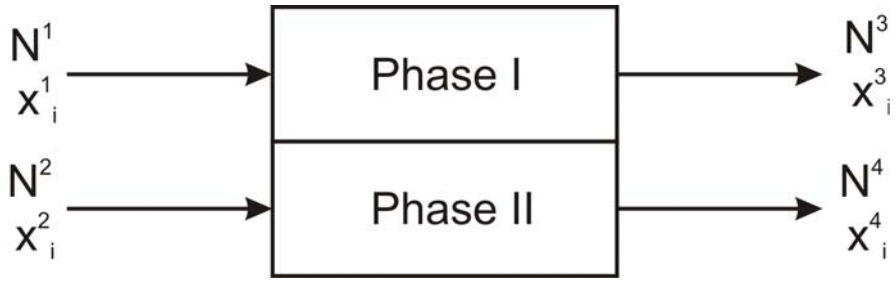

Figure 2.3: Equilibrium modeling scheme

The main idea of equilibrium modeling is assume no further mass transfer is possible, this mean to analyze the selected system at a maximum theoretical efficiency, which is enough for a first design, and let the designer asses the possibilities and disadvantages of his design and decide to go further or to change his design approach.

Figure C.5 is the typical liquid-liquid equilibrium modeling scheme which mass balances are for the ith component:

$$\frac{dN_i^T}{dt} = N^1 x_i^1 + N^2 x_i^2 - N^3 x_i^3 - N^4 x_i^4 \tag{2.5}$$

Where N_i^T is the total mass of i in the vessel and the supper index is the number of the current randomly ordered, as this is a constantly stirred tank model (lumped system), concentrations inside the vessel are assumed to be the same x_i^3 and x_i^4 for its corresponding phase, also x_i^3 and x_i^4 are assumed to be at equilibrium physical and/or chemical, if a chemical reaction takes place. In fact depending on specifical characteristics of the system if a reaction or several reactions take place is up to the designer and modeler criteria to decide if simultaneous chemical and physical equilibrium is reached [39] or just physical equilibrium is attained but the reaction is kinetically driven [40].

Simultaneous chemical and physical equilibrium is the perfect approach for steady state simulation, where dynamic is ignored and design is made based only on the steady state[5].

Simultaneous physical equilibrium and kinetically driven reactions are for the other side a more dynamic approach to equilibrium modeling, the reaction term on the balance equations allows

[5]steady state is the term most commonly used in chemical engineering literature to address equilibrium points, most chemical engineering analysis and design is made based on steady states simulation which means numerically find equilibrium points

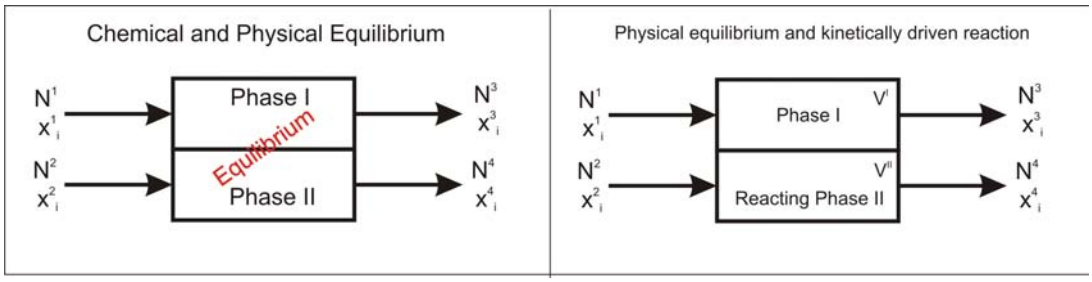

Figure 2.4: Differences between kinetically driven model and simultaneous physical and chemical equilibrium model

the designer and/or researcher to evaluate how phase equilibria affect the reaction development, it also allows to evaluate the multiple equilibrium points (steady states) present and to completely explore the phase space, in order to attain the most accurate dynamic information.

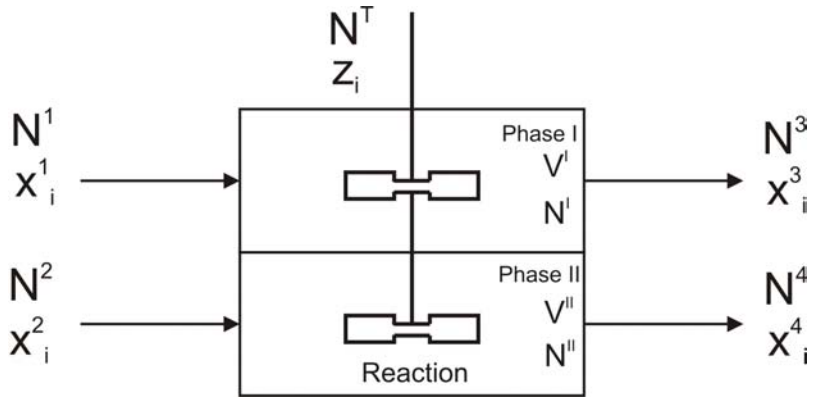

Figure 2.5: Kinetically driven liquid-liquid reactor extractor with one reacting phase

$$\frac{d(N^T \cdot z_i)}{dt} = N^1 x_i^1 + N^2 x_i^2 - N^3 x_i^3 - N^4 x_i^4 \pm \sigma_i \nu(\mathbf{x^4}) \cdot V^{II} \tag{2.6}$$

Figure 2.5 and Equation (2.6) are the diagram and the mass balance for the ith-component respectively, for a two phase physical equilibrium and simultaneous kinetically driven reaction system, where x_i^3 and x_i^4 are in physical but not chemical equilibrium, and the reaction only takes place in phase II with a reaction rate of ν only depending on the volume of phase II (V^{II}), its concentrations ($\mathbf{x}^4 = [x_1^4, x_2^4, ..., x_{C-1}^4, x_C^4]$) and the stoichiometrical coefficient of each component σ_i. If a fixed reactor volume is assumed as V^T and the total mole inside the

reactor (N^T) variation is described by a global mass balance:

$$\frac{dN^T}{dt} = N^1 + N^2 - (N^3 + N^4) + \sum_{i=1}^{C} \sigma_i \nu * V^{II} \tag{2.7}$$

For a C components system, the differential equation system formed by expanding equation (2.6) to $C-1$ components, appended by equation (2.7) has the following algebraic restriction derived from conservative laws:

$$V^T = V^I + V^{II} \tag{2.8}$$
$$\sum_{i=1}^{C} z_i = 1 \tag{2.9}$$
$$\sum_{i=1}^{C} x_i^1 = 1 \tag{2.10}$$
$$\sum_{i=1}^{C} x_i^2 = 1 \tag{2.11}$$
$$\sum_{i=1}^{C} x_i^3 = 1 \tag{2.12}$$
$$\sum_{i=1}^{C} x_i^4 = 1 \tag{2.13}$$
$$x_i^4 = f(\mathbf{x}^3, \mathbf{x}^4, T) \tag{2.14}$$
$$z_i = (1-\theta)x_i^4 + \theta x_i^3 \tag{2.15}$$
$$\frac{N^3}{N^4} = \frac{\theta}{1-\theta} \qquad for \quad \theta \in [0 \quad 1] \tag{2.16}$$
$$V^I = \frac{N^T \theta}{\rho^I} \tag{2.17}$$

Which are explained as follows:

Equation (2.8)**:** Means the reactor volume (V^T) is fixed, and all this volume is occupied by the two liquid phases.

Equations (2.9) **to** (2.13)**:** Are obtained by the fact that the sum of all molar percents present in one current must be equal to 1.

Equation (2.14)**:** Thermodynamic equilibrium relations are imposed by the model itself and its explicit formula and calculations issues will be discussed later in detail.

Equation (2.15)**:** Material balance associated with the physical equilibrium relation, in which a component i is distributed between the two phases, which are also distributed in a specific proportion (θ) of the reactor total mass.

Equation (2.16)**:** Relates the distribution proportion of the phases in the reactor with the outgoing currents (N^3 and N^4). The main assumption made to obtain this relation is that outgoing current flows are in the same proportion that the mass of the phases in the reactor.

Equation (2.17)**:** Relates the Volume of a desired phase (in this case one but can be phase 2) with the number of moles in it ($N^T \cdot \theta$) using the molar density ρ^I (mol/Volume) which can be approximated using the density of pure components and molar percents $\rho^I = \sum_{i=1}^{C} x_i^3 \rho_i$.

This is a differential-algebraic system with the following degrees of freedom:

Table 2.1: Degrees of freedom table for a physical equilibrium and kinetically driven two phase heterogeneous process

Number of differential equations	C	Equations (2.6) and (2.7)
Number of equilibrium relation	C	Equation (2.14)
Number of equilibrium derived mass balances	C-1	Equation (2.15)
Number of molar percent restrictions	5	Equations (2.9) to (2.13)
Number of extra relations	3	Equations (2.8),(2.16) and (2.17)
Number of design Parameters	2C + 1	Input flows and compositions and total reactor Volume
	-	
Number of states	C	$\mathbf{z} = [z_1, z_2, ..., z_{c-2}, z_{c-1}]$ and N^T
Number of variables	4C+8	$\mathbf{x}^1, \mathbf{x}^2, \mathbf{x}^3, \mathbf{x}^4, N^1, N^2, N^3, N^4, V^I, V^{II}, z_C$ and θ
Total	0	

Although this differential-algebraic model seems much more complicated than the mass transfer model, it is indeed the same than solving the mass transfer model once consistent initial conditions are found, also this model takes into account much more aspect that have to be supposed constant or modeled by complex fluid dynamic theories in the mass transfer model. The mass transfer coefficient for example has to be obtained according to the state of the immiscible phases: if a phase is disperse in the other phase or if both phases can be approximated as continuous, different mass transfer correlations have to be used [55], also stirring velocity changes affect surface area and mass transport. Each phase volume has to be supposed or algebraic restrictions have to be imposed making the model differential-algebraic, also as said before if no experimental data is available thermodynamic equilibrium calculations [52] have to be done to calculate the interface concentration which make mass transfer model even more complex than equilibrium model.

2.2.3 General Conclusions of when to use each model

In conclusion both models take into account different aspects both being as complicated as the designers wants.

For processes with limiting mass transfer and/or limiting reaction rate, the mass transfer model approach is recommended as also for complex models where mass, momentum and heat transport occurs simultaneously like in detailed heterogeneous catalytic modeling where mass transfer between the liquid bulk and the catalytic surface is decisive for the designer. Mass transfer approach is the most versatile modeling technique due to its strong theoretical foundations, but some properties are difficult to calculate and it requires complex piecewise dynamical systems to shortcut model the regime changes on mass,heat and momentum transport (i.e a change from laminar to turbulent flow and viceversa, due to perturbations).

For shortcut conceptual design modeling in steady state(equilibrium points), simultaneous physical and chemical equilibrium approach is the best for simplicity, and it has been widely used for decades [56], also many topologically aided design techniques like statics analysis [36] provides a strong theoretic background which helps the designer to make proper decision based on phase space analysis instead of rules of thumb.

For processes with limiting chemical reaction rate but no mass transfer limitations, physically but no chemical equilibrium model (kinetically driven) is the simpler and most accurate ap-

proach, specially for short-cut design where the main aspects of the model are taken into account, but simplifications as the physical equilibrium are possible to accurately assess the future performance of the equipment and to adequately specify most important design parameters as reactor volume and feed ratio.

2.3 BioReactor-Extractor for the Production of Biodiesel Model development

As probed in [2] Biodiesel production limiting step is the chemical reaction. Although [2] treats an alkali catalyzed process, this analysis can be extended to a more complex process like enzyme catalyst, that has multiple and complex inhibitions and interactions with the reaction media.

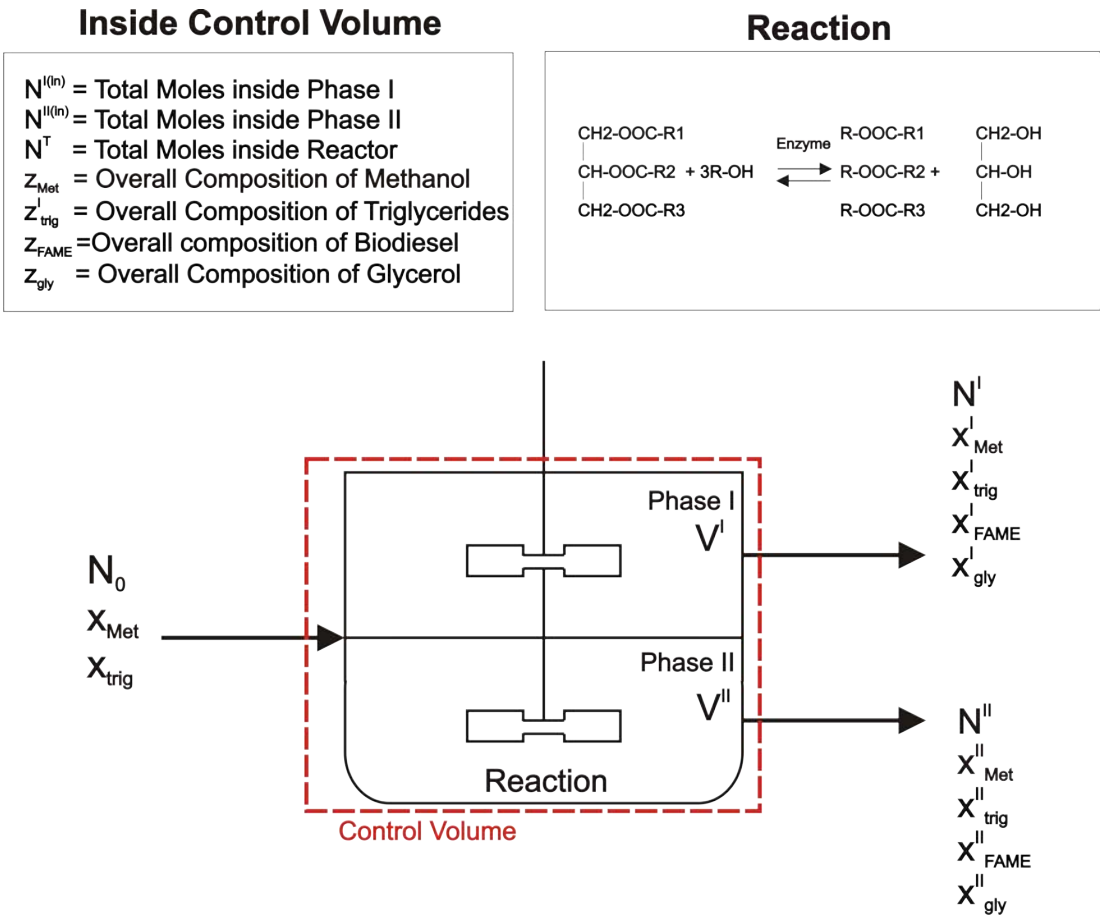

Figure 2.6: General scheme for Biodiesel Production Bioreactor-Extractor Modeling

Figure 2.6 is the general scheme of a bioreactor-extractor for the production of Biodiesel, that uses enzymes as catalyst. From this scheme material balances would be obtained and algebraic restrictions obeying conservation laws will be added to model a physical equilibrium and kinetically driven model that qualitatively and quantitatively describes the behavior of a two phase enzyme catalyzed reactor extractor during its operation.

2.3.1 Material Balances over the Control Volume

The control volume selected for the reactor extractor modeling can be seen in Figure 2.6, the control volume V^T will serve as reference for the capacity of the reactor and as the most important design parameter, the global balance for the selected volume control is:

$$\frac{dN^T}{dt} = N_0 - (N^I + N^{II}) + \sum_i^4 \sigma \upsilon V^{II} \tag{2.18}$$

In which σ is the sum of the stoichiometric coefficients of the transesterification reaction, in this case $\sigma = 1(Triglycerides) + 3(Alcohol) - 3(FAME) - 1(Glycerol) = 0$ (see equation (1.4) on page 5).

Reactor volume V^T is a fixed parameter while the reactor is working and there is no change in the number of moles inside the reactor due to the reaction, then it is possible to assume that the total number of moles inside the reactor is also fixed.

$$0 = N_0 - (N^I + N^{II}) \tag{2.19}$$

Component mass balances for any Alcohol (ROH), any Triglycerde (Trig), any fatty acid methyl ester (FAME or Biodiesel) and Glycerol present on a Transesterification reaction that occurs inside the reactor-extractor are :

$$N^T \frac{d(z_{ROH})}{dt} = N_O \cdot x_{ROH} - (N^I \cdot x^I_{ROH} + N^{II} \cdot x^{II}_{ROH}) - \upsilon_{ROH} \cdot V^{II} \tag{2.20}$$

$$N^T \frac{d(z_{Trig})}{dt} = N_O \cdot x_{Trig} - (N^I \cdot x^I_{Trig} + N^{II} \cdot x^{II}_{Trig}) - \upsilon_{Trig} \cdot V^{II} \tag{2.21}$$

$$N^T \frac{d(z_{FAME})}{dt} = -(N^I \cdot x^I_{FAME} + N^{II} \cdot x^{II}_{FAME}) + \upsilon_{FAME} \cdot V^{II} \tag{2.22}$$

$$N^T \frac{d(z_{Glyc})}{dt} = -(N^I \cdot x^I_{Glyc} + N^{II} \cdot x^{II}_{Glyc}) + \upsilon_{Glyc} \cdot V^{II} \tag{2.23}$$

If the following mole fractions restrictions are added for $i = 1$ for ROH,$i = 2$ for Trig,$i = 3$ for FAME and $i = 4$ for Glyc:

$$\sum_{i=1}^{4} z_i = 1 \tag{2.24}$$

$$\sum_{i=1}^{4} x_i = 1 \tag{2.25}$$

$$\sum_{i=1}^{4} x_i^I = 1 \tag{2.26}$$

$$\sum_{i=1}^{4} x_i^{II} = 1 \tag{2.27}$$

Then the glycerol balance (equation (2.23)) becomes dependent of the other 3 component mass balance equations and the global balance, so only equations (2.20), (2.21), (2.22) and the global balance are useful to describe the behavior of the bioreactor.

2.3.2 Material balance Inside the control Volume

At any fixed time t, the total moles inside the reactor (N^T), the moles inside phase one ($N^I_{(in)}$) and the moles inside phase two ($N^{II}_{(in)}$) are known, also the steady state material balance inside the control volume $N^T(t) = N^I_{(in)}(t) + N^{II}_{(in)}(t)$ and the compositions of each component in each phase. By the CSTR assumption it can be guaranteed that the compositions inside of each phase are the same ones as the compositions in the currents leaving the reactor. Making this assumptions, an instantaneous (fixed t) steady-state mass balance can be done for each component:

$$N^T \cdot z_{ROH} = N^I_{(in)} \cdot x^I_{ROH} + N^{II}_{(in)} \cdot x^I_{ROH} \tag{2.28}$$

$$N^T \cdot z_{Trig} = N^I_{(in)} \cdot x^I_{Trig} + N^{II}_{(in)} \cdot x^I_{Trig} \tag{2.29}$$

$$N^T \cdot z_{FAME} = N^I_{(in)} \cdot x^I_{FAME} + N^{II}_{(in)} \cdot x^I_{FAME} \tag{2.30}$$

$$N^T \cdot z_{Glyc} = N^I_{(in)} \cdot x^I_{Glyc} + N^{II}_{(in)} \cdot x^I_{Glyc} \tag{2.31}$$

Dividing by N^T and replacing $\frac{N^I_{(in)}}{N^T}$ by ϕ :

$$z_{ROH} = \phi \cdot x^{I}_{ROH} + (1-\phi) \cdot x^{II}_{ROH} \tag{2.32}$$

$$z_{Trig} = \phi \cdot x^{I}_{Trig} + (1-\phi) \cdot x^{II}_{Trig} \tag{2.33}$$

$$z_{FAME} = \phi \cdot x^{I}_{FAME} + (1-\phi) \cdot x^{II}_{FAME} \tag{2.34}$$

$$z_{Glyc} = \phi \cdot x^{I}_{Glyc} + (1-\phi) \cdot x^{II}_{Glyc} \tag{2.35}$$

Also equation (2.35) is dependent of the others by the mole fraction restrictions, so for the model to be consistent only equations (2.32),(2.33) and (2.34) would be part of the model.

2.3.3 Thermodynamic Equilibrium Restrictions

In Biodiesel production mass transfer rates are extremely high, so physical equilibrium simplification can be made in order to accurately predict the immiscible phases behavior, this is achieved by the use of standard thermodynamic theory [52] that says that phase equilibrium is achieved only when the chemical potential of all the liquid mixture components in each phase are equal:

$$\mu_i^{\alpha} = \mu_i^{\beta} = \cdots = \mu_i^{\pi} \tag{2.36}$$

In physical equilibrium this relation can be expressed in terms of fugacity as:

$$\hat{f}_i^{\alpha} = \hat{f}_i^{\beta} = \cdots = \hat{f}_i^{\pi} \tag{2.37}$$

For liquid solutions, Gibss energy and fugacity are expressed in terms of its deviation to ideal solutions, for this purpose an excess thermodynamical property (M^E) is defined as the difference between the real property value (M) and the ideal solution property value (M^{is}) at the same temperature and pressure:

$$M^E \equiv M - M^{is} \tag{2.38}$$

The only excess function that will be needed to derive a liquid equilibrium restriction would be

Gibbs free energy:

$$G^E = G - G^{is} \tag{2.39}$$

For a liquid mixture containing n moles in total, equation (2.39) can be multiplied by n and derived with respect to the number of moles of a component n_i for constant temperature, pressure and moles of another component in the mixture n_j:

$$\left[\frac{\partial(nG^E)}{\partial n_i}\right]_{P,T,n_j} = \left[\frac{\partial(nG)}{\partial n_i}\right]_{P,T,n_j} - \left[\frac{\partial(nG^{is})}{\partial n_i}\right]_{P,T,n_j} \tag{2.40}$$

Equation (2.40) has the form of a partial molar property and can be expressed as it:

$$\overline{G}_i^E = \overline{G}_i - \overline{G}_i^{is} \tag{2.41}$$

Using the fugacity definition:

$$d\mu_i = RTd\ln\hat{f}_i \tag{2.42}$$

And the definition of chemical potential:

$$\mu_i = \overline{G}_i \tag{2.43}$$

The following expression can be obtained:

$$\overline{G}_i^E = RT\ln\frac{\hat{f}_i}{f_i} \tag{2.44}$$

Where f_i is the fugacity of the ideal solution. An ideal solution's fugacity is proportional to its molar fraction:

$$f_i = \Re_i x_i \tag{2.45}$$

So replacing equation (2.45) into (2.44) leads to:

$$\overline{G}_i^E = RT \ln \frac{\hat{f}_i}{\Re_i x_i} \tag{2.46}$$

For a reference thermodynamical state it can be established that $\Re_i = f_i^0$, where f_i^0 is the fucacity at the reference thermodynamic state. Replacing this on equation (2.46) and using the activity coefficient definition [52], the following expression is obtained:

$$\overline{G}_i^E = RT \ln \gamma_i \tag{2.47}$$

Where γ_i is the activity coefficient. This defines the activity coefficient as the measure of the deviation of a solution from its ideal behavior and gives an strong theoretical background to the study of thermodynamical equilibrium calculation due to the possibility of using Gibbs excess function models to describe equilibrium behavior in liquid phases.
Then by definition of activity coefficient and fugacity [58] and by using equation (2.37), thermodynamical equilibrium restrictions can be expressed as follows for the Biodiesel production system:

$$x_{ROH}^I \gamma_{ROH}^I = x_{ROH}^{II} \gamma_{ROH}^{II} \tag{2.48}$$

$$x_{Trig}^I \gamma_{Trig}^I = x_{Trig}^{II} \gamma_{Trig}^{II} \tag{2.49}$$

$$x_{FAME}^I \gamma_{FAME}^I = x_{FAME}^{II} \gamma_{FAME}^{II} \tag{2.50}$$

$$x_{Glyc}^I \gamma_{Glyc}^I = x_{Glyc}^{II} \gamma_{Glyc}^{II} \tag{2.51}$$

Activity coefficient (γ_i) models can be found in th Appendix A and its selection for an specific Biodiesel system will be discussed later.

2.3.4 Volumetric Restrictions and Assumptions

Reactor volume V^T is a design parameter and is considered to be fixed, as there is only one reaction phase inside the bioreactor for the production of biodiesel, the only real volume affecting the reaction kinetics would be the volume of reacting phase, that can be approximated

by:

$$V^{II} = \frac{N^{II}_{(in)}}{\rho^{II}} = \frac{N^T \cdot \phi}{\rho^{II}} \tag{2.52}$$

Where ρ^{II} is the density of phase two and can be approximated by the weighted sum of each component density:

$$\rho^{II} \approx \sum_{i=1}^{4} x_i^{II} \cdot \rho_i^{II} = x^{II}_{ROH} \cdot \rho^{II}_{ROH} + x^{II}_{Trig} \cdot \rho^{II}_{Trig} + x^{II}_{FAME} \cdot \rho^{II}_{FAME} + x^{II}_{Glyc} \cdot \rho^{II}_{Glyc} \tag{2.53}$$

Then the reactor total volume V^T would be the maximum volume occupied by phase one and two during the operation to ensure a constant number of moles inside the reactor (N^T).
Last restriction added to the dynamical system is the assumption that the relation between the leaving currents of the reactor are the same that the relation between the moles of the phases inside the reactor:

$$\frac{N^I}{N^{II}} = \frac{N^I_{(in)}}{N^{II}_{(in)}} \tag{2.54}$$

Using ϕ definition on equation (2.54) leads to the final restriction:

$$\frac{N^I}{N^{II}} = \frac{\phi}{1-\phi} \tag{2.55}$$

2.3.5 Kinetic Model and Specifical Reaction Selection

Most of the earlier kinetic studies on lipase-catalyzed esterifications of fatty acids are described by a Ping-Pong kinetic model with competitive inhibition by the alcohol as given below:

$$\upsilon = \frac{V_{max}}{1 + \frac{K_F}{[F]} + \left[1 + \frac{[A]}{K_{IA}}\right] + \frac{K_A}{[A]}} \tag{2.56}$$

Where υ is the reaction rate, V_{max} is the maximum reaction rate, K_F and K_A are the binding constants for the fatty acid (F) and the alcohol (A), and K_{IA} is the inhibition constant for the alcohol, and the brackets denote molar concentration ($mol\ cm^{-3}$).

This mechanism has been modified by incorporating a Ping-Pong Bi-Bi mechanism with inhibition by both of the substrates. However, it was proven experimentally that the substrate (S) (i.e., the ester bond on the triglyceride) does inhibit lipase-catalyzed reactions of vegetable oils [3]. Therefore, this modification is not applicable for the transesterifications of vegetable oils.

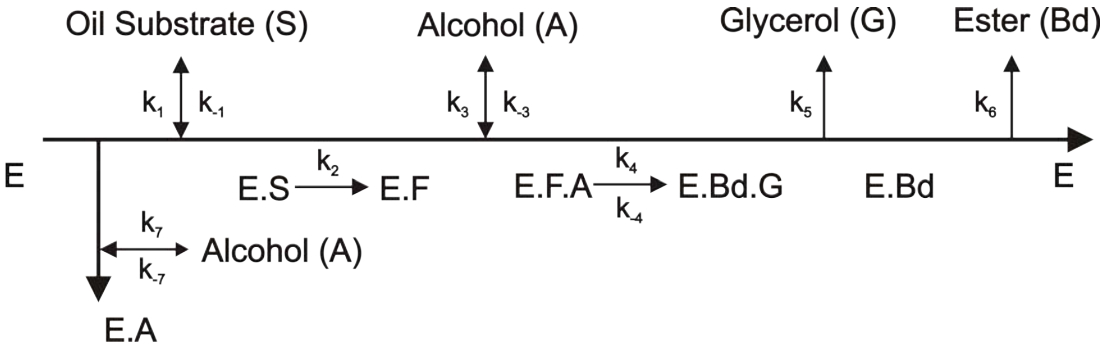

Figure 2.7: Graphical representation of the mechanismic steps of triglyceride ester-bond transesterification form [3]

Figure 2.7 shows a schematic diagram of the mechanismic steps proposed for the esterification of triglycerides with lipases. As proposed in [14], all steps except deacylation of the lipase are assumed to be in quasisteady state. With this proposed mechanism and assumptions, the rate of transesterification of triglycerides can now be expressed as:

$$\upsilon = \frac{V_{max}[S]}{1 + K_{IS}[S] + \frac{K_S}{[S]}\left[1 + \frac{[A]}{K_{IA}}\right] + \frac{K_A}{[A]}} \tag{2.57}$$

Results obtained experimentally in [3] for immobilized *Rhizomucor miehei* (RM) lipase and immobilized *Thermomyces lanuginosa* (TL) lipase, using Sunflower oil and methanol as reactants, for equation (2.56) and (2.57) are presented in the Table 2.2.

In the mass balances obtained previously, all compositions are expressed in molar fraction, and equation (2.57)'s terms are all in molar concentration. Since the molar concentration can be expressed as:

$$[R] = x_R\, \rho \tag{2.58}$$

Table 2.2: Kinetic parameters Obtained in [3] for the Ping Pong kinetics with and without inhibition

	Equation (2.56)		Equation (2.57)	
Parameter	Lipase RM	Lipase TL	Lipase RM	Lipase TL
$V_{max}(min^{-1})$	0.0903	0.0546	0.414	0.197
$K_{IS}(cm^3\ mol^{-1})$	n/a	n/a	0.13	0.13
[Equation (2.56)]$K_F(cm^{-3}\ mol)$	16.34	10.18		
[Equation (2.57)]$K_S(cm^{-3}\ mol))$			0.16	0.44
$K_A(cm^3\ mol^{-1})$	0.19	0.11	0.98E-4	4.82E-4
$K_{AI}(cm^3\ mol^{-1})$	0.1	0.083	1.9	0.9

Where R is any compound into a liquid solution, brackets denote molar Composition ($mol\ cm^{-3}$), x_R is the molar fraction of R ($mol_R/mol_{Solution}$) and ρ is the density of the liquid solution.
If equation (2.58) is substituted into equation (2.57), knowing that every mol of tryglyceride contains 3 mol of ester bonds (Substrate [S]) ando using the notation used in mass balances for phase two (where the reaction takes place), the following expression is obtained:

$$\upsilon = \frac{3V_{max}x^{II}_{Trig}\ \rho^{II}}{1 + 3K_{IS}\ x^{II}_{Trig}\ \rho^{II} + \frac{K_S}{3\ x^{II}_{Trig}\ \rho^{II}}\left(1 + \frac{x^{II}_{ROH}\ \rho^{II}}{K_{IA}}\right) + \frac{K_A}{x^{II}_{ROH}\ \rho^{II}}} \tag{2.59}$$

As reported in [3, 14, 15] equations (2.57) type is much more accurate to predict the tansesterification reaction behavior than equation (2.56). For this reason it would be the selected kinetic model for this work.
As *Rhizomucor miehei* lipase (RM) is immobilized on ion-exchange resin and *Thermomyces lanuginosa* lipase (TL) is immobilized on silica gel, the chosen kinetic model is suitable for reaction-extraction system analysis, because no solvents are added to the reactor, so it would still have the two immiscible phases, also immobilized enzymes report higher yields than free enzymes [11, 34, 59].
With the kinetic model chosen, the reactants and products described in the mass balance are no more general alcohols or triglycerides,now the alcohol(ROH) is methanol (MeOH) and the triglyceride (Trig) are all the triglycerides present in the Sunflower oil.

2.3.6 Activity Coefficient Model Selection

There are two main criteria used to select an activity coefficient model. The first is the physical nature of the process that is going to be simulated (i.e. if its a Vapor-liquid-liquid equilibrium not all models listed in Appendix A are suitable); the second is the experimental data and fitted model parameters availability for the desired substances (All models on Appendix A depend on the availability of experimental data, even group contribution models like UNIFAC use experimental data to estimate group contribution parameters).

Availability of experimental data and correlated parameters is very limited, nevertheless the number of publications of liquid-liquid equilibrium data referring to triglycerides, long chain fatty acid methyl esters, glycerol and alcohol has been rising with the rising interest in biofuels, specially in Biodiesel. As each researcher has its own interests depending on its location and specialty, the available data, correlated models and experimental conditions is diverse as it can be seen on Table 2.3, This reduces considerably the applicability of very specific data to a model like the one proposed in this work.

As Models like Wilson's, NRTL and UNIQUAC need specific data, and specific data for the four component Sunflower Oil+ Methanol+ FAME (Derived from Sunflower oil transesterification with metahnol)+ Glycerol is not currently available in the literature, a group contribution model must be used.

The most widely used and accepted group contribution activity model is UNIFAC and all its variations, the whole family of UNIFAC's group contribution parameters has been correlated from the data stored in the Dortmund Data Bank [67–72].

Original UNIFAC's parameters are correlated only from vapor-liquid equilibrium [70] it is not suitable to be used in liquid-liquid equilibrium, the same happens with UNIFAC DORTMUND whose parameters are correlated from both vapor-liquid and vapor-liquid-liquid equilibrium; thats why Magnussen et al. [73] correlated special group contribution parameters from a limited number of binary and ternary mixtures, this new UNIFAC model parameters for liquid-liquid equilibrium predict within a 10% of molar deviation [73]. This liquid-liquid version of UNIFAC is not recomendable for precting activity coefficients of big molecules, as it can be seen in [73] where 32 different groups are reported, representing hydrocarbons,water, alcohols, low chain organic acids, halogenated hydrocarbons and nitriles.

In a relatively recent article Batista et al. [7] used long chain fatty acids and triglycerides data to

Table 2.3: Available Liquid-Liquid Equilibrium Correlated and Experimental Data

Liquid Mixture	Experimental Conditions	Correlated Activity Model or EoS	Reference
Sunflower Oil+ Ethanol+Carbon Dioxide	Supercritical	GC-EoS	[60]
Cottonseed Oil+Linoleic Acid+ Ethanol	298.2 K	NRTL	
Soybean Oil+Linoleic Acid+Ethanol	298.2 K	NRTL	[61]
Corn Oil+Oleic Acid+Ethanol+Water	298.15 K	NRTL and UNIQUAC	[62]
FAEE+Ethanol+Soybean Oil	300.15 K	Only Exp Data	
FAEE+Ethanol+Glycerol	300.15 K	Only Exp Data	[63]
Corn Oil+Oleic Acid+Methanol	303.15 and 313.15 K	UNIQUAC	
Corn Oil+Oleic Acid+Ethanol	303.15 and 313.15 K	UNIQUAC	[64]
Vegetable Oils+Fatty Acids+Ethanol	293.15,298.18 and 303.15 K	UNIFAC and ASOG	[7]
palm oil+fatty acids+ethanol+ water	318.2	NRTL and UNIQUAC	[65]
sunflower oil+oleic acid+methanol	303.15 and 313.15 K	UNIQUAC	[66]

improve liquid-liquid UNIFAC's accuracy to predict all compounds involved in the Biodiesel reaction, with excellent results reported in the same work (2% of deviationre reported) and in the recent PhD thesis of Luis Fernando Gutierrez [2] where this model was used to predict palm oil and castor oil behaviour during an alkali catalyzed reaction leading to the design of the equipment in Figure 1.9 in page 19 which pattent is pending. Group contibution paramter modifications can be seen in table 2.4.

Table 2.4: Modification to liquid-liquid UNIFAC reported in [7]

m	n	a_{mn}	a_{nm}
$CH=CH$	CH_2COO	-149.180	-2692.200
$CH=CH$	$COOH$	-851.340	194.320
$CH=CH$	OH	1172.400	-2457.900
CH_2COO	$COOH$	17.081	-167.670
CH_2COO	OH	511.190	247.520
$COOH$	OH	-424.310	70.196

This modifications and previous result and experiences in [2] make this kind of modified liquid-liquid UNIFAC perfect for the bioreactor-extractor model proposed in this work.

2.3.7 Final Simplification

The last simplification to be made concerns to the complexity of vegetable oils triglyceride's composition. As described early in Chapter 1 on page 3, triglycerides are defined as a single molecule of glycerol replaced on each OH group by a long chain fatty acid forming an ester bound (see equation (1.4)); in fact any combination of capric, lauric, myristic, palmitic, palmitoleic, oleic, elaidic, arachidic, eicosenoic, behenic, erucic, cerotic, stearic, linoleic and linolenic acid can form a triglyceride. The composition of all the possible triglycerides present in a vegetable oil depends on its source. The chosen sunflower oil is not the exception it is a complex mixture of triglycerides distributed as follows[6]: LLL (33.8 mol%), OLL (29.3 mol%), PLL (10.6 mol%), OOL (8.4 mol%), SLL (7.4 mol%), POL (5.1 mol%), OOO (1.4 mol%) and SOL (2.4 mol%) reported in [74].

The reaction substrate according to kinetics is the ester bond, and any triglyceride has 3 ester

[6] L=Linolein, O=Olein, P=Palmitin, S=Stearin

bonds, so for the selected kinetic model the nature and composition of the used oil is irrelevant; nevertheless the kinetic model parameters are correlated from a reaction with sunflower oil, which means it is not valid to simulate other kind of oils. The problem with the kinetics arises for the product, as the substrate is the ester bond in the triglycerides, the product is the ester bond in the FAME, which is one for any FAME derived from the reaction, sunflower oils triglycerides are 8, the possible FAMES derived from the reaction are 4, but it is impossible to know with the chosen kinetic or with any kinetic published until today, the exact composition of the resulting FAME mixture of a transesterification reaction; this leads to the conclusion that only one FAME should be supposed as the product and one triglyceride supposed as the reactive, to simplify the liquid-liquid equilibrium calculation and eliminate the need of very specific kinetics development, which is out of the scope of this work.

Analyzing the compositions of sunflower oil reported in [74, 75] and on Table 1.2 on page 4, it can be seen that Linolein and Olein are where the most common, being the Linolein the most abundant with 69 mol% [74].

Taking into account the quantity of Linolein present in the sunflower oil, the main interaction of the sunflower oil with the other reactant and the resulting products will be dominated by the interaction of Linolein containing molecules (Triglycerides and FAMEs), so for the purposes of this work sunflower oil will be approximated as Trilinolein and the resulting FAMEs as Methyl Linoleate.

2.4 Bioreactor-Extractor Piecewise Model

2.4.1 Biorreactor-Extractor Start

One of the most important aspects in any chemical or physical process is the star of the equipment. The start of the reactor is not usually taken into account in the first conceptual process design stage because traditionally this design stage is done under steady-state assumption.

Biodiesel Process is catalogued as autoextractive[7] [2] so a special start algorithm must be used to generate from the reactives a two liquid phases system. This could be achieved by making the reactor extractor to behave as a batch CSTR:

The process consist into load the reactor with a mixture of reactives and catalyst, then close the

[7] There is no need to add solvents to provoke a phase split

output and input valves of the reactor and turn on the agitation fast enough to make the reactor-extractor work as close to a CSTR as possible; as the reaction begins, glycerol and Biodiesel will be produced, and when certain time t_s is reached and a certain amount of immiscible products is produced, inputs and output valves of the reactor-extractor will be opened, and agitation speed will be reduced to the optimal value, where phase split and reaction will occur simultaneously.

Mass Balances Over the Control Volume

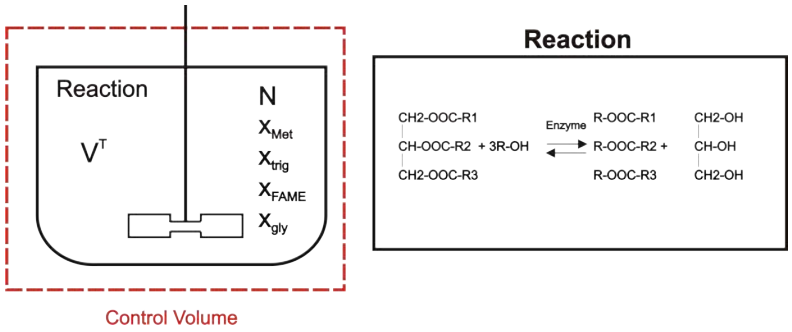

Figure 2.8: Start of the Bioreactor

As shown before, using Figure 2.8 mass balances are derived for a no inputs no outputs reactor.
Global balance:

$$\frac{dN^T}{dt} = \sum_i^4 \sigma \upsilon V^T \tag{2.60}$$

As proved before for the Biodiesel production reaction $\sigma = 0$ so the total change of moles inside the reactors is null.
Component balance:

$$N^T \frac{dz_{ROH}}{dt} = -\upsilon_{ROH} V^T \tag{2.61}$$

$$N^T \frac{dz_{Trig}}{dt} = -\upsilon_{Trig} V^T \tag{2.62}$$

$$N^T \frac{dz_{FAME}}{dt} = \upsilon_{FAME} V^T \tag{2.63}$$

$$N^T \frac{dz_{Glyc}}{dt} = \upsilon_{Glyc} V^T \tag{2.64}$$

$\sum z = 1$, then z_{Glic} is a dependent variable, this makes equation (2.64) dependent and is eliminated from the model.

Initial Value Problem

The bioreactor-extractor start model mathematically reduces the start of the reactor-extractor to the solution of an initial value problem in ordinary differential equations, the main idea of this is to determine a time t_s to switch the bioreactor from start to operation mode. This t_s has to be chosen carefully to ensure that the bioreactor-extractor will reach the desired steady-state, which can be previously selected numerically analyzing all the possible steady-states and basins of attraction of the model described in section 2.3.
Initial values are also part of the design problem as a design parameter, in this particular case the main assumption will be that the bioreactor-extractor in the starting stage will be totally full of methanol and sunflower oil, so N is fixed as the capacity of the reactor-extractor depending on the total volume V^T, then the design parameter R will be the proportion between the reactants in zero time:

$$R = \frac{z_{ROH}(t=0)}{z_{Trig}(t=0)} \tag{2.65}$$

2.4.2 Piecewise Bioreactor-Extractor Model

Each one of the models developed in section 2.3 and subsection 2.4 can be analyzed separately, but also they can be analyzed together as a single piecewise model which will describe a simplified operation trajectory on the thermodynamic limit, this is specially useful as a tool to predict at least approximately, the behavior of the reactor-extractor in presence of disturbances, but not accurate enough to be a model suitable for the implementation of a controller due to its multiple simplifications.

The Piecewise Simplification

Th switch between the starting and operating mode in real is not a simple step, it includes complex fluid dynamics and simultaneous reaction, while the transition between the high agitation rate's CSTR like induced behavior and the optimal agitation's two phase reaction-extraction

regime takes place; this phenomena is the one that will be simplified as a switch between the two models, this indeed leaves the complex simulation and modeling of this transition to further design stages in which this phenomena can be modeled or experimentally recreated to improve the start algorithm of the bioreactor extractor, the reason for this is that for a first estimate of the start parameters of the bioreactor-extractor there is no need to use complex fluid dynamics.

The Model

The resulting Piecewise non lineal model is a combination of the two previously formulated models:

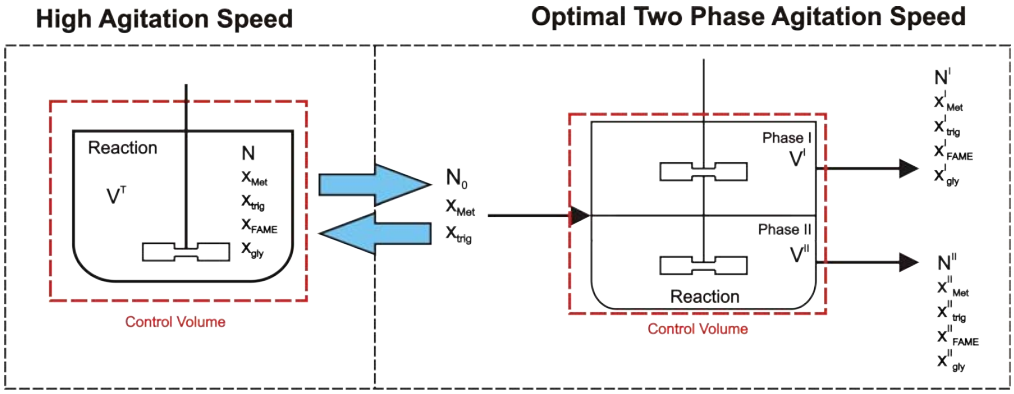

Figure 2.9: Piecewise Bioreactor-Extractor Model Scheme

For the Operation Stage:

$$0 = N_0 - (N^I + N^{II}) \tag{2.66}$$

$$N^T \frac{d(z_{ROH})}{dt} = N_0 \cdot x_{ROH} - (N^I \cdot x^I_{ROH} + N^{II} \cdot x^{II}_{ROH}) - \upsilon_{ROH} \cdot V^{II} \tag{2.67}$$

$$N^T \frac{d(z_{Trig})}{dt} = N_0 \cdot x_{Trig} - (N^I \cdot x^I_{Trig} + N^{II} \cdot x^{II}_{Trig}) - \upsilon_{Trig} \cdot V^{II} \tag{2.68}$$

$$N^T \frac{d(z_{FAME})}{dt} = -(N^I \cdot x^I_{FAME} + N^{II} \cdot x^{II}_{FAME}) + \upsilon_{FAME} \cdot V^{II} \tag{2.69}$$

$$z_{ROH} = \phi \cdot x^I_{ROH} + (1-\phi) \cdot x^{II}_{ROH} \tag{2.70}$$

$$z_{Trig} = \phi \cdot x^I_{Trig} + (1-\phi) \cdot x^{II}_{Trig} \tag{2.71}$$

$$z_{FAME} = \phi \cdot x^I_{FAME} + (1-\phi) \cdot x^{II}_{FAME} \tag{2.72}$$

$$\sum_{i=1}^{4} z_i = 1 \tag{2.73}$$

$$\sum_{i=1}^{4} x^I_i = 1 \tag{2.74}$$

$$\sum_{i=1}^{4} x^{II}_i = 1 \tag{2.75}$$

$$x^I_{ROH}\gamma^I_{ROH} = x^{II}_{ROH}\gamma^{II}_{ROH} \tag{2.76}$$

$$x^I_{Trig}\gamma^I_{Trig} = x^{II}_{Trig}\gamma^{II}_{Trig} \tag{2.77}$$

$$x^I_{FAME}\gamma^I_{FAME} = x^{II}_{FAME}\gamma^{II}_{FAME} \tag{2.78}$$

$$x^I_{Glyc}\gamma^I_{Glyc} = x^{II}_{Glyc}\gamma^{II}_{Glyc} \tag{2.79}$$

$$V^{II} = \frac{N^T \cdot \phi}{\rho^{II}} \tag{2.80}$$

$$\frac{N^I}{N^{II}} = \frac{\phi}{1-\phi} \tag{2.81}$$

For the Start or CSTR like stage:

$$N^T \frac{dz_{ROH}}{dt} = -\upsilon_{ROH} V^T \tag{2.82}$$

$$N^T \frac{dz_{Trig}}{dt} = -\upsilon_{Trig} V^T \tag{2.83}$$

$$N^T \frac{dz_{FAME}}{dt} = \upsilon_{FAME} V^T \tag{2.84}$$

$$\sum_{i=1}^{4} z_i = 1 \tag{2.85}$$

To switch form start stage to operation stage the last value of the vector **z** is now the initial value of equation (2.66) to (2.69), and consistent initial values for the other variables must be calculated using the globally stable liquid-liquid equilibrium algorithm developed for this work in Appendix C, and then integrate the resulting differential algebraic system. The only condition to do this switch is that the liquid-liquid equilibrium exists for the values of the vector **z**, otherwise the transition isn't possible in real life.

To switch from the operation stage to the CSTR like stage i.e to recover from a disturbance, The final values of vector **z** are taken as the initial values of equations (2.82) to (2.85), and the ODE system is integrated.

Chapter 3

Differential Algebraic Equation's Integration by Effective Order Singly Implicit Runge-Kutta Methods

In Order to numerically integrate the model purposed on Chapter 2 by any type of Runge-Kutta Method, it is necessary to understand the properties of nonlinear Differential-Algebraic equations and how they affect the stability and convergence of the numerical method used to its solution, it is also important to know the numerical method inherent stability and convergence properties, to make an adequate selection of method and order, taking into account the precision, stability and computational costs associated with each method.

The present chapter gives a brief introduction to DAEs, its properties and mathematical characterization, as also its integration by Runge-Kutta methods, analyzing the stability of both implicit and explicit integration schemes making a special emphasis into singularly implicit Runge-Kutta methods, effective order and the combination of both concepts to create the numerically implementable and stable, Effective Order Implicit Runge-Kutta Methods (ESIRK). Its numerical implementation for the solution of DAEs of order one, with fixed and variable stepsize schemes will be discussed as long with the possibility of exploiting variable order algorithms in the DAE integration.

3.1 Differential Algebraic Equations Generalities

The desirability of working directly with DAE's has been recognized for over 30 yrs by scientist and engineers in several areas [76]. The most straight forward way of studying DAE's, certainly from the view point of applied mathematics, is to use the singular perturbation analysis. The

singular perturbation problem is considered

$$y' = f(y, z), \quad y(0) = y_0 l \tag{3.1}$$

$$\epsilon z' = g(y, z), \quad z(0) = z_0 \tag{3.2}$$

If $\epsilon \to 0$, the following reduced equation is obtained,

$$y' = f(y, z) \tag{3.3}$$

$$0 = g(y, z) \tag{3.4}$$

A practical way of looking at the equations (3.3) to (3.4) is to consider them as differential equations for which the solution is constrained to lie on a manifold $g(y, z) = 0$, this can appreciated in the model developed on chapter 2, where the solution of the bioreactor-extractor is constrained to the physical equilibrium manifold which represents an idealization of maximum achievable separation efficiency. As the solution lies on the manifold also the initial values must lie on the same manifold [77], so they have to satisfy,

$$g(y_0, z_0) = 0 \tag{3.5}$$

3.1.1 Differential Algebraic Equations Indices

Differential Index

A general DAE takes the form

$$f(y', y, t) = 0 \tag{3.6}$$

where f and y are in $\mathbb{R}^n$. The differential index d_i, of the system is the minimum integer m, such that the system of equations (3.6) and

$$\begin{aligned} \tfrac{df(y',y,t)}{dt} &= 0 \\ \tfrac{d^2 f(y',y,t)}{dt^2} &= 0 \\ &\vdots \\ \tfrac{d^m f(y',y,t)}{dt^m} &= 0 \end{aligned}$$

can be solved for $y' = y'(y)$, This explicit ODE is often called the underlying ODE, it is important to take into account the three first differential indexes:

Differential Index One Consider the system of equations (3.3) and (3.4). If $g_z = \frac{\partial g}{\partial z}$ is invertible in a neighborhood of the solution, the the problem has differential index one since in this case the differentiation of (3.4) gives a first order ODE for z. The initial conditions are required to satisfy the condition (3.5).

Differential Index Two Consider the semi-explicit form,

$$y' = f(y, z) \tag{3.7}$$

$$0 = g(y) \tag{3.8}$$

Differentiating the constraint with respect to y,

$$0 = g_y \frac{dy}{dx} = g_y f(y, z) \tag{3.9}$$

Relation (3.9) is often referred to as the hidden constraint. Differentiating again with respect to z, (3.7) and (3.8) are of index two if $g_y\ f_z$ is invertible in a neighborhood of the solution.

Differential Index Three Consider the system,

$$y' = k(y, z, w) \tag{3.10}$$

$$z' = f(y, z) \tag{3.11}$$

$$0 = g(z) \tag{3.12}$$

This problem is in Hessenberg form [76] and has index three if and only if $g_z\ f_y\ k_w$ is invertible in a neighborhood of the solution.

Perturbation Index

Hairer et al [4] defined the perturbation index p_i, as the smallest value of the integer m such that the difference between the solution of (3.6) and the solution for the perturbed equation

$$f(z', z, t) = e(t) \tag{3.13}$$

can be bounded by an expression of the form

$$\begin{aligned} \max \|z(t) - y(t)\| \quad \leq \quad & K[\|z(0) - y(0)\|] + \max(\|e(t)\|) + \\ & \max(\|\dot{e}(t)\|) + \ldots + \max(\left\| e^{(m-1)}(t) \right\|] \end{aligned} \tag{3.14}$$

over a finite interval $t \in [0, T]$.

The perturbation index is clearly an important factor in the numerical solution of a DAE since it will play a major role in determining the impact of roundoff errors. The expected round-off errors would be of the order δ/h^{p-1}, because the method will be performing a numerical differentiation on roundoff errors assumed to be order of δ. [4].

3.1.2 Relation to Stiffnes and Order Reduction

In the early 1950's as a result of the work by Curtiss and Hirschfelder [78] stiff ODEs were identified as "equations were certain implicit methods, and in particular backward-differentiation formula (BDFs) perform better, usually tremendously better than explicit ones", although this definition is not all precise it does encapsulate an intuitive idea of what stiffness is [77]. Another intuitive idea of the nature of stiffness is that they are multi-scale problems. That is, stiff equations represent coupled physical systems having components which vary on very different time-scales.

There is a close relationship between DAE systems and stiff ode systems, as it was seen before, the system of equations (3.1) and (3.2) tends to be the semi explicit system of equation (3.3) and (3.4) as $\epsilon \to 0$. Thus it is natural to expect that there will be a relationship between the behavior of numerical ODE methods when applied to the related DAE. This can be interpreted as a multi-scale problem where the "time" scales of y and z become extremely different as long as ϵ tends to zero.

Order reduction is a phenomenon that was noted in 1974 by Prothero and Robinson. They studied the stiff model problem

$$y'(t) = \lambda y(t) + g'(t) - \lambda g(t), \quad \lambda << 0 \tag{3.15}$$

and noted that when an Rungue-Kutta method was applied to solve the above equation, the error order of the solution was bellow the expected one for the applied numerical method. Some of the numerical results reported in [4] illustrate the order reduction of singular perturbation problems as function of ϵ and confirm the order reduction predicted in theory, so order reduction is expected for DAE systems.

3.2 Runge-Kutta Methods for DAE's

The idea of generalizing the Euler method, by allowing for a number of evaluations of the derivative to take place in a step, is generally attributed to Runge (1895). Further contributions were made by Heun (1900) and Kutta (1901). The latter completely characterized the set of Runge-Kutta methods of order 4, and proposed the first methods of order 5. Special methods for second order differential equations were proposed by Nyström (1925), who also contributed to the development of methods for first order equations. It was not until the work of Huta (1956,1957) that sixth order methods were introduced.

Since the advent of digital computers, fresh interest has been focused on Runge-Kutta methods, and a large number of research workers have contributed to recent extensions to the theory, and to the development of particular methods [79].

Runge-Kutta methods have originally been conceived for numerical solution of ordinary differential equations $y' = f(x, y)$ [1]. From an approximation y_n of the solution at x_n these one-step methods construct an approximation y_{n+1} at $x_{n+1} = x_n + h$ via the formulas

$$y_{n+1} = y_n + h \sum_{i=1}^{s} b_i Y'_{ni} \tag{3.16}$$

where Y'_{ni} is called stage derivative and is defined by

$$Y'_{ni} = f(x_n + c_i h, Y_{ni}) \tag{3.17}$$

with internal stages Y_{ni} given by

$$Y_{ni} = y_n + h \sum_{j=1}^{s} a_{ij} Y'_{ni} \qquad \text{for } i = 1, \ldots, s \tag{3.18}$$

Here a_{ij}, b_i and c_i are the coefficients which determine the method, and s is the number of stages. The most common way to represent an s-stage Runge-Kutta Methods is by the

[1] Since now the independent variable of differential equations will be noted by x, aiming to have a more general notation than the former t

Butcher's tableau:

$$\begin{array}{c|cccc} c_1 & a_{11} & a_{12} & \cdots & a_{1s} \\ c_2 & a_{21} & a_{22} & \cdots & a_{2s} \\ \vdots & \vdots & \vdots & \ddots & \vdots \\ c_{s-1} & a_{(s-1)1} & a_{(s-1)2} & \cdots & a_{(s-1)s} \\ c_s & a_{s1} & a_{s2} & \cdots & a_{ss} \\ \hline & b_1 & b_2 & \cdots & b_s \end{array} \tag{3.19}$$

It can also be noted in a more compact notation as $(\mathbf{A}, \mathbf{b}, \mathbf{c})$ or,

$$\begin{array}{c|c} \mathbf{c} & \mathbf{A} \\ \hline & \mathbf{b}^T \end{array} \tag{3.20}$$

where $\mathbf{A}$ is the matrix of a_{ij}, $\mathbf{b}$ and $\mathbf{c}$ are the vectors of b_i and c_i respectively. If $a_{ij} = 0$ for $i \leq j$, the internal stages $Y_{n1}, \ldots, Y_{ns}$ can be computed one after the other from equation (3.18) by explicit functions evaluations. Such methods are called explicit. Otherwise equation (3.18) constitutes a non linear system for the internal s stages, and the method is called implicit. If Kronecker tensor product ($\otimes$) is used, a s-stages Runge-Kutta method $(\mathbf{A}, \mathbf{b}, \mathbf{c})$ applied to a system of N ODEs, can be compactly described by the following equations

$$\mathbf{Y} = \mathbf{e} \otimes y_n + h(\mathbf{A} \otimes \mathbf{I}) f(\mathbf{Y}) \tag{3.21}$$

$$y_{n+1} = y_n + h(\mathbf{b}^T \otimes \mathbf{I}) f(\mathbf{Y}) \tag{3.22}$$

where $\mathbf{Y}$ is the Ns elements vector of the stages of the method, $\mathbf{e}$ being the s elements vector of ones, $\mathbf{I}$ the $N \times N$ Identity matrix and h is the stepsize ($h = x_n - x_{n-1}$).

3.2.1 Order Conditions

To describe any Implicit Runge-Kutta method is necessary to introduce

$$c_i = \sum_{j=1}^{s} a_i j \ (i = 1, \ldots, s) \tag{3.23}$$

and the following algebraic conditions:

$$B(p) \quad : \quad \sum_{i=1}^{s} b_i c_i^{k-1} = \frac{1}{k} \qquad \text{for } k = 1, \ldots, p \tag{3.24}$$

$$C(q) \quad : \quad \sum_{j=1}^{s} a_i j c_j^{k-1} = \frac{c_i}{k} \qquad \text{for } k = 1, \ldots, q \tag{3.25}$$

$$D(r) \quad : \quad \sum_{i=1}^{s} b_i c_i^{k-1} a_{ij} = \frac{b_j}{k}(1 - c_j^k) \qquad \text{for } k = 1, \ldots, r \tag{3.26}$$

Condition $B(p)$ means that the quadrature formula with weights $b_1 \ldots, b_s$ and nodes $c_1, \ldots, c_s$ integrates polynomials up to degree $p-1$ exactly on the interval $[0, 1]$, and condition $C(q)$ says that polynomials up to degree at least $q-1$ are integrated exactly on the interval $[0, c_i]$, for each i,, by the quadrature formula with weights $a_{i1}, \ldots, a_{is}$, a deduction of this conditions based on the rooted tree theory applied to the Taylor series expansion of the exact and the approximated solution can be found in [79] and [80].

One of the most important conditions to this work is $C(q)$, By comparing both the Taylor expansions of formula (3.18) and $y(x_n + c_i h)$ the following expression is obtained,

$$Y_i = y(x_n + c_i h) + O(h^{q+1}) \tag{3.27}$$

This means that the stage is an approximation with error of order $q + 1$ of the solution at $x_n + c_i h$, then if $q = s$ no lower order approximations will be used to estimate the solution y_n, this avoids order reduction [81].

3.2.2 Stability Functions of The Runge-Kutta Methods

Since the identification of stiff differential equations [78], the investigation of numerical methods to overcome stiffness started, bringing very interesting and enlightening results in 1963 by the mathematician Germund Dahlquist [82]. Dahlquist simple but yet very useful approach to the stability, reduces the problem to a numerical method applied to the equation

$$y'(x) = \mathbf{q}y(x), \quad y(x_0) = y_0. \tag{3.28}$$

where $\mathbf{q}$ is a complex constant with negative real part.

One of the most notorious members of the Runge-Kutta method family is the implicit Euler

method, if this method is applied to the Dahlquist equation 3.28,

$$\frac{y(x_{n+1}) - y(x_n)}{h} = qy(x_{n+1}) \tag{3.29}$$

making this equation explicit in $y(x_{n+1})$

$$y(x_{n+1}) = \frac{y(x_n)}{1 - h\mathbf{q}} \tag{3.30}$$

replacing $h\mathbf{q}$ by z and using the initial condition, the following difference equation is obtained:

$$y_n = \left(\frac{1}{1-z}\right)^n y_0, \quad \text{for } n = 1, \ldots \tag{3.31}$$

The stability function of the implicit Euler method is then

$$R(z) = \frac{1}{1-z} \tag{3.32}$$

Using difference equation stability theory, $R(z)$ is stable, if and only if $|R(z)| \leq 1$, which for the Euler method gives the following stability region:

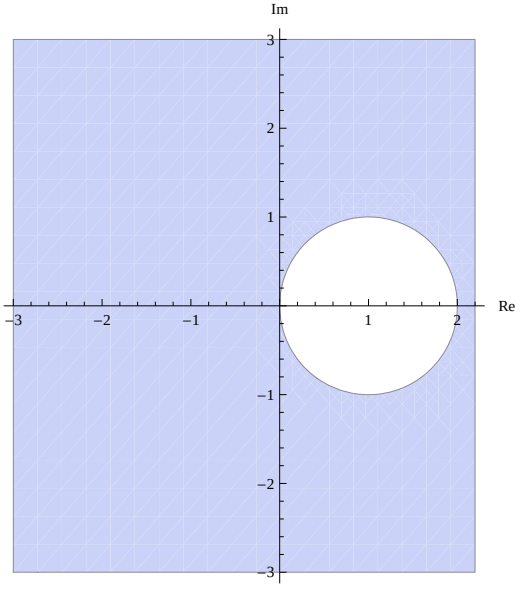

Figure 3.1: Stability Region of the Implicit Euler Method

Definition 3.1. *The function $R(z)$ is called the stability function of the method. It can be interpreted as the numerical solution after one step for*

$$y'(x) = qy(x), \quad y_0 = 1, \quad z = hq \tag{3.33}$$

the famous Dahlquist test equation, The set

$$S = \{z \in \mathbb{C}, |R(z)| \leq 1\} \tag{3.34}$$

is called the stability domain of the method.

Definition 3.2 (Dahlquist, 1963)**.** *A method whose stability domain contains the whole of the left complex half plain is called* ***A-stable***

A more flexible definition of A-stability called A(α)-stability was purposed by Widlund in 1967 [83].

Definition 3.3 (Widlund, 1967)**.** *A method is called A(α)-stable if its stability domain includes*

$$S_\alpha = \{z \in \mathbb{C}, |arg(-z)| \leq \alpha\} \tag{3.35}$$

Runge-Kutta Methods Stability Function

For an s-stage Runge-Kutta method defined by the Tableau

$$\begin{array}{c|c} \mathbf{c} & \mathbf{A} \\ \hline & \mathbf{b}^T \end{array} \tag{3.36}$$

the vector Y, made up from the s stages values satisfies

$$Y = \mathbf{e}y_0 + h\mathbf{A}qY = y_0 + z\mathbf{A}Y \tag{3.37}$$

where y_0 is the incoming approximation. It follows that

$$Y = (\mathbf{I} - z\mathbf{A})^{-1}\mathbf{e}y_0 \tag{3.38}$$

Substituting this into the solution approximation leads to

$$y_1 = y_0 + z\mathbf{b}^T(\mathbf{I} - z\mathbf{A})^{-1}y_0 = R(z)y_0 \tag{3.39}$$

where

$$R(z) = 1 + z\mathbf{b}^T(\mathbf{I} - z\mathbf{A})^{-1}\mathbf{e} \tag{3.40}$$

Another Interesting result can be found applying the Kramer's rule to find y_1 in terms of y_0

$$R(z) = \frac{det(\mathbf{I} - z\mathbf{A} + z\mathbf{e}\mathbf{b}^T)}{det(\mathbf{I} - z\mathbf{A})} \tag{3.41}$$

3.2.3 Stability Domains of Runge-Kutta Methods

From the resulting equivalent stability functions (3.40) and (3.41), stability domains can be obtained and analyzed:

Explicit Runge-Kutta Stability Domain If $\mathbf{A}$ is strictly lower triangular, it is clear that the stability function (3.41) would be a polynomial of the form

$$R(z) = 1 + z + \frac{z}{2!} + \ldots + \frac{z}{p} + O(z^{p+1}) \tag{3.42}$$

where p is the order of the method.

This means Explicit Runge-Kutta methods will always have bounded stability regions, therefore any explicit Runge-Kutta method would be A-stable, this is an undesirable characteristic for integrating stiff ODEs and DAEs.

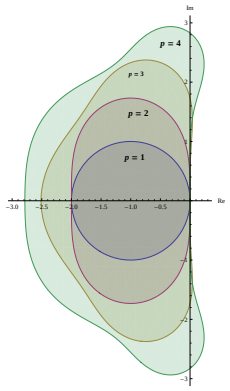

Figure 3.2: Stability Domain for Explicit Runge-Kutta Mehtods of order p

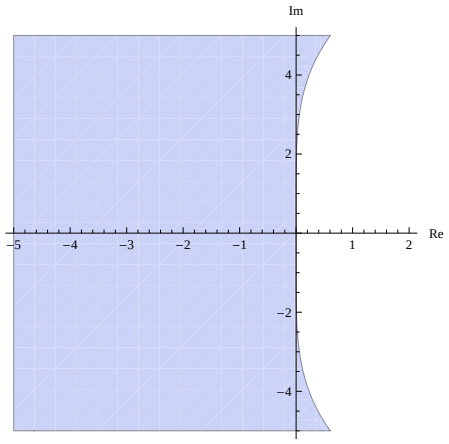

Figure 3.3: Radau IIA Stability Domain ($p = 5,\ s = 3$)

Implicit Runge-Kutta Stability Domain Implicit Runge-Kutta methods is the opposite case, as their stability function is rational, its stability domain is not necessarily bounded. The famous RadauIIA method based on the Radau quadrature, implemented by Hairer et al. and discussed in several books and articles [4, 80, 84, 85] is probe of an A-stable and stiffly accurate 3 stages and order 5 method. It's Tableau is:

$$\begin{array}{c|ccc} \frac{4-\sqrt{6}}{10} & \frac{88-7\sqrt{6}}{360} & \frac{296-169\sqrt{6}}{1800} & \frac{-2+3\sqrt{6}}{225} \\ \frac{4+\sqrt{6}}{10} & \frac{296+169\sqrt{6}}{1800} & \frac{88+7\sqrt{6}}{360} & \frac{-2-3\sqrt{6}}{225} \\ 1 & \frac{16-\sqrt{6}}{36} & \frac{16+\sqrt{6}}{36} & \frac{1}{9} \\ \hline & \frac{16-\sqrt{6}}{36} & \frac{16+\sqrt{6}}{36} & \frac{1}{9} \end{array} \tag{3.43}$$

and its stability domain is shown in Figure 3.3.

Implicit Runge-Kutta are ideal for the integration of stiff ODEs and DAEs due to its strong stability properties, but they still present the order reduction phenomenon.

3.2.4 Numerical Solution of Index 1 DAEs by Runge-Kutta Methods

Considering the differential-algebraic system

$$\begin{aligned} y' &= f(y,z) \\ 0 &= g(y,z) \end{aligned} \tag{3.44}$$

where f and g are sufficiently differentiable. System (3.44) is an index 1 problem only if

$$\left\|(g_z(y,z))^{-1}\right\| \leq M \tag{3.45}$$

in a neighborhood of the exact solution, also consistent initial values y_0, z_0 are assumed for system .

Solution of the equivalent ordinary differential equation

Condition (3.45) implies that in a neighborhood of the solution the second equation in system (3.44) can be formally transformed into $z = G(y)$ by the implicit function theorem, so that system (3.44) becomes

$$y' = f(y, G(y)) \tag{3.46}$$

It is possible to apply an arbitrary (explicit or implicit) Runge-Kutta method to equation (3.46) and to determine the z-component by $z_n = G(y_n)$. This is equivalent to solve the system

$$\mathbf{Y} = \mathbf{e} \otimes y_n + h(\mathbf{A} \otimes \mathbf{I})\mathbf{Y}' \tag{3.47}$$

$$y_{n+1} = y_n + h(\mathbf{b}^T \otimes \mathbf{I})\mathbf{Y}' \tag{3.48}$$

where

$$\mathbf{Y}' = f(\mathbf{Y}, \mathbf{Z}) \tag{3.49}$$

$$0 = g(\mathbf{Y}, \mathbf{Z}) \tag{3.50}$$

and z_{n+1} is given by

$$0 = g(y_{n+1}, z_{n+1}) \tag{3.51}$$

In this case all the classical results about the order, convergence and asymptotic expansions of the Runge-Kutta methods hold [4].

The direct approach

Solve the equivalent differential equation approach does not correspond to the definition of the method given in equations (3.21) and (3.22), for which formulas (3.47),(3.48),(3.49) and (3.50) hold but (3.51) is replaced by

$$z_{n+1} = z_n + h(\mathbf{b}^T \otimes \mathbf{I})\mathbf{Z}' \tag{3.52}$$

$$\mathbf{Z} = \mathbf{e} \otimes z_n + h(\mathbf{A} \otimes \mathbf{I})\mathbf{Z}' \tag{3.53}$$

Relation (3.53) defines $\mathbf{Z}'$ uniquely if the Runge-Kutta matrix $\mathbf{A}$ is invertible, which will be assumed since now on.

Convergence

For both approaches the y-component of the numerical solution can be interpreted as the numerical result for the ordinary differential equation (3.46). Therefore the following result always hold

$$y_n - y(x_n) = O(h^p) \tag{3.54}$$

where y_n is the exact solution, $y(x_n)$ is the approximated solution by a Runge-Kutta method and p is the classical order of the Runge-Kutta method. The same convergence result is also obtained for the z-component in the equivalent ODE approach, because $z_n - z(x_n) = G(y_n) - G(y(x_n)) = O(h^p)$.

For the convergence of the z-component in the direct approach, the condition $C(q)$, defined in as the algebraic condition (3.25), becomes important. The limit of the stability function as tends to ∞ plays a decisive role for differential algebraic equations. For invertible $\mathbf{A}$ it is given by

$$R(\infty) = 1 - \mathbf{b}^T \mathbf{A}^{-1} \mathbf{e} \tag{3.55}$$

The following theorem's respective probe can be found in [4].

Theorem 3.1 (Hairer et al.)**.** *Suppose that the condition* (3.45) *holds in a neighborhood of the solution* $(y(x), z(x))$ *of system* (3.44)*, and that that the initial values are consistent. Consider the Runge Kutta method defined by formulas* (3.47) *and* (3.48) *of classical order* p*, satisfying C(q), with* $p \geq q + 1$ *and having invertible coefficient matrix* $\mathbf{A}$

1. *If* b_i =a_{si} *for all* i*, the the global error for the* z*-component satisfies for* $x_n = nh \leq Const$

$$z_n - z(x_n) = O(h^p)$$

2. *If* $-1 \leq R(\infty) < 1$ *then*

$$z_n - z(x_n) = O(h^{q+1})$$

3. *Ir* $R(\infty) = 1$ *then*

$$z_n - z(x_n) = O(h^q)$$

4. *If* $|R(\infty)| > 1$ *then the numerical solution diverges.*

3.3 Implementable Implicit Runge-Kutta Methods

The implicit nature of the this methods, requires the solution of an algebraic system for every step. For an s-stage method applied to an N-dimensional problem (N is the sum of algebraic and differential states for DAEs), there are sN unknowns to evaluate and these satisfies sN equations. If f and therefore g are nonlinear, then the large system of equations to be solved is non-linear. However there are linear parts of it, and it may be possible to exploit this in the numerical solution.

A typical simplification to the solution of this kind of systems is to use the simplified newton approach. The application of a Runge-Kutta method to an index one semi-explicit DAE with N differential states and M algebraic estates, leads to the non linear system:

$$\mathbf{Y} - \mathbf{e}_s \otimes y_n - h(\mathbf{A} \otimes \mathbf{I_N}) f(\mathbf{Y}, \mathbf{Z}) = 0 \tag{3.56}$$

$$g(\mathbf{Y}, \mathbf{Z}) = 0 \tag{3.57}$$

If $\begin{pmatrix} \mathbf{Y} - \mathbf{e}_s \otimes y_n \\ \mathbf{Z} - \mathbf{e}_s \otimes z_n \end{pmatrix}$ is substituted by $\mathbf{\Gamma} = \begin{pmatrix} \Gamma_1 \\ \Gamma_2 \end{pmatrix}$ then the jacobian of the system at $\mathbf{\Gamma} = 0$ is

$$\begin{pmatrix} (\mathbf{I}_s \otimes \mathbf{I}_N) - h\mathbf{A} \otimes f_y & -h\mathbf{A} \otimes f_z \\ \mathbf{I}_s \otimes g_y & \mathbf{I}_s \otimes g_z \end{pmatrix} \tag{3.58}$$

which leads to the newton iteration

$$\begin{pmatrix} (\mathbf{I}_s \otimes \mathbf{I}_N) - h\mathbf{A} \otimes f_y & -h\mathbf{A} \otimes f_z \\ \mathbf{I}_s \otimes g_y & \mathbf{I}_s \otimes g_z \end{pmatrix} \Delta\mathbf{\Gamma} = \begin{pmatrix} -\Gamma_1 + h(\mathbf{A} \otimes \mathbf{I}_N) f(\mathbf{\Gamma}) \\ -g(\mathbf{\Gamma}) \end{pmatrix} \tag{3.59}$$

with

$$\mathbf{\Gamma}^{k+1} = \mathbf{\Gamma}^k + \Delta\mathbf{\Gamma} \tag{3.60}$$

The cost measured solely in terms of linear algebra costs, divides into two components. First, the factorization o the jacobian carried from time to time in the computation costs a small

multiple of of $s^3(N+M)^3$ floating point operations. Secondly the back substitution for the solution of equation (3.59) costs a small multiple of $s^2(N+M)^2$.
Implementable Runge-Kutta aim to lower the factors s^3 in the occasional part of the cost and to lower the factors s^2 in the per iteration parts of the cost.

3.3.1 Diagonally Implicit Runge-Kutta Methods

Becuase the cost in evaluating the stages in a fully implicit Runge-Kutta method, Alexander [86] developed the Diagonally Implicit Runge-Kutta methods or DIRK. For this methods $\mathbf{A}$ has a lower triangular structure with equal elements on the diagonal, the computational advantage of this methods is that the stage can be evaluated sequentially rather than as one big implicit system.
Results of the implementation of this methods to singulary perturbed problems and the development of diagonally singly implicit methods with explicit first stage, were treated in [87] with very interesting results, also important numerical analysis results were published on about "**DIRK**" methods on [88], this methods use the embedded Runge-Kutta approach for error estimations, which is not the case in the RadauIIA implemented in the code Radau5 by Hairer et al. [4, 80, 84, 85]

3.3.2 Singly Implicit Runge-Kutta Methods

For large dimensional systems LU decomposition and backsubstitution have big computational costs[2]. In order to overcome this difficulties, Butcher [89] proposed to reduce the computational cost by using the jordan canonical form of $\mathbf{A}$ instead of $\mathbf{A}$ in the newton iteration. That is for any $\mathbf{A}$ matrix, there exists a nonsingular matrix $\mathbf{T}$ such that $\mathbf{T}^{-1}\mathbf{A}\mathbf{T} = \bar{\mathbf{A}}$. Because of this transformation called "Butcher transformation" the operations for the LU factorization will become proportional to dN^3, being d the number of distinct eigenvalues of $\mathbf{A}$, and the operations of the back substitution are reduced to sN^2 [79, 81, 90].
From this point of view it is clear to see that the biggest reduction in the computational costs occurs when the coefficient matrix $\mathbf{A}$ has one point spectrum. The factorization cost will then reduce to N^3. Method with this property are called "**SIRK**" (singly-implicit Runge-Kutta)

[2] Once simplified newton approach is used the major cost is not the evaluation of the jacobian but its LU decomposition and the solution of linear system in the newton iteration

methods.

"SIRK" Linear Transformations

First transformation to reduce the number of operations in LU decomposition was $\mathbf{T}^{-1}\mathbf{A}\mathbf{T} = \bar{\mathbf{A}}$ which applied to DAEs gives

$$\begin{pmatrix} (\mathbf{I}_s \otimes \mathbf{I}_N) - h\bar{\mathbf{A}} \otimes f_y & -h\bar{\mathbf{A}} \otimes f_z \\ \mathbf{I}_s \otimes g_y & \mathbf{I}_s \otimes g_z \end{pmatrix} \Delta\bar{\mathbf{\Gamma}} = \begin{pmatrix} -\bar{\Gamma}_1 + h(\bar{\mathbf{A}} \otimes \mathbf{I}_N)\bar{F} \\ -\bar{G} \end{pmatrix} \tag{3.61}$$

where

$$\Delta\mathbf{\Gamma} = \begin{pmatrix} (\mathbf{T} \otimes \mathbf{I}_N)\Delta\bar{\mathbf{\Gamma}}_\mathbf{1} \\ (\mathbf{T} \otimes \mathbf{I}_M)\Delta\bar{\mathbf{\Gamma}}_\mathbf{2} \end{pmatrix} \tag{3.62}$$

$$\bar{\Gamma}_1 = (\mathbf{T}^{-1} \otimes \mathbf{I}_N)\Gamma_1 \tag{3.63}$$

$$\bar{F} = (\mathbf{T}^{-1} \otimes \mathbf{I}_N)F \tag{3.64}$$

$$\bar{G} = (\mathbf{T}^{-1} \otimes \mathbf{I}_M)G \tag{3.65}$$

Transformation matrix $\mathbf{T}$ causes high operation cost and it has to be made into a lower triangular matrix by the transformation $\mathbf{T} = \mathbf{U}\mathbf{L}$ this implies

$$\mathbf{U}^{-1}\mathbf{A}\mathbf{U} = \hat{\mathbf{A}} \tag{3.66}$$

With this the new newton iteration is:

$$\begin{pmatrix} (\mathbf{I}_s \otimes \mathbf{I}_N) - h\hat{\mathbf{A}} \otimes f_y & -h\hat{\mathbf{A}} \otimes f_z \\ \mathbf{I}_s \otimes g_y & \mathbf{I}_s \otimes g_z \end{pmatrix} \Delta\hat{\mathbf{\Gamma}} = \begin{pmatrix} -\bar{\Gamma}_1 + h(\hat{\mathbf{A}} \otimes \mathbf{I}_N)\hat{F} \\ -\hat{G} \end{pmatrix} \tag{3.67}$$

where

$$\Delta\mathbf{\Gamma} = \begin{pmatrix} (\mathbf{U} \otimes \mathbf{I}_N)\Delta\hat{\mathbf{\Gamma}}_\mathbf{1} \\ (\mathbf{U} \otimes \mathbf{I}_M)\Delta\hat{\mathbf{\Gamma}}_\mathbf{2} \end{pmatrix} \tag{3.68}$$

$$\hat{\Gamma}_1 = (\mathbf{U}^{-1} \otimes \mathbf{I}_N)\Gamma_1 \tag{3.69}$$

$$\hat{F} = (\mathbf{U}^{-1} \otimes \mathbf{I}_N)F \tag{3.70}$$

$$\hat{G} = (\mathbf{U}^{-1} \otimes \mathbf{I}_M)G \tag{3.71}$$

Where $\hat{\mathbf{A}}$ is a lower triangular matrix with one single diagonal element.
Making $\mathbf{M} = \lambda\hat{\mathbf{A}}^{-1}$, and multiplying equation (3.67) by $\mathbf{M}$ gives

$$\begin{pmatrix} (\mathbf{M}\otimes\mathbf{I}_N) - h\lambda(\mathbf{I}_s\otimes f_y) & -h\lambda\mathbf{I}_s\otimes f_z \\ \mathbf{I}_s\otimes g_y & \mathbf{I}_s\otimes g_z \end{pmatrix} \Delta\hat{\mathbf{\Gamma}} = \begin{pmatrix} -\tilde{\Gamma}_1 + h\lambda(\mathbf{I}_s\otimes\mathbf{I}_N)\hat{F} \\ -\hat{G} \end{pmatrix} \quad (3.72)$$

where

$$\tilde{\Gamma}_1 = (\mathbf{M}\otimes\mathbf{I}_N)\hat{\Gamma}_1 \quad (3.73)$$

$$(3.74)$$

3.4 Efective Order Singly Implicit Runge Kutta Methods

SIRK with $s \geq 3$ possess the undesirable property that some of their abscissae, because of the A-stability requirement, lie outside the integration inteval. One solution to this problem was to use extra stages, but this add implementation disadvantages, instead of this Butcher and Chartier [91] applied a concept used to overcome the well known butcher barrier called effective order and they created effective order SIRK. by adopting the more general definition of order, "efective order", these new methods allow more freedom in the choice of their parameters without loosing the high stage order property.

3.4.1 Effective Order

In order to overcome the famous difficulty shown in the following theorem, Butcher introduced "effective order"

Theorem 3.2. *When $s \geq 5$, no s-stage explicit Runge-Kutta method can attain order s.*

This is the well-known "Butcher barrier" . With the aid of th is new interpretation of order, Butcher was able to construct 5-stage explicit Runge-Kutta methods which were of order 5. In that design, two different 5-stage explicit Runge-Kutta methods of order 3 are used to integrate the first step and the final step respectively, and a 5-stage explicit method of order 4 is used to integrate the remaining $n-2$ steps (if total integration steps are n). It turns out that after this combination, the final output numerical solution will be of order 5. [81]

When any Order p numerical method is used to integrate a differential equation $y'(x) = f(y(x))$ the local error is

$$y(x_n) - y_n = O(h^{p+1}) \tag{3.75}$$

If the function $\phi(y(x_{n-1}))$ is used to represent the numerical solution obtained using a method after the first step then the above equation can be written as

$$y(x_{n-1} + h) - \phi(y(x_{n-1})) = O(h^{p+1}) \tag{3.76}$$

Similarly if ψ and ϕ are assumed as the mappings associated with a starting method and an effective order p method respectively, then from the definition of effective order:

$$y(x_{n-1} + h) - \psi^{-1}(\phi(\psi(y(x_{n-1})))) = O(h^{p+1}) \tag{3.77}$$

this leads to the following definition,

Definition 3.4. *A method is said to have effective order p at x_n, if it satisfies*

$$\psi(y(x_{n-1} + h)) - \phi(\psi(y(x_{n-1}))) \tag{3.78}$$

where ψ and ϕ are the mappings associated with the starting method and the method itself.

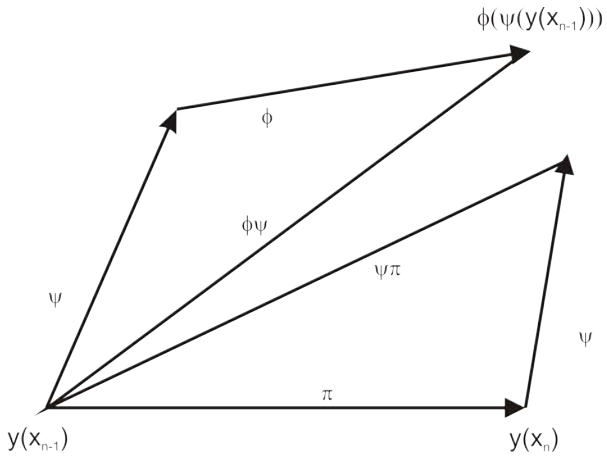

Figure 3.4: Effective order method ϕ and the starting method ψ

From this definition the "exact solution" at x_n for an effective order method ϕ can be treated as the perturbation using the starting method ψ at x_n. this is illustrated on figure 3.4.
Any effective order integration has to have an stating method for the first and the last steps and an effective order method which integrates the $n - 2$ steps, if n is the number of steps in the integration.

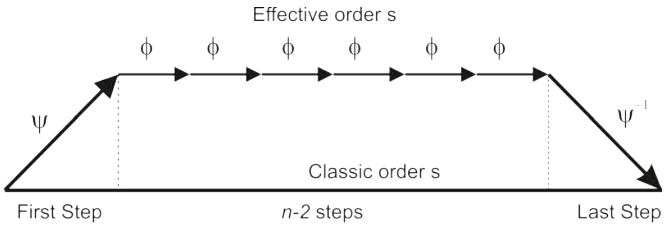

Figure 3.5: Integration procedure for effective order methods

3.4.2 Effective order of Runge-Kutta methods

The classical order SIRK methods have restrictions in their abscissae because they are collocation methods, collocation method's abscissae is restricted to be formed from Laguerre's polynomials zeros [79, 81], for which the L-stability requirement dictates that the some values of theabscissae c_i would lie outside the integration interval."Effective order" definition frees the abscissae from its restriction by defining the expansion of the exact solution $\psi(y(x_{n-1}))$ around x_{n-1} as a weighted Taylor series

$$y(x_{n-1}) + \alpha_1 h y(x_{n-1}) + \alpha_2 h y''(x_{n-1}) + \ldots + \alpha_s h y^{(s)}(x_{n-1}) \tag{3.79}$$

Hence, s free parameters are introduced. With this s parameters, the abscissae c_i can be chosen freely as long they are distinct. For conviniece the following notation is given

$$B_{s,h}(\alpha, y(x_{n-1})) = y(x_{n-1}) + \alpha_1 h y(x_{n-1}) + \alpha_2 h y''(x_{n-1}) + \ldots + \alpha_s h y^{(s)}(x_{n-1}) \tag{3.80}$$

where $y(x_{n-1})$ is the exact solution at the n-th step and $\alpha = [\alpha_1, \alpha_2, \ldots, \alpha_s]^T \in \mathbb{R}^s$. $B_{s,h}(\alpha, y(x_{n-1}))$ will be called the "Butchered Solution". The definition of a SIRK method which has effective order s can now be given.

Definition 3.5. *An s-stage SIRK method is said to have effective order s at x_{n-1} if it satisfies*

$$B_{s,h}(\alpha, y(x_{n-1})) - \phi(B_{s,h}(\alpha, y(x_{n-1}))) = O(h^{s+1}) \tag{3.81}$$

where ϕ is the associated mapping of the method.

the procedure to obtain effective order singly implicit methods or ESIRK from a chosen abscissae vector $\mathbf{c}$ can be found in chapter 4 of [81], with its respective deduction.

3.4.3 Variable stepsize for ESIRK methods and their stability

Stepsize selection is crucial to the starting method and the method itself, not only for convergence reasons but for precision. Many integration problems require variable stepsize because the numerical behavior change along the integration region, the error will change with it, augmenting the local error and affecting the error propagation. However representative difficulties arise when variable stepsize is used for effective order methods.
When definition 3.5 is interpreted, it is taken for granted that the same stepsize h is used for

1. The perturbation of the incoming approximation $B_{s,h}(\alpha, y(x_{n-1}))$.
2. the step represented by ϕ_h.
3. the stepsize expected in the following step.

In order to have a new stepsize (say rh) the ESIRK method need to be built to have an approximation of the butchered solution $B_{s,rh}(\alpha, y(x_{n-1}+h))$ so the step size can be changed repitedly, this is achieved by the derivation of a new vector b as a function of the stepsize changing ratio r. the deduction and procedure to achieve this in a ESIRK is given in [81].
The final result is a ESIRK in function of the stepsize changing ratio, this affects the stability of the method under successive stepsize changes, this is mainly because the stability function of a Runge-Kutta method always depends on b, then a stability function depending on r and z must be derived in order to study the stability of the method

Theorem 3.3 (Chen and Butcher)**.** *For an s stage ESIRK method, if the stepsize for the present step and the next step are h and rh respectively, then the stability function $\widehat{R}(z,r)$ for the step is*

$$\widehat{R}(z,r) = \frac{P(z,r)}{(1-\lambda z)^s} \tag{3.82}$$

where

$$P(z,r) = \frac{(1-\lambda z)^s \exp z\phi(rz)}{\phi(z)} + O(z^{s+1}) \tag{3.83}$$

and

$$\phi(z) = 1 + \alpha_1 z + \alpha_2 z^2 + \ldots + \alpha_s z^s \tag{3.84}$$

moreover, as the step changing occurs in two successive steps the stability function is

$$\widehat{R}_2(z,r) = \widehat{R}(z,r)\widehat{R}(rz),\frac{1}{r}) = \frac{P(z,r)}{(1-\lambda z)^s}\frac{P(rz,\frac{1}{r})}{(1-\lambda z)^s} \tag{3.85}$$

Applying the E-polynomial criteria, Chen [81] investigated the stability A stability of several abscissae vectors some of its result are listed in the following table:

Table 3.1: r-intervals for A-stability of ESIRK

s	Abscissae	r-interval
2	$[3-2\sqrt{2},1]$(SIRK)	$(0,\infty)$
2	$[0,1]$	$[.355047, 2.81653]$
2	$[\frac{7-4\sqrt{2}}{3},1]$	$[0.235576, 4.24431]$
3	$[2.7415165, 0.1812222, 1]$(SIRK)	$(0,\infty)$
3	$[0,\frac{1}{2},1]$	$[0.444787, 2.24827]$
3	$[0,\frac{1}{5},1]$	$[0.559114, 1.78855]$
4	$[0,\frac{1}{3},\frac{2}{3},1]$	$[0.368532, 2.71347]$
4	$[-1,0,0.5,1]$	$[0.378442, 2.64472]$
5	$[0,\frac{1}{4},\frac{1}{2},\frac{3}{4},1]$	$[0.707239, 1.41395]$
5	$[-1,-0.5-0,0.5,1]$	$[0.788534, 1.26818]$

Graphical representations of the domains of stability for $s=3,\ c=[0,\frac{1}{2},1]$ and $s=4,\ c=[0,\frac{1}{3},\frac{2}{3},1]$ can be seen on figure 3.6.

3.5 Implementation of ESIRK for DAEs

3.5.1 Error estimation

Error estimation is crucial for practical pourpuses. The concept of Richardson deferred approach to the limit can be used to estimate the local truncation error of any integration method but, specially for Implicit Runge-Kutta methods this is numericaly costly. Another very common way of error estimation is called "embedding", this error estimation used on Runge-Kutta methods consist in build another method $(A,\overline{b}^T,c)$ of order one higher, say $p+1$, if the original method (A,b^T,c) has order p, then the solutions obtained by the order $p+1$ and p are $\overline{y}_n$ and

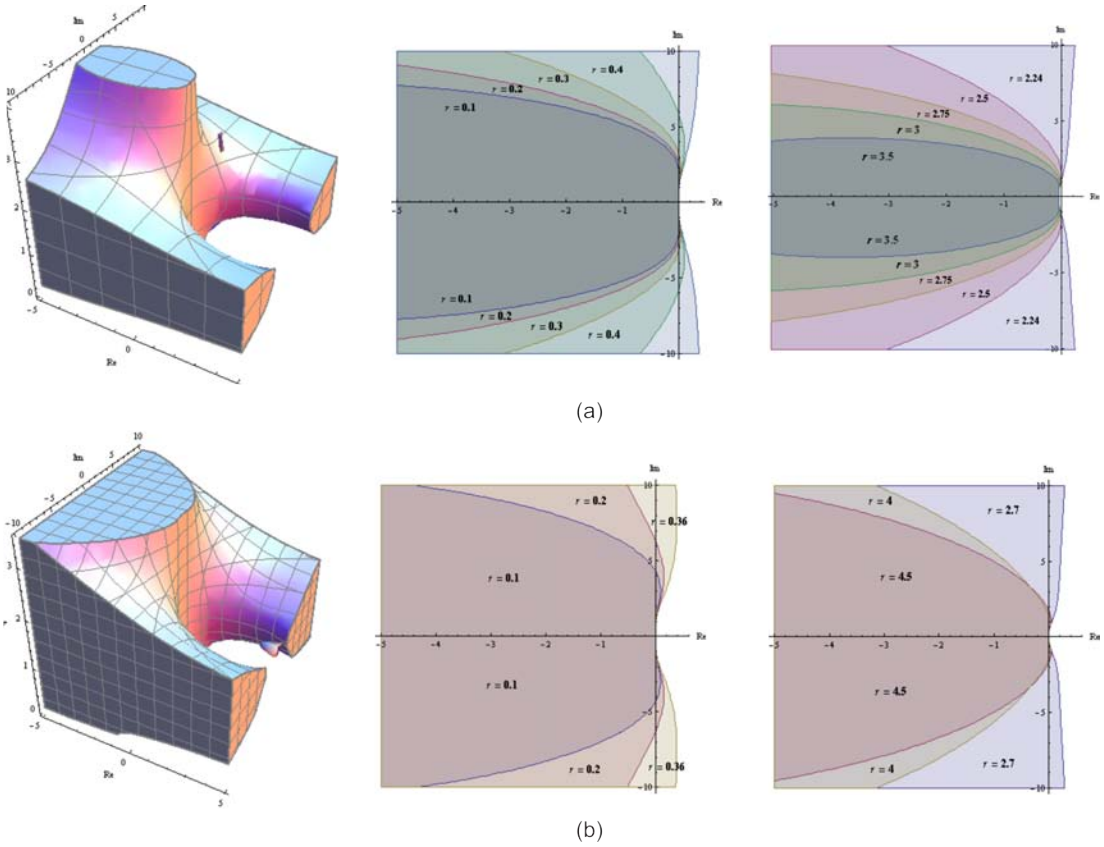

Figure 3.6: $s = 3$ and $s = 4$ ESIRK Stability Domains

y_n respectively then the local truncation error can be deducted as follows:

$$y(x_n) - y_n = \delta + O(h^{p+2}) \tag{3.86}$$

$$y(x_n) - \bar{y}_n = O(h^{p+2}) \tag{3.87}$$

$$\tag{3.88}$$

therefore the local error δ can be estimated by

$$\delta = \bar{y}_n - y_n + O(h^{p+2}) = h(\bar{b}^T - b^T)\mathbf{Y}' \tag{3.89}$$

Although DIRK or semi-implicit methods are built under "embedding" strategy, there is no need for this approach or for Richardson extrapolation in ESIRK methods, it is because it has the advantage that the stage order is equal to the number of stages that Nordsieck vector can be used for the purpose of estimating the local truncation error. Nordsiek vector can be approximated as follows form the previous stage derivatives form the $n - 1$ step of the integration

$$hF^{[n-1]} = (\mathbf{W} \otimes \mathbf{I}_n)\zeta^{[n-1]} + O(h^{s+1}) \tag{3.90}$$

where

$$\mathbf{W} = \begin{pmatrix} 1 & c_1 & \frac{c_1^2}{2} & \cdots & \frac{c_1^{s-1}}{(s-1)!} \\ 1 & c_1 & \frac{c_1^2}{2} & \cdots & \frac{c_1^{s-1}}{(s-1)!} \\ \vdots & \vdots & \vdots & \ddots & \vdots \\ 1 & c_s & \frac{c_s^2}{2} & \cdots & \frac{c_s^{s-1}}{(s-1)!} \end{pmatrix} \tag{3.91}$$

Nordsieck vector is

$$\zeta^{[n-1]} = \begin{bmatrix} hy'(x_{n-1}) \\ h^2y''(x_{n-1}) \\ \vdots \\ h^s y^{(s)}(x_{n-1}) \end{bmatrix} \tag{3.92}$$

and

$$hF = \begin{bmatrix} hf(Y_1) \\ hf(Y_2) \\ \vdots \\ hf(Y_s) \end{bmatrix} \tag{3.93}$$

This and the $C(s)$ condition allows the construction of the following error estimator

$$h^{s+1}y^{(s+1)} = \mathbf{e}_{s+1}^T(\widehat{\mathbf{W}} \otimes \mathbf{I_n})h\widehat{F}^{[n-1]} \tag{3.94}$$

where

$$\widehat{\mathbf{W}} = \begin{pmatrix} 1 & c_i - 1 & \frac{(c_i-1)^2}{2} & \cdots & \frac{(c_i-1)^s}{s!} \\ 1 & c_1 & \frac{c_1^2}{2} & \cdots & \frac{c_1^s}{s)!} \\ 1 & c_1 & \frac{c_1^2}{2} & \cdots & \frac{c_1^s}{s!} \\ \vdots & \vdots & \vdots & \ddots & \vdots \\ 1 & c_s & \frac{c_s^2}{2} & \cdots & \frac{c_s^s}{s!} \end{pmatrix} \tag{3.95}$$

s	C
2	0.04044011451988
3	0.02589708465063
4	0.02725898678972
5	0.00053004823515
6	0.00034135121283
8	0.00000268206244

Table 3.2: Absolute value of error constant for ESIRK methods

and $h\widehat{F}^{[n-1]} = [hf(Y_i^{[n-2]}, Z_i^{[n-2]}), hf(Y_1^{[n-1]}, Z_1^{[n-1]}), hf(Y_2^{[n-1]}, Z_2^{[n-1]}), \ldots, hf(Y_s^{[n-1]}, Z_s^{[n-1]})]$.
So it is possible to approximate the truncation error $h^{s+1}y^{(s+1)}$ as long as $c_i - 1 \neq c_j,\ \forall j$
This local error estimation is only good if the stepsize hasn't changed in two consecutive steps, which is restrictive for a variable stepsize method, thats why using

$$h^s y^{(s)}(x_n) - h^s y^{(s)}(x_{n-1}) = h^{s+1} y^{(s+1)}(x_n) + O(h^{s+2}) \tag{3.96}$$

yields to the following theorem

Theorem 3.4. *For an s-stage ESIRK method with distinct abscissae $c_1, c_2, \ldots, c_s$, suppose δ_1 and δ_2 satisfy*

$$\delta_1 = \left(\frac{h}{r}\right)^s y^{(s)}(x_{n-2}) + O(h^{s+1}), \qquad \delta_2 = h^s y^{(s)}(x_{n-1}) + O(h^{s+1}) \tag{3.97}$$

where r is defined as the stepsize change ratio $r = \frac{h_{new}}{h_{old}}$. then the principal local truncation error is given by

$$Ch^{s+1}y^{s+1}(x_n) = C\frac{sr}{s + (r-1)\sum_{i=1}^{s} c_i}(\delta_2 - r^s\delta_1) + O(h^{s+2}) \tag{3.98}$$

and C is the associated error constant.

δ_1 and δ_2 have the form

$$\delta_1 = \sum_{i=1}^{s} \frac{h}{r} d_i f(Y_i^{[n-2]}, Z_i^{[n-2]}) \tag{3.99}$$

$$\delta_2 = \sum_{i=1}^{s} h d_i f(Y_i^{[n-1]}, Z_i^{[n-1]}) \tag{3.100}$$

and $\mathbf{d}$ can be estimated using

$$\mathbf{d} = \mathbf{e}_s^T \mathbf{W}^{-1} \tag{3.101}$$

where $\mathbf{e}_s^T = [0, 0, \ldots, 1]_s$ and $\mathbf{W}$ is the modified Vandermond matrix.

3.5.2 Newton Iterations Convergence

When solving then nonlinear algebraic equations for Implicit Runge-Kutta methods, a good question to make is, When to stop the Newton iterations and accept the approximations of the iterations?. The way this question is answered affects greatly the efficient of a numerical implementation. It is hoped to obtain an expected accuracy in the solution at the lowest computational cost. This criteria has been studied widely as long with the stepsize control [79, 80, 92–95].

Suppose $T^{[n]}$ is the n-th Newton update during the iteration in a certain step, then the quantity

$$\Theta^{[n]} = \frac{\left\| T^{[n+1]} - T^{[n]} \right\|}{\left\| T^{[n]} - T^{[n-1]} \right\|} \tag{3.102}$$

is the convergence rate. If $\Theta^{[n]} > 1$, the iteration is not contracting and the iteration should be terminated. If τ is the expected error bound and its related to the desired accuracy ϵ in the solution, then the test for stopping the iteration is given by

$$\frac{\Theta}{1-\Theta} \left\| T^{[n+1]} - T^{[n]} \right\| \leq \tau \tag{3.103}$$

In general if the user defined tolerance $tol = \epsilon$, then $\tau = 0.1\ \epsilon$. For stiff problems relative tolerance $rtol$ and absolute tolerance $atol$ are recommended to be used as follows

$$\frac{\Theta}{1-\Theta} \left\| T^{[n+1]} - T^{[n]} \right\| \leq 0.1 \left(atol + \max_i(\|y_i\|) rtol \right) \tag{3.104}$$

where y_i denotes the i-th component of the numerical solution.

3.5.3 Estimation of the next stepsize

For robustness, a stepsize controller has to respond as smoothly as possible to abrupt changes in behavior. This means that the stepsize should not decrease or increase from one step to the next by an excessive ratio. Also, if the user-specified tolerance, given as a bound on the norm of the local truncation error estimate, is ever exceeded, recomputation and loss of performance will result. Hence, to guard against this as much as possible, a "safety factor" is usually introduced into the computation. If h is the estimated stepsize to give a predicted truncation error equal to the tolerance, then some smaller value, such as $0.9\ h$, is typically used instead. Combining all these ideas, we can give a formula for arriving at a factor r, to give a new stepsize rh, following a step for which the error estimate is est. The tolerance is written as tol, and it is assumed that this previous step has been accepted. The ratio r is given by [79]

$$r = \max\left(\alpha, \min\left(\beta, fac\left(\frac{tol}{\|err\|}\right)^{1/(s+1)}\right)\right) \tag{3.105}$$

where α and β are design factors associated with the A-stability domain of the ESIRK method, and fac is a safety factor.

3.6 Conclusions

By using the general definition of order "effective order" Butcher et al achieved to develop A-stable and numerically implementable Runge-Kutta methods that are perfect for integrating extremely stiff ODEs and DAEs up to differential order 2, because of its high stage order this methods deal with the order reduction in both ODEs and DAEs. The great problem with effective order methods comes when variable stepsize schemes are applied to it, this affects the error estimation and also the method itself, Butcher tableaus for constant and variable stepsize were derived using procedures in [81] and the can be found in Appendix B.

Chapter 4

Numerical Experiments and Bioreactor-Extractor Simulation

4.1 Preliminary Numerical Experiments

To test the accuracy and efficiency of the ESIRK implementation for DAEs, Two main test subjects were analyzed to see the behavior of the integrator on Index 1 semi-implicit DAE systems, this are the well known pendulum equation and the residue curve map, which is a direct application of physical equilibrium manifold restricted systems, used to describe ideal operations on chemical engineering.

4.1.1 The Pendulum

The simplest constrained mechanical system is the pendulum. The equations of motion of a point-mass m suspended at a massless rod of length l under the influence of a gravity g in cartesian coordinates (p, q) are

$$\dot{p} = u \tag{4.1}$$

$$\dot{q} = v \tag{4.2}$$

$$m\dot{u} = -p\lambda \tag{4.3}$$

$$m\dot{v} = -q\lambda - g \tag{4.4}$$

$$0 = p^2 + q^2 - l^2 \tag{4.5}$$

where (u, v) is the velocity and λ is the rod tension. This formulations is an index 3 DAE. Its

reduction to index one can be found in [4], and consist on replacing the equation (4.5) by

$$0 = m(u^2 + v^2) - gq - l^2\lambda \tag{4.6}$$

Numerical Simulations

Several successful numerical simulations were carried on for the pendulum differential index one DAE system, ESIRK methods of order 2,3,4 and 5 were used. The only restriction of this ESIRK methods was the value of $h = 0.01$ as the maximum stepize where the simplified newton algorithm and regular newton algorithm were convergent.

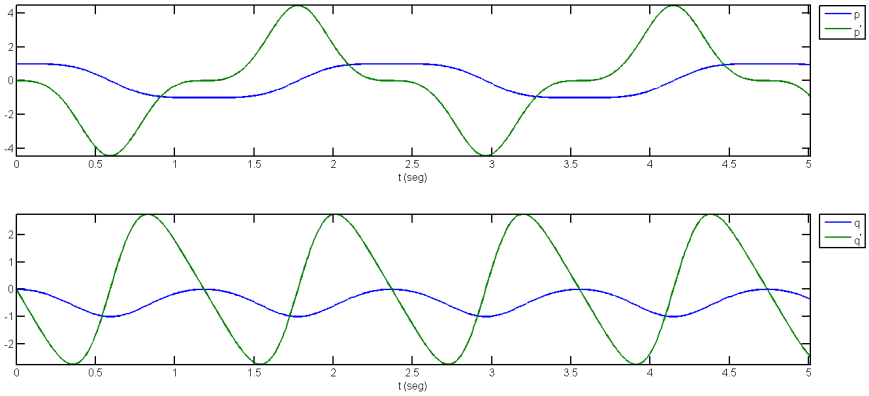

Figure 4.1: Numerical Simulation of the pendulum using ESIRK of order 5 with $h = 0.01$

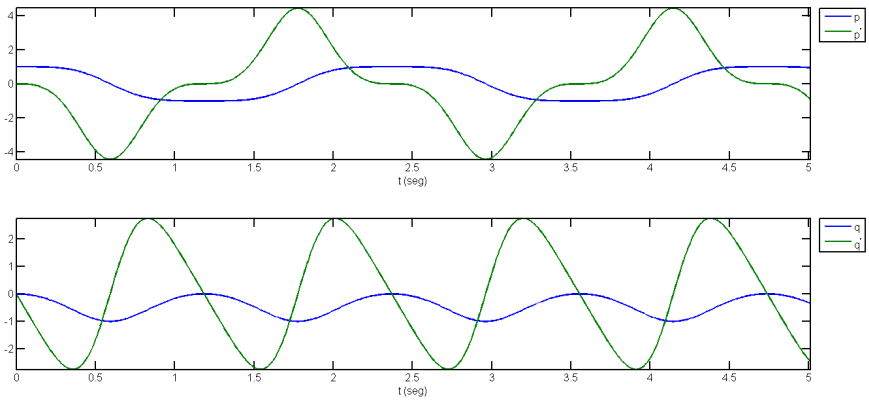

Figure 4.2: Numerical Simulation of the pendulum using ESIRK of order 3 with $h = 0.01$

Local Error Estimates in dependence of h

A good way to evaluate a numerical integration algorithm is to plot the behavior of the local error in dependence of h, here the maximum local error of 100 integration steps was plotted against the step of integration h.

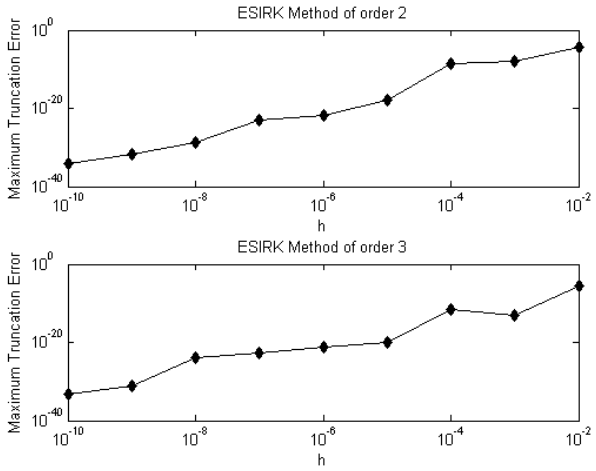

Figure 4.3: Maximum Truncation Error Behavior along 100 integration steps with different stepsizes h

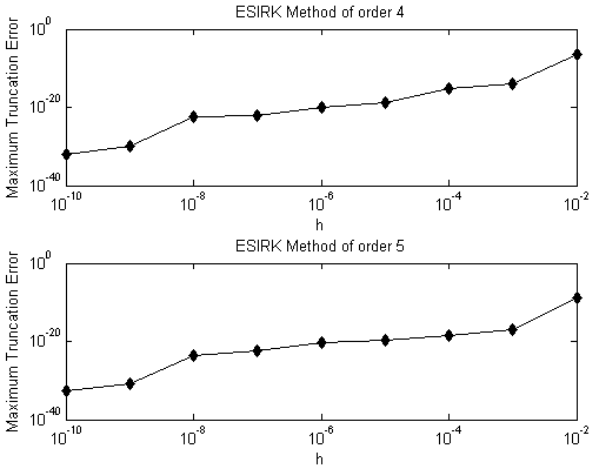

Figure 4.4: Maximum Truncation Error Behavior along 100 integration steps with different stepsizes h

4.1.2 Residue Curve Map

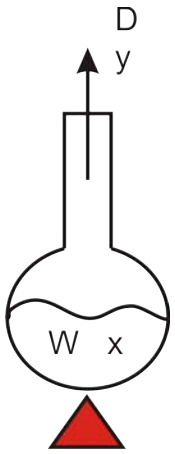

Figure 4.5: Residue curve map experimental set up

Residue curve maps are useful to know in advance to any kind of design the separation feasibility of a certain given mixture by distillation. Figure 4.5, Shows the residue curve map main idea. First it can be seen a heated vessel with mixture of some liquid components, total moles in the vessel are $W(t)$. As it is heated, the mixture evaporates, the vapor stream $D(t)$ goes to a Condenser and is turned again into liquid.Note than $W(t)$ is in molar units, and $D(t)$ is in

$mole/time$ units.

The molar percent of a liquid component will be noted as x with subscript i for an specific component of the mixture with c number of components, the molar percent of a vapor component will be noted as y with subscript i for an specific component,of a vapor mixture with c number of components. In order to obtain the Residue Curve DAE system is necessary to perform the material balance:

Global Material Balance

$$\frac{dW(t)}{dt} = -D(t) \tag{4.7}$$

This means that the evaporation rate ($\frac{dW(t)}{dt}$) of the whole liquid mixture in a time t is equal to the evaporation stream ($D(t)$) in a time t. The negative sign means that the total mass of the liquid mixture is decreasing in the vessel.

$i-th$ **component Material Balance**

$$\frac{d\left(W(t)\cdot x_i(t)\right)}{dt} = -D(t)\cdot y_i(t) \tag{4.8}$$

This means that the evaporation rate ($\frac{d(W(t)\cdot x_i(t))}{dt}$) in a time t of a component i is equal to the evaporated stream ($D(t)\cdot y_i(t)$) of the same component in a time t. The negative sign mean that component i in the liquid mixture is leaving the vessel in form of vapor.

Expanding the evaporation rate component mass balance leads to:

$$\frac{dW(t)}{dt}x_i(t) + \frac{dx_i(t)}{dt}W = -D(t)\cdot y_i(t) \tag{4.9}$$

Replacing (4.7) into (4.9) gives

$$\frac{W(t)}{dt}x_i(t) + \frac{dx_i(t)}{dt}W = \frac{dW(t)}{dt}\cdot y_i(t) \tag{4.10}$$

Canceling dt at both sides and reordering

$$dx_i(t) = \frac{dW(t)}{W}\cdot y_i(t) - \frac{dW(t)}{W}\cdot x_i(t) \tag{4.11}$$

replacing $-\frac{dW(t)}{W}$ of (4.11) by $-dln(W(t) = d\tau$ leads to the residue curve DAEs:

$$\frac{dx_i(\tau)}{d\tau} = x_i(\tau) - y_i(\tau) \tag{4.12}$$

This system is very useful in conceptual design of distillation towers because it is an idealization of a distillation column, and is possible based on its analysis to determine without much effort if a separation of a mixture by distillation is feasible [44]. As it can be seen there's no chemical reaction, and the algebraic constraints are not explicit yet. To make the algebraic constrains explicit is necessary to establish the thermodynamical relationship between the composition of a boiling liquid mixture component ($x_i(\tau)$) with its vapor composition:

$$x_i \cdot \gamma_i(\mathbf{x}, T) \cdot P_i^{SAT}(T) = y_i \cdot \phi_i(\mathbf{y}, t, P) \cdot P \tag{4.13}$$

where $P_i^{SAT}(T)$,γ_i and ϕ_i are the saturation pressure, activity and fugacity coefficients of the component i respectively, which are strong nonlinear functions of $\mathbf{y}, \mathbf{x}, T$ and P which are the vapor composition vector $\mathbf{y} = [y_1, y_2, \ldots, y_n]^T$, the liquid composition vector $\mathbf{x} = [x_1, x_2, \ldots, x_n]^T$, the temperature and the pressure of the thermodynamic system.

ϕ and γ computation is not a trivial step, this functions are intricate and there is no explicit solution for them.

Finally adding the thermodynamical equilibrium manifolds restriction and the percentage restrictions the DAE system for a c component mixture that only behaves as what is know as vapor liquid equilibrium, the following index one DAE is obtained

$$\frac{dx_i(\tau)}{d\tau} = x_i(\tau) - y_i(\tau) \tag{4.14}$$

$$x_i(\tau) \cdot \gamma_i(\mathbf{x}, T) \cdot P_i^{SAT}(T) - y_i(\tau) \cdot \phi_i(\mathbf{y}, T, P) \cdot P = 0 \tag{4.15}$$

$$\sum_{i=1}^{c} x_i(\tau) - \sum_{i=1}^{c} y_i(\tau) = 0 \tag{4.16}$$

$$1 - \sum_{i=1}^{c} x_i(\tau) = 0 \tag{4.17}$$

Numerical Simulation

For the integration of residue curve map equations, a well known study case has been selected, this is the Ethanol-Isobutylene-ETBE distillation [40, 45], where the Unifac Dortmund Activity Coefficient Model [72] and the PSRK model with adjusted α constants was chosen to be simple and accurate enough to predict the tricky vapor liquid equilibrium of this ternary thermodynamic system.

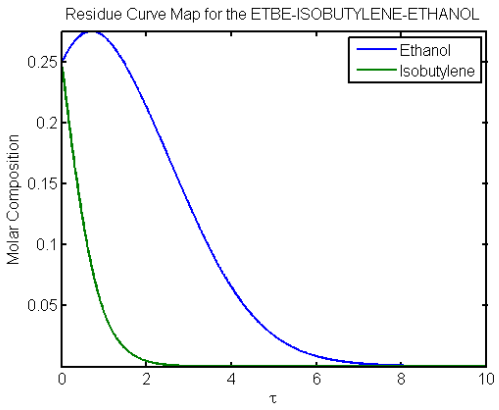

Figure 4.6: Numerical simulation of residue curve DAEs with ESIRK of order 2

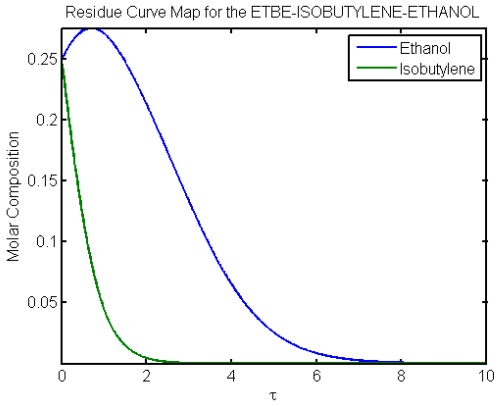

Figure 4.7: Numerical simulation of residue curve DAEs with ESIRK of order 4

Local Error Estimates in dependence of h

Also local error estimates in dependence of different h were calculated for the residue curve map problem, with excellent results.

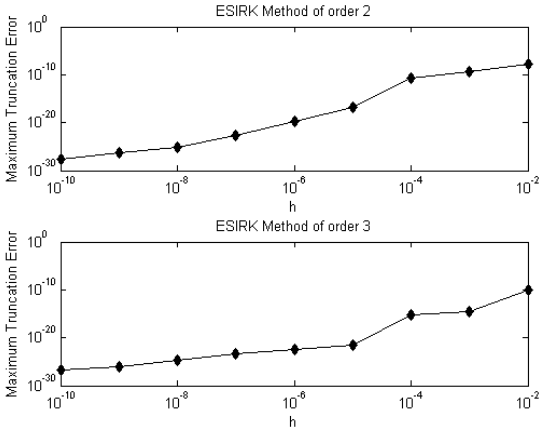

Figure 4.8: Maximum Truncation Error Behavior along 100 integration steps with different stepsizes h

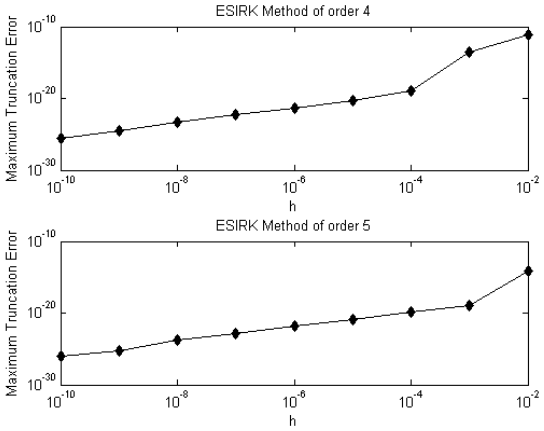

Figure 4.9: Maximum Truncation Error Behavior along 100 integration steps with different stepsizes h

4.2 Bioreactor Extractor Simulation

The bioreactor-extractor DAE system is more complicated to simulate than the previous examples, its differential index is two, this mean as stated in [4, 80] that the convergence of the simplified newton iteration will be slower and the restrictive h will randomly be under the restrictive value (0.01). The main advantage of ESIRK methods on the integration of DAEs of order at least two, is that the stage order is equal to the order of the method, this overcome the conventional Runge-Kutta order reduction for the algebraic and differential components of the DAE.

The selected parameters chosen for the numerical simulation were $N_0 = 120\, mol/day$, $N^T = 100\ mo$, and the feed parameter $R = x_{MeOH}/x_{Trig}$ was varied between 1 and 4.

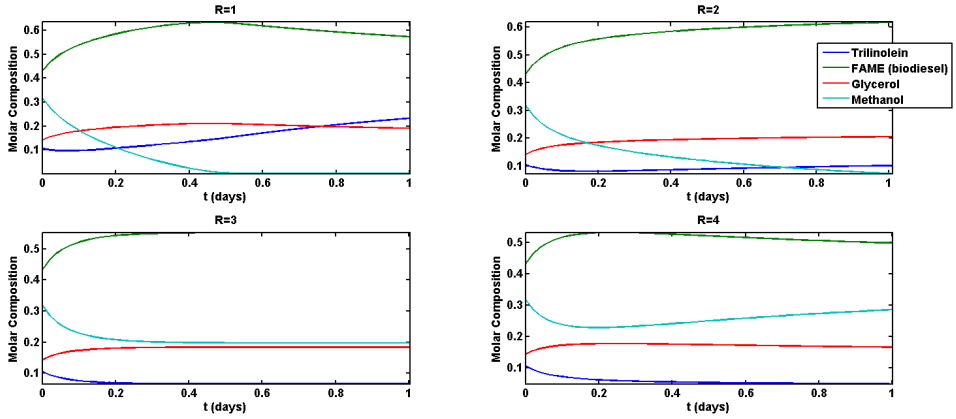

Figure 4.10: Simulation of the Bioreactor-Extractor under different feed ratios R

The simulations were carried on with a constant stepsize of $h = 0.01$, and local errors were about the order of $1E-6$. The sparsity pattern of both, the jacobian and its inverse on the newton iteration of the ESIRK method applied to this system in particular can be seen on Figures 4.12 and 4.13 respectively.

Local Error Estimates in dependence of h

Local error estimates of the ESIRK methods of different orders were calculated in dependence of the stepsize h (Figures 4.14 and 4.15), although the resulting truncation errors were not as low as with the index one systems of the pendulum and the residue curve maps, the always

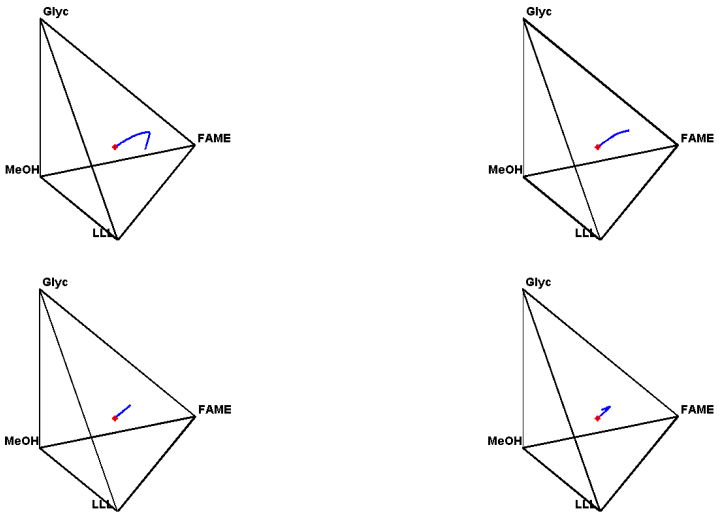

Figure 4.11: Phase plots of the simulations in Figure 4.10

decreasing tendency of the error as h decreases is good enough to show the ESIRK methods are appropriate for high accuracy integration of differential index two DAEs.

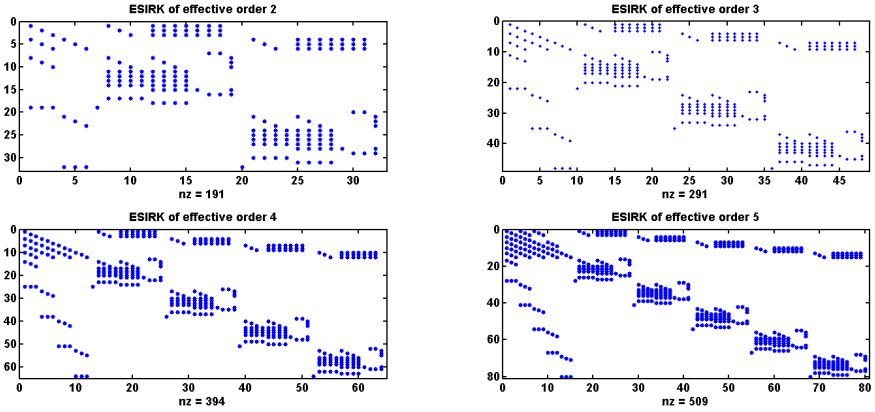

Figure 4.12: Sparsity pattern of the jacobian in the newton iteration

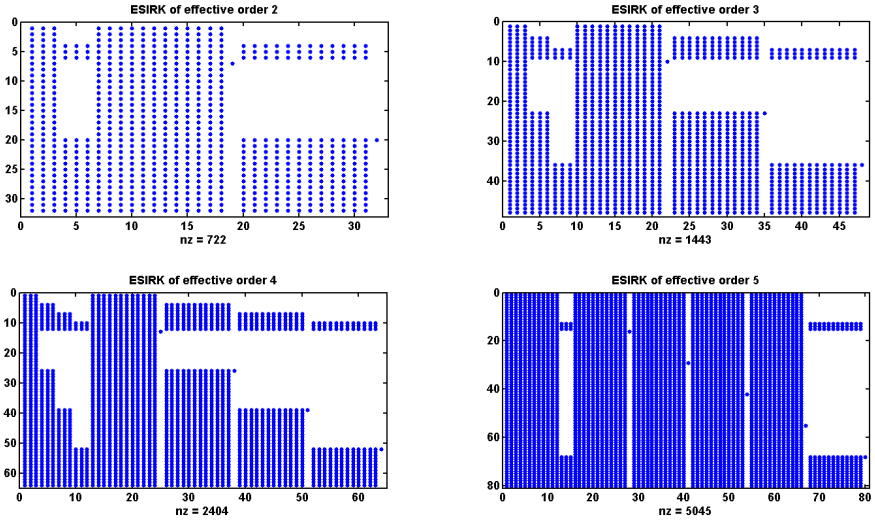

Figure 4.13: Sparsity pattern of the inverse of the jacobian in the newton iteration

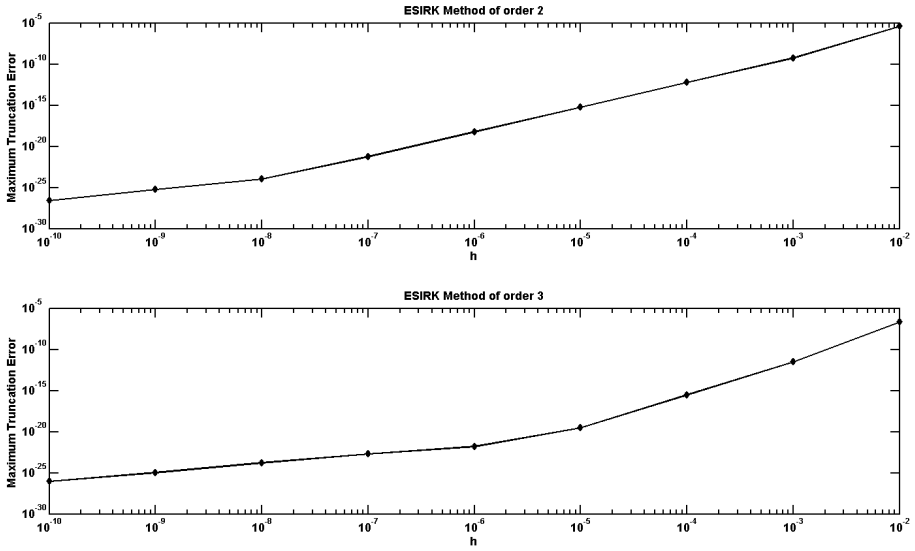

Figure 4.14: Local error estimtes in dependence of h for 500 integration steps

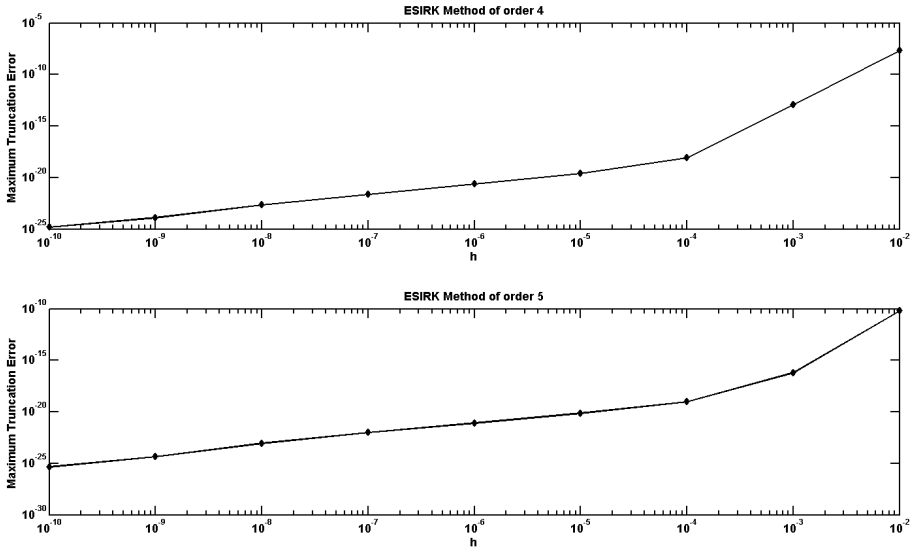

Figure 4.15: Local error estimtes in dependence of h for 500 integration steps

4.3 Conclusions

Although the restrictive stepsize of $h = 0.01$ is a difficulty to be solved in the future, ESIRK methods are really superior to conventional Implicit Runge-Kutta methods as RadauIIA, this can be deducted by the simple observation of Figure 4.16, where local error estimates in dependence of h for different pairs of methods were plotted.
Comparing the local errors achieved by ESIRK methods of orders 2,3,4 and 5 in common differential algebraic problems with the same errors reported in [4] for common implicit Runge-Kutta methods applied to the pendulum equation (Figure 4.16), many advantages can be seen:

- Higher Accuracy
- Monotonic decreasing error as stepsize h decreases
- Error behavior stability
- Lower cost on the Jacobian inversion, which for some problems compensates the restrictive stepsize $h = 0.01$ with the accuracy gained in comparison with traditional implicit Runge-Kutta schemes
- No order reduction due to the high stage order
- No need for an embedded Runge-Kutta scheme for error estimation
- Implementability

The main advantage for the bioreactor-extractor is accuracy. ESIRK methods are capable to integrate DAEs to order up to 2 with as much accuracy as needed, the high stage order guarantees high orders of convergence in the simplified newton iteration [4] and no order reduction for the error on algebraic and differential variables [80, 81].

Conventions for Figure 4.16

$\square$ Radau IIA ($s = 2$) and Radau IIA ($s = 3$)

$+$ SDIRK (see [88] for examples) and Radau IIA ($s = 3$)

$\times$ Lobatto IIIC ($s = 2$) and Lobatto IIIC ($s = 3$)

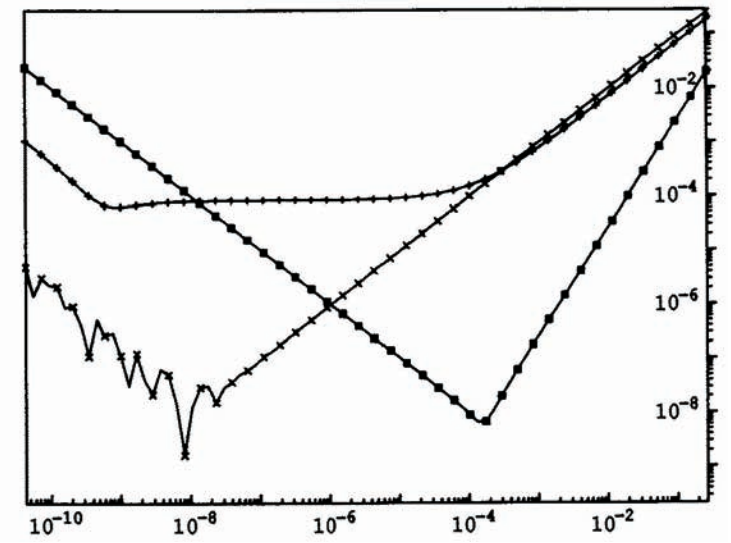

Figure 4.16: Local Error estimates in dependence of h from [4]

Chapter 5

Bioreactor-Extractor Analysis

...beware of mathematicians, and all those who make empty prophecies.
The danger already exists that the mathematicians have made a covenant
with the devil to darken the spirit and to confine man in the bonds of Hell.
Saint Augustine, De Genesi ad Litteram

5.1 Bioreactor Start Dynamics

The most important parameter to vary during the Bioreactor start is the relation of Reactants, noted as $R = \frac{x_{MeOH}}{x_{Trig}}$. Twelve simulation were done to determine a good reactants relation R, results can be seen on Figure 5.1 where the behavior of the reactants during the start phase was plotted for a time of 24 hours.

The most efficient starting R is 3, as it can be seen in the Figures 5.1 and 5.2, where almost all the reactants were consumed in less than 10 hours, giving the best conversion. From this simple analysis of the bioreactor extractor in the starting stage, derived from its simulation, the best theoretical reactant relation R has been selected.

5.1.1 Starting time

The determination of a good starting time for the bioreactor-extractor is important due to the possibility of reaching operation mode faster. A practical criteria to choose a good switching time is the change percent of the molar composition along time, if a threshold is selected to be the minimum change percent allowed during a period of time for the reactor to continue operating on batch mode, then a good switching time estimate can be selected to ensure a good reactants conversion along time.

It can be seen that the starting time should be less than 12 hours, after 12 hours of batch

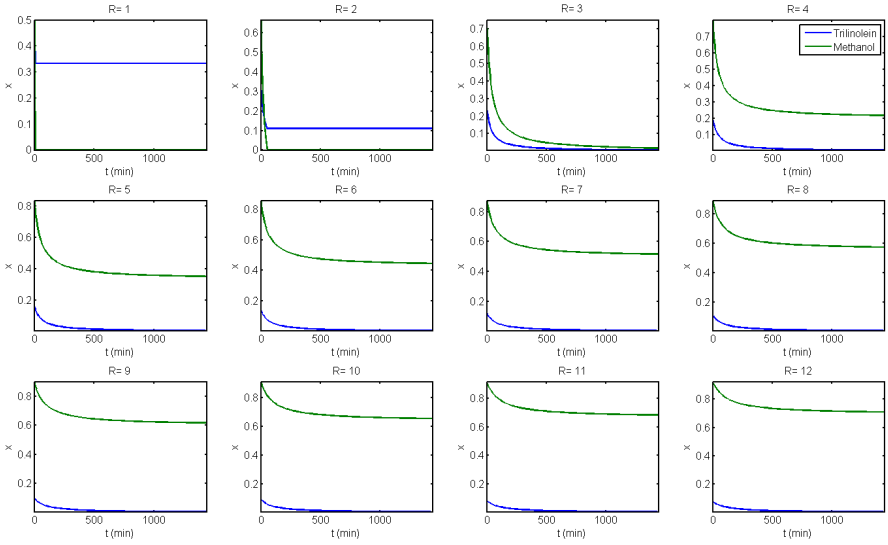

Figure 5.1: Start Dynamic behavior of the bioreactor varying parameter R

operation the percent of change in the biodiesel concentration is less than 5 % (Figure 5.3), also after 6 hours of operation no change over 10% in the biodiesel concentration is achieved, from there the changes in the Trilinolein conversion become less significative (i.e. a conversion of 10% is achieved after an hour of operation, after 6 hours to achive a change from 37.95% to 46.63% 3 hours are needed, see Figure 5.4). Using a threshold of 10% of change per hour in biodiesel production a reasonable switching time for the biorreactor extractor is 6 hours.

5.1.2 Bioreactor start and operational behavior

Figure5.5 shows how the reactor extractor behaves when it is switched from batch to operation (continue) mode. After the reactor is switched form batch (starting) to operation mode, it can be noted a drastic acceleration in the reaction rate that leads the bioreactor toward a steady state relatively fast, the stable steady state reached is a high conversion steady state, where the degree of separation between glycerol and FAME (biodiesel) is almost complete.

This result shows the feasibility of the continuous reaction-extraction technology, and the utility of shortcut methods and its dynamic extension to foresee the stability of a new process.

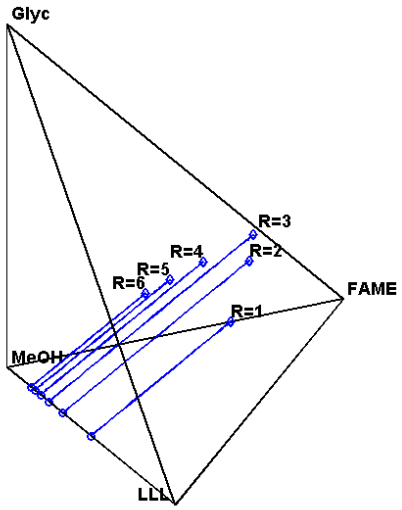

Figure 5.2: Batch Bioreactor phase plot varying the paramter R

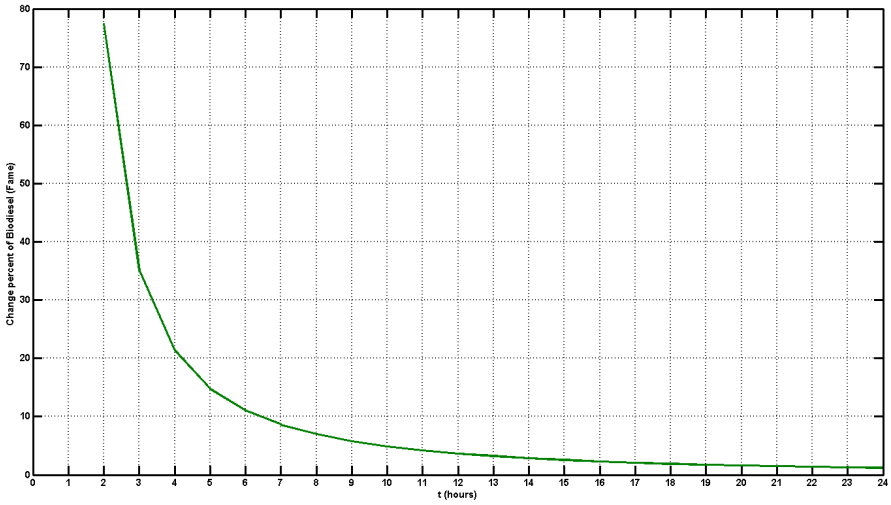

Figure 5.3: Percent of change of the biodiesel molar composition and reactive along time

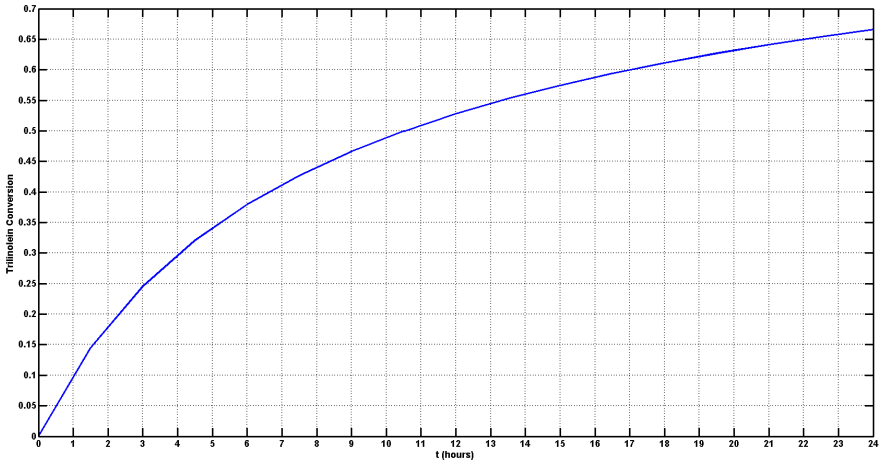

Figure 5.4: Conversion of Triolein for the batch operation stage

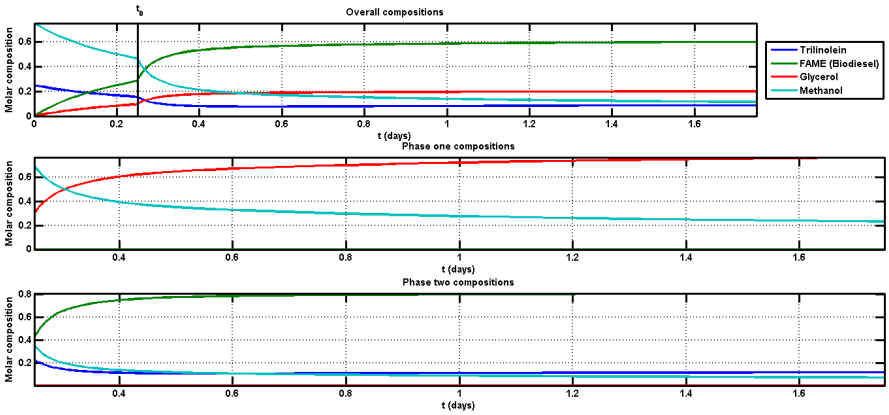

Figure 5.5: Biorreactor Start and operation mode switch at 6 hours

5.2 Biorreactor's Parametric Space Exploration

Bifurcation of differential-algebraic equations is a new field of study in mathematics, theres a general lack of articles, books and software dedicated to this new topic. This has difficulted the analysis of the bioreactor-extractor system, limiting its continuation and bifurcation search drastically, as the software and algorithms used to detect bifurcations tend to take into account the eigenvalues associated to algebraic states of the system. Singular perturbation theory was also discarded for this analysis as bifurcations were inducted by the variation of the singular perturbation parameter affecting the result and generating doubts about the real meaning of this

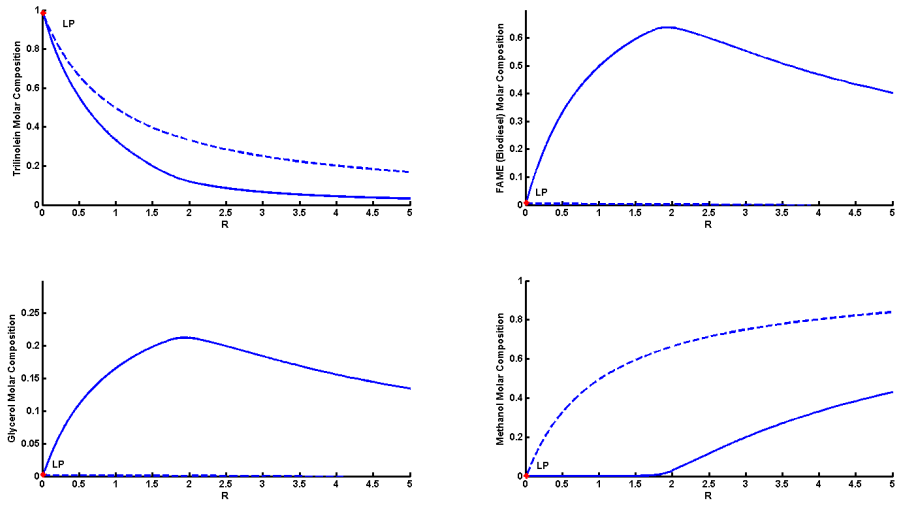

Figure 5.6: Bifurcation Diagram of the four differential states varying the parameter R

kind of bifurcations on an engineering analysis.

Therefore the bifurcation and stability analysis of this system was carried on using the implicit function theorem and basic numerical procedures based on newton and newton-like algorithms to infer the real stability of the three differential variables.

5.2.1 One Parameter Bifurcation Analisys

For the codimension one bifurcation analysis two independent design parameters were selected in order to obtain physically significant bifurcations, this parameters were the relation of reactives at the inlet of the reactor (R) and the reactor dilution rate ($D = \frac{N_0}{N^T}$) which are decisive control and design parameters.

Behavior under variations on Parameter R

Figure 5.6 show the behavior of the four differential sates as the parameter R is varied and D is fixed at 1.2. It is possible to observe the appearance of a Saddle-Node bifurcation joining the stable and the unstable equilibrium points of the bioreactor-extractor, this means that under normal reactions conditions the variation of R is possible in wide ranges, but operation of the reactor is not possible when R is under 0.011. The presence of a maximum biodiesel concentration at $R = 1.933$ show that the slightest perturbation in the reactor's feed would

affect the production negatively, which means that a disturbance rejection control might be necessary to ensure the reactor to be operating at as near as possible of his maximum.

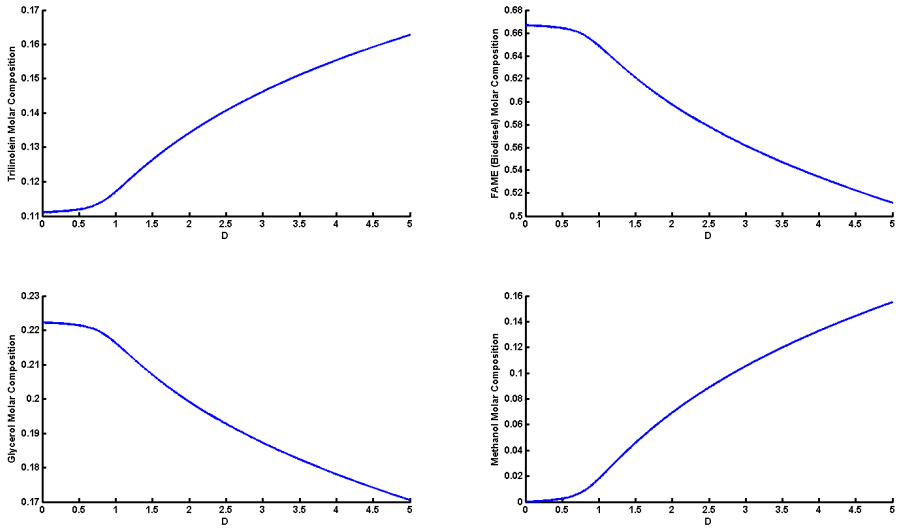

Figure 5.7: Bifurcation Diagram of the four differential states varying the parameter D

Behavior under variations on Parameter D

Figure 5.7 is a less less explicit on the behavior of the reactor than Figure 5.6 but still important conclusions cane be derived from its analysis. The Dilution rate of the reactor is another important design and control parameter that has to be taken into account, it can be associated with the reactor sizing, valve selection and with the control during the operation of the equipment. As a design parameter dilution rate is associated with the size of the reactor, when the dilution rate D decreases under 0.75 no appreciable change on the biodiesel concentration is observed, so the bioreactor sizes increases (for a desired production) but no significant benefits are obtained. As control parameter the implications are less severe because no instability could be generated from the variation of the dilution rate, but the decrease or increase of it should cause the decrease on the production or the decrease of the bioreactor-extractor efficiency.

Bioreactor-Extractor's Equilibrium Manifolds

Bioreactor-extractor's equilibrium manifold is the space region where the bioreactor reaches its physical and chemical equilibrium simultaneously, it differs from the physical and chemical equilibrium manifold because it takes into account the reaction kinetics which present dynamical phenomenons like inhibition and multiple stable solutions, that finally alters the equilibrium manifold. The use of the bioreactor's equilibrium manifold instead of the physical and chemical equilibrium manifold is a more realistic way to approaching bioreactor's design when the mass transfer rates are faster than the reaction kinetic rates (like the present case).

Figure 5.8 shows the behavior of the equilibrium manifold as R varies between 0 and 5, the most important characteristic that can be observed in this figure, is the Saddle-Node bifurcation meaning on physical equilibrium systems. As R reaches the bifurcation value of 0.011 the global composition values get closer to one of the phases compositions, and in the bifurcation point they become equal, this means the bioreactor global equilibrium composition touches the physical equilibrium manifold, no possible bioreactor operation can be achieved outside the physical equilibrium manifold, then the Saddle-Node bifurcation can be interpreted as the lowest R value were the reactor-extractor can operate or the point where the physical equilibrium manifold and the bioreactor's equilibrium manifold touch.

Bioreactor-extractor's global compositions are always restricted to be inside the physical equilibrium manifold, once they touch it, a bifurcation occurs due the impossibility of the bioreactor-extractor to operate outside the physical equilibrium manifold.

5.2.2 Two Parameter Operation Curve Analysis

As no codimension two bifurcations with physical meaning where found there was no possibility to perform a significant two parameter bifurcation analysis, therefore the analysis was done over the system's operation surfaces which are a very good source of information for further design and optimization.

Global, phase one and phase two compositions response surface analysis

The main phenomenon observed in this curves is the inhibition due to the methanol, as R and the molar composition of methanol at the inlet current in the reactor rises, the inhibition of

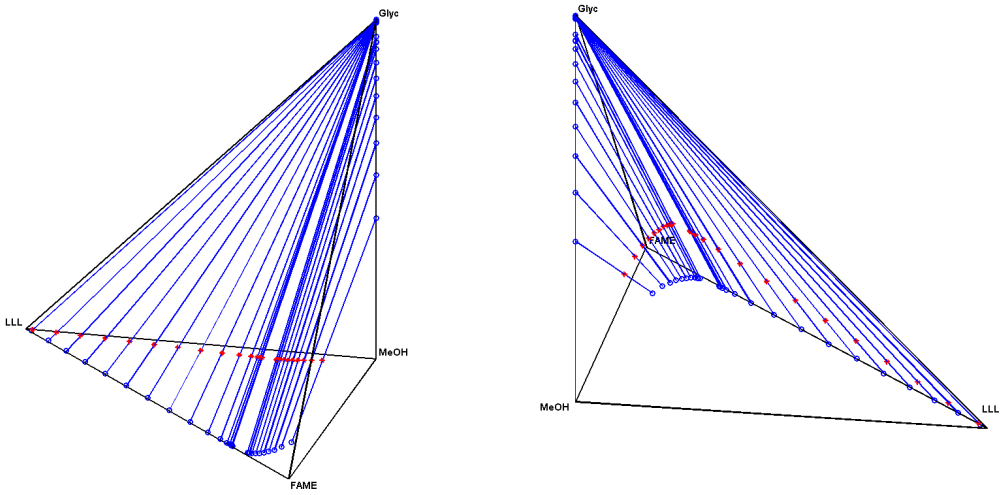

∗ Equilibrium global compositions, ○ Phase one and two compositions, − Material balance lines

Figure 5.8: Two different views of the bioreactor's equilibrium manifold generated when R varies between 0 and 5

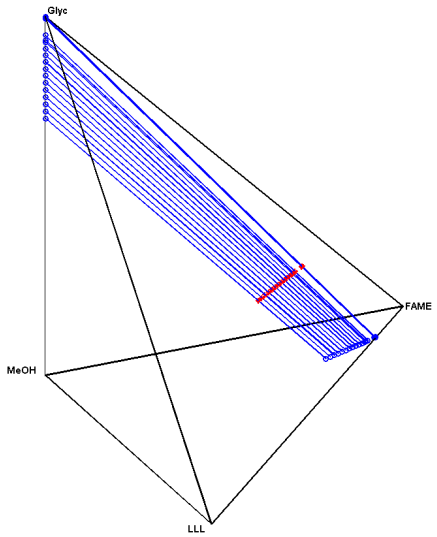

∗ Equilibrium global compositions, ○ Phase one and two compositions, − Material balance lines

Figure 5.9: Bioreactor's Equilibrium manifold generated when D varies between 0 and 5

the enzymatic reaction mechanism is more evident, if D decreases and R increases the non inhibition zone (see Methanol composition on Figure 5.10) becomes more narrow; the reactor should be operated in this zone to avoid the excess of methanol in the reactors outlet which would cause the necessity of its evaporation and also high yields of unreacted triglyceride in the Biodiesel composition (See Figure 5.12 and Figure 5.15 where the non inhibition zone is in white).

Due to the inhibition caused by the Methanol on the lipases, phase two outlet composition of trilinolein would be at least 10% with methanol traces(See Figure 5.12), this will difficult the obtention of biodiesel because an extra separation of the biodiesel and the triglyceride should be done as post processing causing extra costs. This kind of a priori observations based on shortcut modelling can be discarded in further steps of the design such as the rigurous model or optimization stage, where more than one reaction and separation stage would be taken into account.

Something important to remark is that due to the shape of the operation surfaces it is not possible to optimize the production of biodiesel only based on the operation surfaces or combinations of both, but it is possible to reduce optimization space with simple analysis.

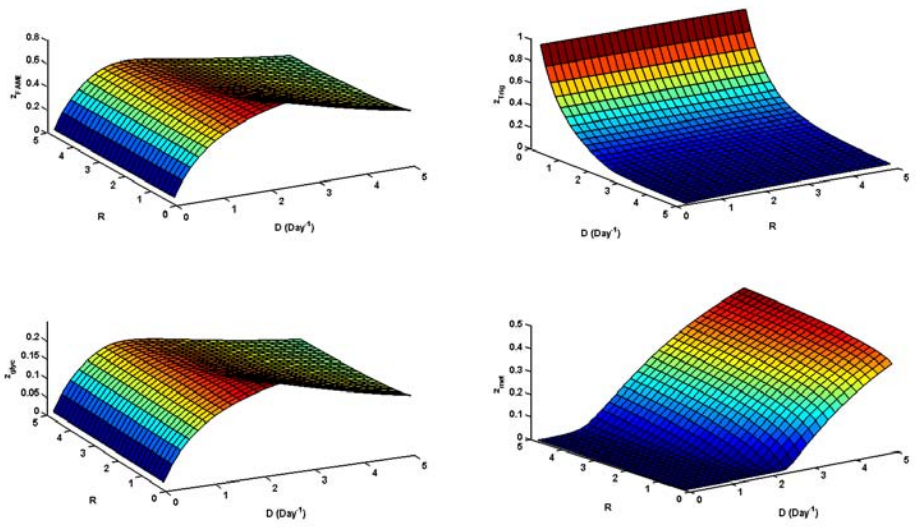

Figure 5.10: Global composition operation surface

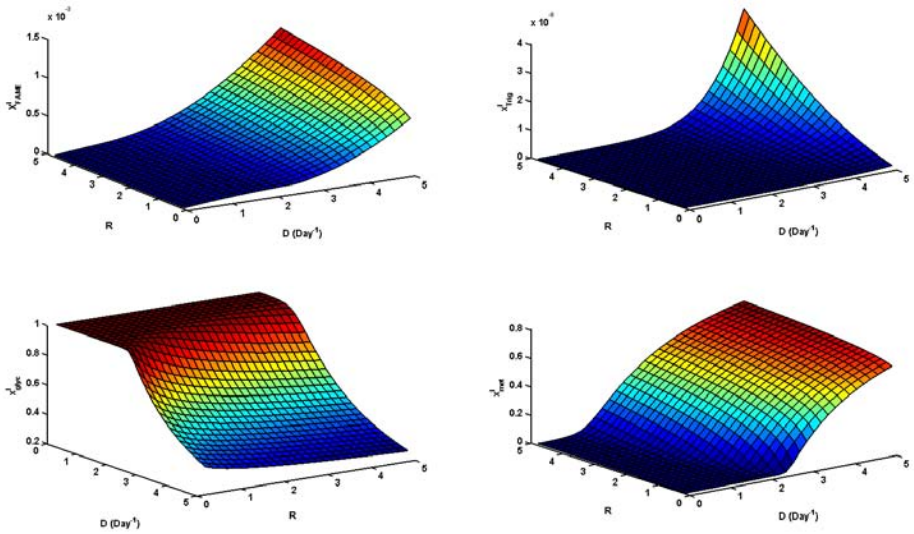

Figure 5.11: Phase one operation surface

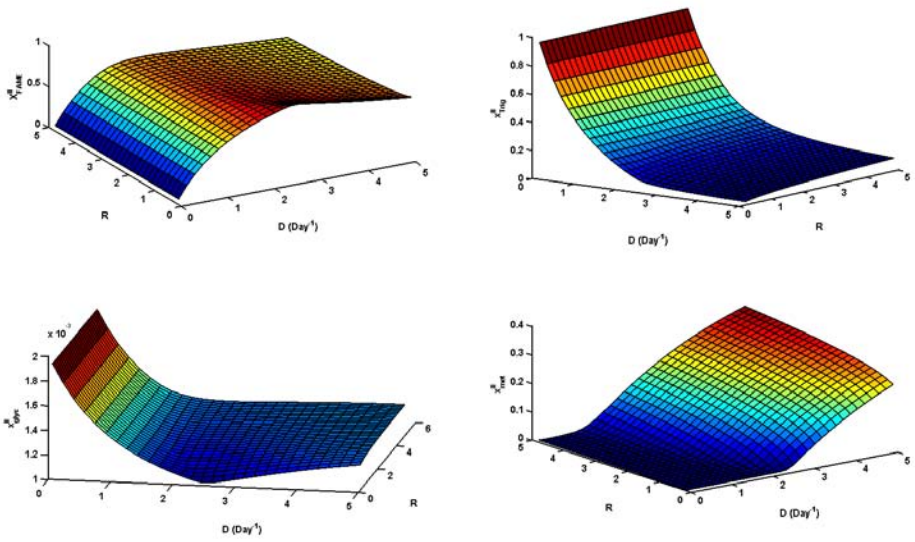

Figure 5.12: Phase two operation surface

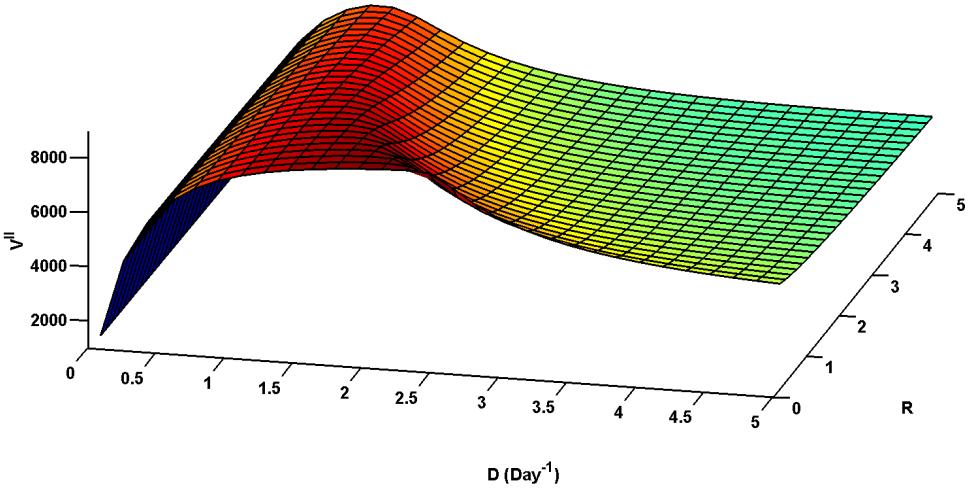

Figure 5.13: Reaction volume operation surface

Reactor volume and Total production analysis

The Reaction volume is an important variable on the design of the bioreactor-extractor, the volume occupied by the reaction's phase is decisive on the bioreactor's design. To complete a successful design at least the reaction volume should be guaranteed to ensure the biodiesel's rate of production. Figure 5.13 shows how the reaction volume or phase two volume varies as the principal design parameters (D and R) are varied between 0 and 5, reaction volume reach its maximum a R tends to zero due to the high amount of unreacted trilinolein on the reaction phase, so this high volumes are apparent and don't mean that the higest biodiesel production yields are being reached. Nevertheless the volume graph presents a constant ridge that represents the highest achievable volume if the parameter R is kept constant. The volume response surface can't be interpreted directly, it has to be part of a cost minimization objective function where the bioreactor's biodiesel yield benefits and costs are pondered, this has to be done in a further design step because in the conceptual design stage there is not enough information to do a realistic estimation.

Figure 5.15 shows the low methanol composition zone (in white) overlaid with the production isoclines. Using this Figure two study cases have been selected to show the utility of surface

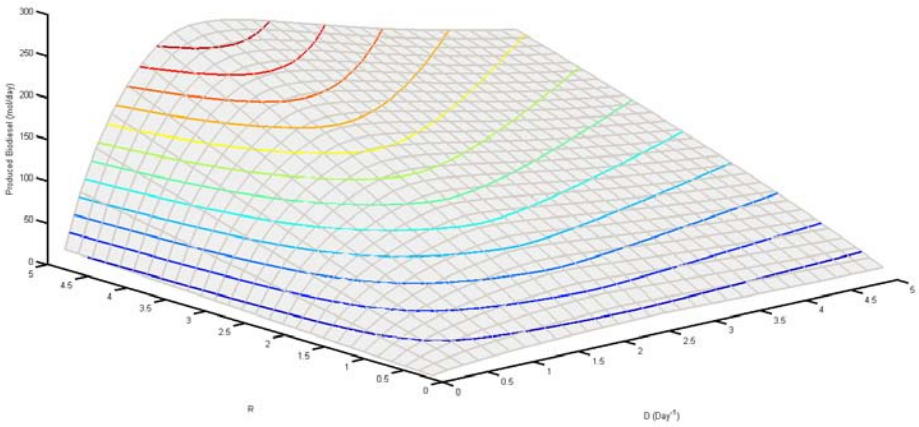

Figure 5.14: Total production surface, with production isoclines
for 20,40,60,80,100,120,140,160,180,200,220,240 mol/day of biodiesel

response analysis to obtain a desired response, the first one located in the non inhibition zone with $R = 1.5$ and $D = 3.22$ for a production of $160\ mol/day$ and the second one located in the blue region of the figure with $R = 3.5$ and $D = 4.27$ for a production of $160\ mol/day$. Figure 5.16 and Figure 5.17 show the operational behavior of the reactor when this this different values of the design parameters are varied to be in an out the low methanol composition zone with a fixed production rate.

Using Figure 5.18 and fixing the desired average of the molar compositions of methanol and triglyceride on 0.07 the parameter values $R = 2.25$ and $D = 0.732$ are obtained to shape the response of the reactor to the desired response than can bee seen in Figure 5.19, were the outlet compositions of reactives were reduced as desired.

In conclusion the response curve analysis is a good way to shape the desired response of a reactor without much computational effort, although it has big limitations it is adequate for shortcut models and the level of detail they involve.

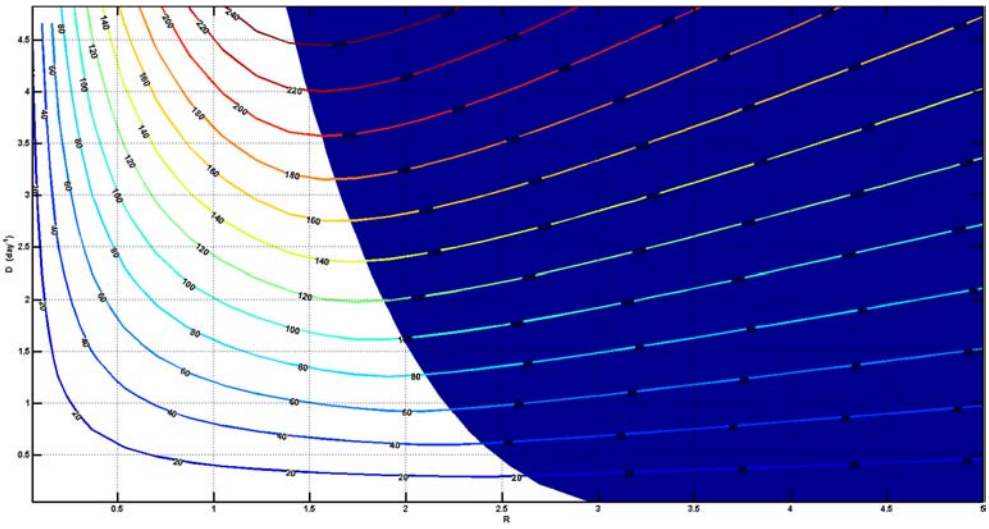

Figure 5.15: Non inhibition reaction zone and production isoclines

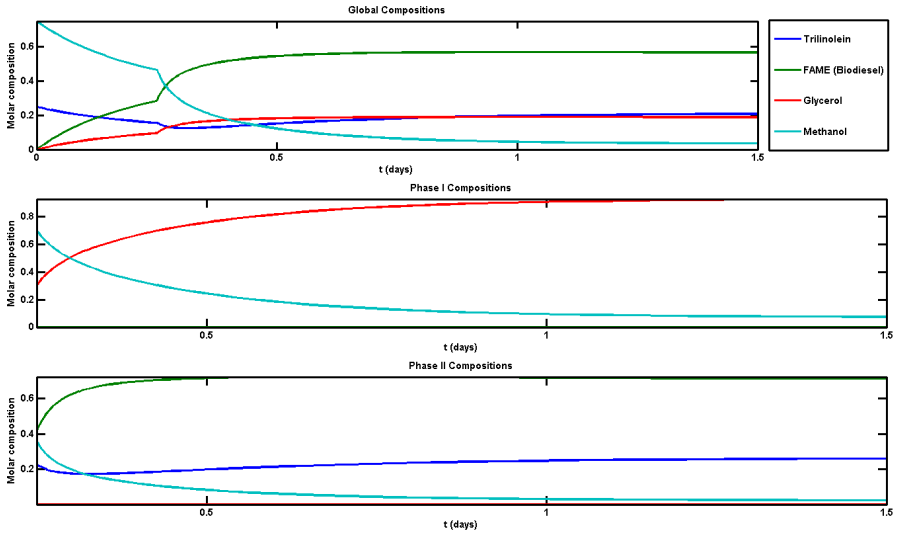

Figure 5.16: biorreactor operational behavior when $R = 1.5$ and $D = 3.22$

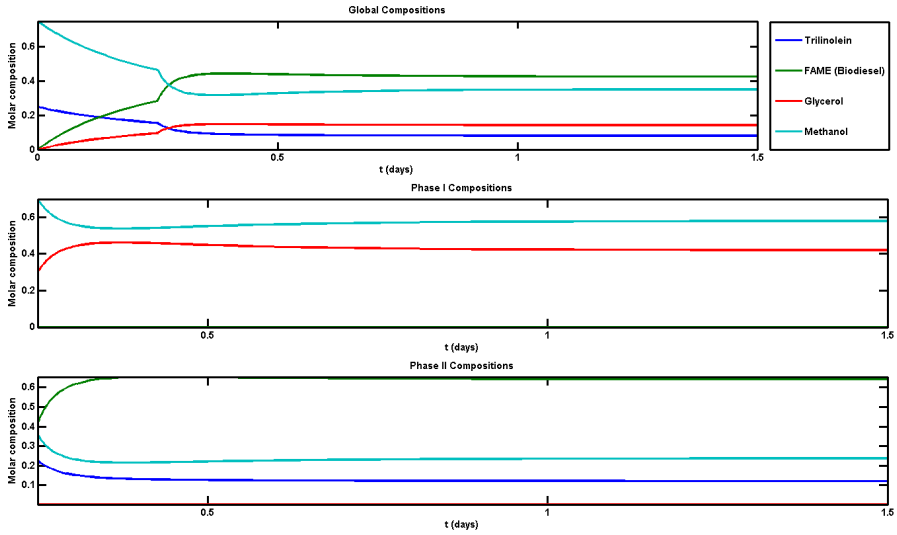

Figure 5.17: biorreactor operational behavior when $R = 3.5$ and $D = 4.27$

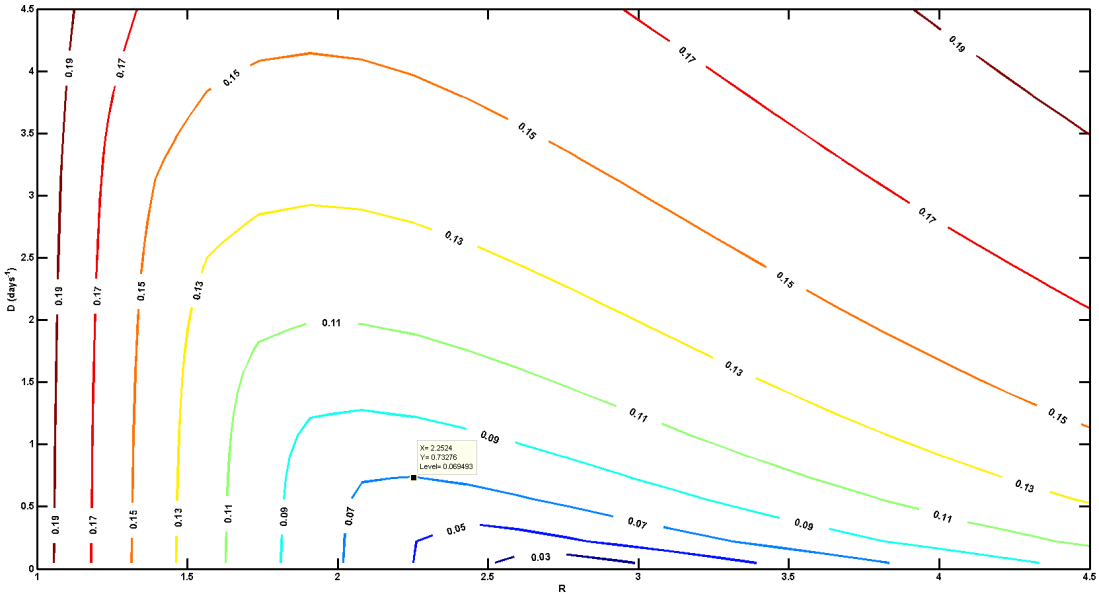

Figure 5.18: Average between x_{met}^{II} and x_{trig}^{II} isoclines

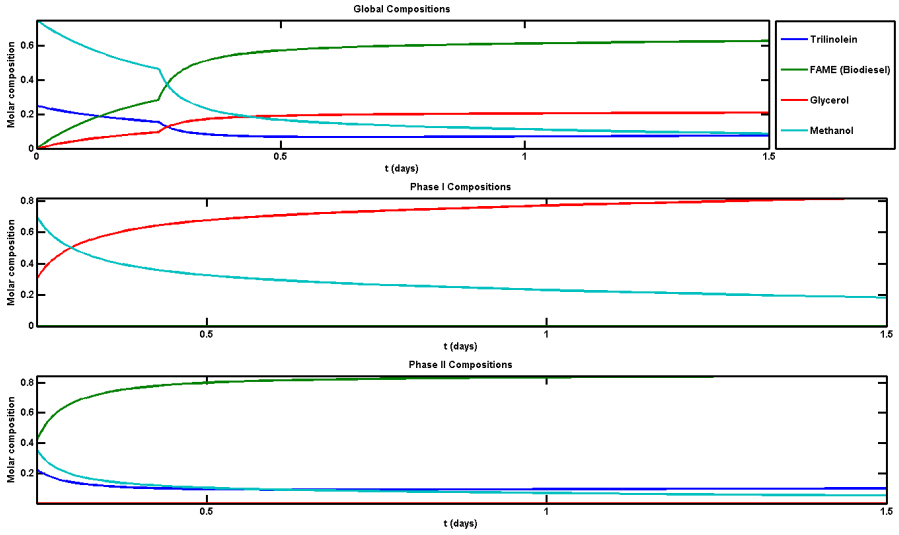

Figure 5.19: biorreactor operational behavior when $R = 2.25$ and $D = 0.732$

Chapter 6

Final Conclusions

6.1 About Biodiesel Production

Biofuels market is a new born opportunity for Colombia economically speaking but the lack of solid relations between academy and industry tend to isolate the academical research in lonely efforts that don't have repercussions on national reality. The most evident case was the law 693 of 2001, that benefited only the big sugar company's and promoted the creation of several new work vacancies (less than were promised), but the technological quota of the national universities and even of national companies on the construction of this new process plants was minimum. Biodiesel production is the new opportunity the country has to amend the mistakes made in the past and create new bonds between industry and universities that will benefit not only the industries as in the past but a complete academic community that is eager for the opportunity of make the difference.

6.2 About Shortcut Modeling

Shortcut modeling strategies as residue curve map and finite reflux residue curve map modeling has proven to be great tools of analysis and design, they are dynamic tools but they are used for steady state or static design and analysis. Dynamic design takes into account important operational factors that static design doesn't. With the formulation of the bioreactor-extractor shortcut design model the best qualities of both dynamic and static models were combined to produce a much more complete model that takes into account stability and the reactor start dynamics but not loosing the "simplicity" of thermodynamical equilibrium and infinite efficiency that has been used on shortcut design for years. The main idea in the formulation of dynamic

shortcut model is to asses the possible benefits and withdraws of a new technology with the information thats already available in the literature, this aloud the investigator or the designer of the new equipment to accept or discard new technologies as the combined reaction and extraction as the solution to specific problems, and to know in advance if this unit would have the expected better performance than conventional technology, without having to spend enormous amounts of time in laboratory design or rigorous modeling.

6.3 About the Bioreactor-Extractor

The combined reaction and extraction has been used in some applications mostly at pilot scale but always with the addition of a solvent, there are not many works in the available literature about auto inducted reaction and extraction processes, this work contributes to the state of the art in auto inducted reaction-extraction design doing as an extension of the previous work done in the PhD thesis of Dr. Luis Fernando Gutierrez, and adds the dynamic and stability analysis to shortcut design.

The enzymatic production of Biodiesel has had several withdraws with the inhibition caused by the the glycerol on enzymes, reaction-extraction technology is a solution to this problem because using the concentration field redistribution principle it concentrates the produced glycerol in a different phase that the phase where the reaction is taking place avoiding the inhibition.

In general the use of enzymes seems like a promising technology specially if immobilized enzymes are used, because of the high selectivity, but the lack of complete kinetics for this kind of processes make the analysis difficult and theoretical solutions to problems like inhibition cant be complete because the available models in the literature don't take into account all the inhibitions present in the reactions at the same time, further developments in the enzymatic kinetics and enzyme technology would do the labor of shortcut modeling and design much more precise and reliable.

In conclusion the reaction-extraction technology is appropriate to deal with the problems generated by the use of enzymes being much more suitable that the use of membranes due to the high cost of this.

6.4 About the Numerical Methods used in this Work

Non linear modeling and design bring new challenges to the modern engineer one of them is that the computational solution of this problems is not as easy as it used to be for much more simple approaches. The use of simple fixed point iterations is a common practice in the chemical engineering world but its an archaic practice, that has proven to be slow, inefficient and in some cases inaccurate. The numerical methods used in this work were specially selected to overcome the archaic practice of using simple fixed points iterations and to improve this by the use of topology and general differential-algebraic techniques developed over the past two decades.
this work attacked several numerical problems:

Material Stability: the first successfully solved problem that made the realization of the whole analysis possible was the creation of a new algorithm described in appendix C that allows an easy, precise and accurate solution of one of the biggest problems in liquid-liquid calculations, the material stability has been topic of research for decades and although the algorithm developed in Appendix C is not the ultimate answer to the problem of globals stability it give a good grade of certainty that the solution to the problem is correct but without spending ridiculous amounts of time on numerical and global optimizations that don't guarantee anything.

Differential-Algebraic Equations Integration: With the first implementation of ESIRK methods for the solution of DAEs this work contributes to the state of the art in numerical integration of DAEs with very good results. The use of ESIRK probed to be the right choice for the integration of the index 2 differential algebraic equation derived from the modeling of the reactor-extractor, this become more evident when Matlab's algorithms failed to integrate successfully this DAE system in several occasions. ESIRK proved to be superior to existing DAE integration algorithms due to its high order stage and the effective order concept that made this algorithm a perfect choice for high accuracy.

Numerical Continuation and Bifurcation Search: This work evidenced the lack of available software and literature about differential-algebraic equation's bifurcations, as conventional software as Matcont proved to be ineffective to predict the bifurcation of the

differential variables in the DAE systems due to the bifurcations inducted by single perturbation theory, the implementation of a continuation algorithm and implicit function theorem newton based Matlab routines to establish the real stability of the system was necessary and it proved to be effective in the analysis. Still DAE Bifurcation is a new born field of investigation and there are many questions that this work was unable to answer.

Bibliography

[1] M. A. Dubé, A. Y. Tremblay, and J. Liu. Biodiesel production using a membrane reactor. *Bioresource Technology*, 98(3):639–647, 2007.

[2] Luis Fernando Gutiérrez Mosquera. *Estudio y Diseño de Procesos Reacción Extracción Simultáneos*. PhD thesis, Universidad Nacional de Colombia Sede Manizales, 2007.

[3] S. Al-Zuhair. Production of biodiesel by lipase-catalyzed transesterification of vegetable oils: A kinetics study. *Biotechnol. Prog.*, 21(5):1442–1448, 2005.

[4] Ernst Hairer, Michel Roche, and Christian Lubich. *The Numerical Solution of Differential-Algebraic Systems by Runge-Kutta Methods*. Springer-Verlag, 1989.

[5] Matt Johnston and Tracey Holloway. A global comparison of national biodiesel production potentials. *Environ. Sci. Technol.*, 41(23):7967–7973, 2007.

[6] Ayhan Demirbas. Biodiesel production from vegetable oils via catalytic and non-catalytic supercritical methanol transesterification methods. *Progress in Energy and Combustion Science*, 31(5-6):466–487, 2005.

[7] Luiz Stragevitch Carla G. Pina Cintia B. Goncü alves Eduardo Batista, Sandra Monnerat and Antonio J. A. Meirelles. Prediction of liquid-liquid equilibrium for systems of vegetable oils, fatty acids, and ethanol. *J. Chem. Eng. Data*, 44,:1365–1369, 1999.

[8] Ayhan Demirbas. *Biodiesel*. Springer-Verlag, 2008.

[9] Andrea Salis Maura Monduzzi and Vincenzo Solina. *Industrial Enzymes*, chapter Use of Lipases for the Production of Biodiesel, pages 317–339. Springer-Verlag, 2007.

[10] J. M. Marchetti, V. U. Miguel, and A. F. Errazu. Possible methods for biodiesel production. *Renewable and Sustainable Energy Reviews*, 11(6):1300–1311, 2007.

[11] Srivathsan Vembanur Ranganathan, Srinivasan Lakshmi Narasimhan, and Karuppan Muthukumar. An overview of enzymatic production of biodiesel. *Bioresource Technology*, 99(10):3975–3981, 2008.

[12] Palligarnai Vasudevan and Michael Briggs. Biodiesel production-current state of the art and challenges. *Journal of Industrial Microbiology and Biotechnology*, 35(5):421–430, 2008. 10.1007/s10295-008-0312-2.

[13] Ayahan Demirbas. Biodiesel fuel via transesterification in supercritical methanol. *Energy Convers Manage*, 2002.

[14] Ana L. Paiva, Victor M. Balcão, and F. Xavier Malcata. Kinetics and mechanisms of reactions catalyzed by immobilized lipases[small star, filled]. *Enzyme and Microbial Technology*, 27(3-5):187–204, 2000.

[15] Sulaiman Al-Zuhair, Fan Wei Ling, and Lim Song Jun. Proposed kinetic mechanism of the production of biodiesel from palm oil using lipase. *Process Biochemistry*, 42(6):951–960, 2007.

[16] Mittlebach Michael. Lipase catalyzed alcoholysis of sunflower oil. *Journal of American Oil chemical Society*, 67:168–170, 1990.

[17] Valérie Dossat, Didier Combes, and Alain Marty. Lipase-catalysed transesterification of high oleic sunflower oil. *Enzyme and Microbial Technology*, 30(1):90–94, 2002.

[18] Noureddini H. X. Gao and R.S. Philkana. Immobilized *Pseudomonas cepacia* lipase for biodiesel fuel production from soybean oil. *Bioresource Technology*, 96:769–777, 2005.

[19] N. R Kamini and H Iefuji. Lipase catlysed methanolisis of vegetable oil in aqueous medium by *Criptococcus*. *Process Biochem*, 37:405–410, 2001.

[20] K.C Jones Hsu A.F and T.A Foglia. Immobilized lipase-catalysed production of alkyl esters of restaurant grease as biodiesel. *Journal of American Oil Chemical Society*, 36:181–186, 2002.

[21] T. Samukawa. A. Sugihara J. Noda H. Fukuda Shimada Y., Y. Watanabe and Y. Tominaga. Conversion of vegetable oil to biodiesel using immobilized *Candida Antartica* lipase. *J. Am. Oil. Chem. Soc.*, 76(7):789–793, 1999.

[22] T. A. Foglia Lee K. T. and K. S. Chang. Production of alkyl esters as biodiesel from fractioned lard and restaurant grease. *J. Am. Oil. Chem. Soc.*, 79:191–195, 2002.

[23] W. T. Wu Chen J. W. Regeneration of immobilized *Candida antartica* lipase for transesterification. *J. Biosci. Bioeng*, 2003.

[24] A. Sugihara Watanabe Y. Y. Shimada and Y. Tominaga. Conversion of degummed soybean oil to biodiesel fuel with immobilized *Candida antartica* lipase. *J. Mol Catal B Enzym*, 17:151–155, 2002.

[25] J. Zeng Du W., Y. Chu and D. Liu. Novozym 435-catalysed transesterification of crude soya bean oil for biodiesel production in solvent free medium. *Biotech. Appl- Biochem*, 40:187–190, 2004.

[26] R.S. Vali Y. H Ju Lai C.C., S. Zullaikai. Lipase catalized production of biodiesel from rice bran oil. *J. Chem. Technol. Biotechnol*, 80:331–337, 2005.

[27] J. Zeng Xu, Y. W. Du and D. Liu. Conversion of soybean oil to biodiesel fuel using lipozyme tl im in a solvent-free medium. *Biocatal. Biotrasnf*, 22:45–48, 2004.

[28] D. Combes Dossat V. and A. marty. Continuos enzymatic transesterification of high oleic sunflower oil in a packed-bed reactor: influence of the glycerol production. *Enzyme. Microb. Tech.*, 25:194–200, 1999.

[29] F. Kovács L. Gubicza Beláfi-Bakó, K. and J. Hancsók. Enzymatic biodiesel production from sunflower oil by *Candida antartica* lipase in a solvent-free system. *Biocatal. Biotransf.*, 20:437–439, 2002.

[30] Peigang Cao, Marc A. Dubé, and André Y. Tremblay. High-purity fatty acid methyl ester production from canola, soybean, palm, and yellow grease lipids by means of a membrane reactor. *Biomass and Bioenergy*, 32(11):1028–1036, 2008.

[31] Peigang Cao, Marc A. Dubé, and André Y. Tremblay. Methanol recycling in the production of biodiesel in a membrane reactor. *Fuel*, 87(6):825–833, 2008.

[32] L. Guerreiro, J. E. Castanheiro, I. M. Fonseca, R. M. Martin-Aranda, A. M. Ramos, and J. Vital. Transesterification of soybean oil over sulfonic acid functionalised polymeric membranes. *Catalysis Today*, 118(1-2):166–171, 2006.

[33] Shinji Hama, Sriappareddy Tamalampudi, Takahiro Fukumizu, Kazunori Miura, Hideki Yamaji, Akihiko Kondo, and Hideki Fukuda. Lipase localization in rhizopus oryzae cells immobilized within biomass support particles for use as whole-cell biocatalysts in biodiesel-fuel production. *Journal of Bioscience and Bioengineering*, 101(4):328–333, 2006.

[34] Kaili Nie, Feng Xie, Fang Wang, and Tianwei Tan. Lipase catalyzed methanolysis to produce biodiesel: Optimization of the biodiesel production. *Journal of Molecular Catalysis B: Enzymatic*, 43(1-4):142–147, 2006.

[35] Carlos A. Cardona and R Marcela. Análisis de procesos simultaneos reacción extracción a nivel productivo: Generalidades del proceso, equlibrio fásico y quimico simultáneo. *Ingenieria y Competitividad*, 6:17 – 25, 2004.

[36] Paola Andrea Solano Arias Carlos Ariel Cardona, Luis Carlos Gallego. *Introducción a las Operaciones de Separacion no Convencionales*. Arcano, 2007.

[37] Luis Fernando Gutierrez Mosquera Carlos A.Cardona, Luis Geronimo Matallana Perez. Aplicación de la destilación reactiva en la producción de biocombustibles. Ponencia en la Cuarta conferencia internacional sobre energía renovable, ahorro de energía y educación energética, 2005.

[38] Leonid A Serafimov Yua pisarenko, Carlos Ariel Cardona Alzate. Reactive distillation with fast irreversible chemical reactions. ACHEMA 2002. 1st International Congress in Process Technologies, March 2002.

[39] Felipe Antonio Perdomo. Diseño coneptual y simulacion de columnas de destilacion reactiva via termodinamica topologica a condiciones finitas de operacion. Master's thesis, Universidad Nacional de Colombia sede Manizales, 2007.

[40] Christian Thiel, Kai Sundmacher, and Ulrich Hoffmann. Synthesis of etbe: Residue curve maps for the heterogeneously catalysed reactive distillation process. *Chemical Engineering Journal*, 66(3):181–191, 1997.

[41] Carlos A. Cardona and Oscar J. Sanchez. Fuel ethanol production: Process design trends and integration opportunities. *Bioresource Technology*, 98(12):2415–2457, 2007.

[42] Michael F. Doherty David B. Van Dongen. Design and synthesis of homogeneous azeotropic distillations. 1. problem formulation for a single column. *Ind. Eng. Chem. Fundamen*, 24(24):454–463, 1985.

[43] Michael F. Doherty Sanford G. Levy, David B. Van Dongen. Design and synthesis of homogeneous azeotropic distillations. 2. minimum reflux calculations for nonideal and azeotropic columns. *Ind. Eng. Chem. Fundam*, 24:463–474, 1985.

[44] E. Blass A. W. Westerberg O. M. Wahnschafft, J. W. Koehler. The product composition regions of single-feed azeotropic distillation columns. *Ind. Eng. Chem. Res*, 31(10):2345–2362, 1992.

[45] Ross Taylor Angelo Luci, Amit Amalea. Distillation pinch points and more. *Computers and Chemical Engineering*, 32:1342–1364, 2008.

[46] Ayhan Demirbas. Biofuels sources, biofuel policy, biofuel economy and global biofuel projections. *Energy Conversion and Management*, 49(8):2106–2116, 2008.

[47] Kailas L. Wasewar, A. Bert M. Heesink, Geert F. Versteeg, and Vishwas G. Pangarkar. Reactive extraction of lactic acid using alamine 336 in mibk: equilibria and kinetics. *Journal of Biotechnology*, 97(1):59–68, 2002.

[48] Vera Zimmermann, Ines Masuck, and Udo Kragl. Reactive extraction of n-acetylneuraminic acid–kinetic model and simulation of integrated product removal. *Separation and Purification Technology*, 63(1):129–137, 2008.

[49] Vera Zimmermann and Udo Kragl. Reactive extraction of n-acetylneuraminic acid–a new method to recover neuraminic acid from reaction solutions. *Separation and Purification Technology*, 61(1):60–67, 2008.

[50] D. Cascaval, A. I. Galaction, N. Nicuta, and A. C. Blaga. Selective separation of gentamicins from the biosynthetic mixture by reactive extraction. *Separation and Purification Technology*, 57(2):264–269, 2007.

[51] M. M. Bora, S. Borthakur, P. G. Rao, and N. N. Dutta. Study on the reactive extraction and stripping kinetics of certain [beta]-lactam antibiotics. *Chemical Engineering and Processing: Process Intensification*, 47(1):1–8, 2008.

[52] Van-Ness H. C. Smith J.M. *Introducción a la Termodiámica en Ingeniería Química*. McGraw-Hill., 1989.

[53] H. J. Bart, C. Drumm, and M. M. Attarakih. Process intensification with reactive extraction columns. *Chemical Engineering and Processing: Process Intensification*, 47(5):745–754, 2008.

[54] Ville Alopaeus, Jukka Koskinen, and Kari I. Keskinen. Simulation of the population balances for liquid-liquid systems in a nonideal stirred tank. part 1 description and qualitative validation of the model. *Chemical Engineering Science*, 54(24):5887–5899, 1999.

[55] J. A. Wesselingh and A. M. Bollen. Single particles, bubbles and drops: Their velocities and mass transfer coefficients. *Chemical Engineering Research and Design*, 77(2):89–96, 1999.

[56] Robert Ewald Treybal. *Liquid extraction*. McGraw-Hill, New York, 2nd ed edition, 1963.

[57] Glenn A. Caldarola Michael F. Doherty. Design and synthesis of homogeneous azeotropic distillations. 3. the sequencing of columns for azeotropic and extractive distillations. *Ind. Eng. Chem. Fundam*, 24(4):474–485, 1985.

[58] J. M Prausnitz. *Molecular thermodynamics of fluid-phase equilibria*. Prentice-Hall, Upper Saddle River, N.J, 3rd ed edition, 1999.

[59] Fangrui Ma and Milford A. Hanna. Biodiesel production: a review. *Bioresource Technology*, 70(1):1–15, 1999.

[60] Francisco J. Senorans Guillermo Reglero Elvis J. Hernandez, Guillermo D. Mabe and Tiziana Fornari. High-pressure phase equilibria of the pseudoternary mixture sunflower oil + ethanol + carbon dioxide. *J. Chem. Eng. Data*, 53:2632–2636, 2008.

[61] Eduardo Batista Ronei J. Poppi Marcelo Lanza, Waldomiro Borges Neto and Antonio J. A. Meirelles. Liquid-liquid equilibrium data for reactional systems of ethanolysis at 298.3 k. *J. Chem. Eng. Data*, 53:5–15, 2008.

[62] Eduardo Batista Cintia B. Gonalves and Antonio J. A. Meirelles. Liquid-liquid equilibrium data for the system corn oil + oleic acid + ethanol + water at 298.15 k. *J. Chem. Eng. Data*, 47:416–420, 2002.

[63] Yujun Wang Xuejun Liu, Xianglan Piao and Shenlin Zhu. Liquid-liquid equilibrium for systems of (fatty acid ethyl esters + ethanol +soybean oil and fatty acid ethyl esters + ethanol + glycerol). *J. Chem. Eng. Data*, 53:359–362, 2008.

[64] Mohsen Mohsen-Nia and Mahdi. Dargahi. Liquid-liquid equilibrium for systems of (corn oil + oleic acid + methanol or ethanol) at (303.15 and 313.15) k. *J. Chem. Eng. Data,*, 53:910–914, 2007.

[65] Antonio J.A. Meirelles Cintia B. Gonçalves. Liquid-liquid equilibrium data for the system palm oil + fatty acids + ethanol + water at 318.2k. *Fluid Phase Equilibria*, 221:139–150, 2004.

[66] M. Mohsen-Nia and A. Khodayari. De-acidification of sunflower oil by solvent extraction: (liquid + liquid) equilibrium data at t = (303.15 and 313.15) k. *The Journal of Chemical Thermodynamics*, 40(8):1325 – 1329, 2008.

[67] Juergen Gmehling, Peter Rasmussen, and Aage Fredenslund. Vapor-liquid equilibriums by unifac group contribution. revision and extension. 2. *Industrial and Engineering Chemistry Process Design and Development*, 21(1):118–127, 1982.

[68] Henrik K. Hansen, Peter Rasmussen, Aage Fredenslund, Martin Schiller, and Juergen Gmehling. Vapor-liquid equilibria by unifac group contribution. 5. revision and extension. *Industrial and Engineering Chemistry Research*, 30(10):2352–2355, 1991.

[69] Eugenia Almeida Macedo, Ulrich Weidlich, Juergen Gmehling, and Peter Rasmussen. Vapor-liquid equilibriums by unifac group contribution. revision and extension. 3. *Industrial and Engineering Chemistry Process Design and Development*, 22(4):676–678, 1983.

[70] Steen Skjold-Jorgensen, Barbel Kolbe, Jurgen Gmehling, and Peter Rasmussen. Vapor-liquid equilibria by unifac group contribution. revision and extension. *Industrial and Engineering Chemistry Process Design and Development*, 18(4):714–722, 1979.

[71] Detlef Tiegs, Peter Rasmussen, Juergen Gmehling, and Aage Fredenslund. Vapor-liquid equilibria by unifac group contribution. 4. revision and extension. *Industrial and Engineering Chemistry Research*, 26(1):159–161, 1987.

[72] Ulrich Weidlich and Juergen Gmehling. A modified unifac model. 1. prediction of vle, he, and .gamma..infin. *Industrial and Engineering Chemistry Research*, 26(7):1372–1381, 1987.

[73] Thomas Magnussen, Peter Rasmussen, and Aage Fredenslund. Unifac parameter table for prediction of liquid-liquid equilibriums. *Industrial and Engineering Chemistry Process Design and Development*, 20(2):331–339, 1981.

[74] Andrzej. Stolyhwo, Henri. Colin, and Georges. Guiochon. Analysis of triglycerides in oils and fats by liquid chromatography with the laser light scattering detector. *Analytical Chemistry*, 57(7):1342–1354, 1985.

[75] Stefanie Bail Sabine Krist, Gerald Stuebiger and Heidrun Unterweger. Detection of adulteration of poppy seed oil with sunflower oil based on volatiles and triacylglycerol composition. *J. Agric. Food Chem*, 57:6385–6389, 2006.

[76] Kathryn Eleda Brenan, Stephen La Vern Campbell, and Linda R. Petzold. *Numerical Solution of Initial-Value Problems in Differential-Algebraic Equations*. North-Holland, New York, 1989.

[77] J. R. Cash. Review paper. efficient numerical methods for the solution of stiff initial-value problems and differential algebraic equations. *Proceedings: Mathematical, Physical and Engineering Sciences*, 459(2032):797–815, 2003.

[78] J. O. Hirschfelder C. F. Curtiss. Integration of stiff equations. *Poc. Natl Acad Sci.*, 38:235–243, 1952.

[79] J. C Butcher. *Numerical Methods for Ordinary Differential Equations*. John Wiley & Sons, Ltd, 2008.

[80] G. Wanner E. Hairer. *Solving Ordinary Differential Equations II: Stiff and Differential Algebraic Problems.* Springer-Verlag, 1991.

[81] David Jen Lung Chen. *The Effective Order of Singly-Implicit Methods for Stiff Differential Equations*. PhD thesis, The University of Auckland (New Zeland), 1998.

[82] Germund G. Dahlquist. A special stability problem for linear multistep methods. *BIT Numerical Mathematics*, 3:27–43, 1963.

[83] Olof B. Widlund. A note on unconditionally stable linear multistep methods. *BIT Numerical Mathematics*, 7:65–70, 1967.

[84] G.Wanner E. Hairer, S. P. Nørsett. *Solving Ordinary Differential Equations I: Nonstiff Problems*. Springer-Verlag, 2008.

[85] Ernst Hairer, Gerhard Wanner, and Christian Lubich. *Geometric Numerical Integration*. Springer-Verlag, 2006.

[86] Robert Alexander. Diagonally implicit runge-kutta methods for stiff odes. *Siam journal of Numerical Analysis*, 14:1006–1021, 1977.

[87] Roger K. Alexander and James J. Coyle. Runge-kutta methods and differential-algebraic systems. *SIAM Journal on Numerical Analysis*, 27(3):736–752, 1990.

[88] A. Kvaerno. Singly diagonally implicit runge-kutta methodswith an explicit first stage. *BIT Numerical Mathematics*, 44:489–502, 2004.

[89] J. C. Butcher. On the implementation of implicit runge-kutta methods. *BIT Numerical Mathematics*, 16(3):237–240, September 1976.

[90] J. M. Varah. On the efficient implementation of implicit runge-kutta methods. *Mathematics of Computation*, 33:557–561, 1979.

[91] J.C. Butcher and P. Chartier. The effective order of singly-implicit runge-kutta methods. *Numerical Algorithms*, 20(4):269–284, August 1999.

[92] K. Burrage, J. C. Butcher, and F. H. Chipman. An implementation of singly-implicit runge-kutta methods. *BIT Numerical Mathematics*, 20(3):326–340, September 1980.

[93] J.C. Butcher and M.T. Diamantakis. Desire: diagonally extended singly implicit runge-kutta effective order methods. *Numerical Algorithms*, 17(1):121–145, May 1998.

[94] Gennady Y. Kulikov. *Computational Science ICCS 2004*, chapter An Advanced Version of the Local-Global Step Size Control for Runge-Kutta Methods Applied to Index 1 Differential-Algebraic Systems, pages 596–569. Springer-Verlag, 2004.

[95] J. Butcher and Z. Jackiewicz. A reliable error estimation for diagonally implicit multistage integration methods. *BIT Numerical Mathematics*, 41(4):656–665, September 2001.

[96] Peter Albrecht. The runge–kutta theory in a nutshell. *SIAM Journal on Numerical Analysis*, 33(5):1712–1735, 1996.

[97] E. L. ALLGOWER and K.GEORG. Continuation and path following. *Acta numerica*, 2:1–64, 1993.

[98] Carmen Arévalo and Per Lötstedt. Improving the accuracy of bdf methods for index 3 differential-algebraic equations. *BIT Numerical Mathematics*, 35(3):297–308, 1995.

[99] Uri M. Ascher and Linda R. Petzold. *Computer Methods for Ordinary Differential Equations and Differential-Algebraic Equations*. Society for Industrial and Applied Mathematics, Philadelphia, PA, USA, 1998.

[100] G. Bader and P. Deuflhard. A semi-implicit mid-point rule for stiff systems of ordinary differential equations. *Numerische Mathematik*, 41(3):373–398, 1983.

[101] Jürgen Bausa and Wolfgang Marquardt. Quick and reliable phase stability test in vlle flash calculations by homotopy continuation. *Computers and Chemical Engineering*, 24(11):2447–2456, 2000.

[102] Roland Bulirsch and Josef Stoer. Numerical treatment of ordinary differential equations by extrapolation methods. *Numerische Mathematik*, 8(1):1–13, 1966.

[103] J. Butcher. High order a-stable numerical methods for stiff problems. *Journal of Scientific Computing*, 25(1):51–66, October 2005.

[104] J. Butcher. The effective order of runge-kutta methods, 1969.

[105] J.C. Butcher and T.M.H. Chan. Variable stepsize schemes for effective order methods and enhanced order composition methods. *Numerical Algorithms*, 26(2):131–150, February 2001.

[106] J.C. Butcher and A.D. Heard. Stability of numerical methods for ordinary differential equations. *Numerical Algorithms*, 31(1):59–73, December 2002.

[107] J. C. Butcher. Order and stability of parallel methods for stiff problems. *Advances in Computational Mathematics*, 7(1):79–96, March 1997.

[108] J. C. Butcher. On fifth order runge-kutta methods. *BIT Numerical Mathematics*, 35(2):202–209, June 1995.

[109] J. C. Butcher. A generalization of singly-implicit methods. *BIT Numerical Mathematics*, 21(2):175–189, June 1981.

[110] J. C. Butcher. Ona-stable implicit runge-kutta methods. *BIT Numerical Mathematics*, 17(4):375–378, December 1977.

[111] J. C. Butcher. A stability property of implicit runge-kutta methods. *BIT Numerical Mathematics*, 15(4):358–361, December 1975.

[112] Roger K. Alexander; James J. Coyle. Runge-kutta methods and differential-algebraic systems. *SIAM Journal on Numerical Analysis*, 27:736–752, 1990.

[113] Juan Lanz Cristina Gonzlez, Jos M. Resa and M. Angeles Fanega. Properties of mixing of systems that contain sunflower oil with ketones. *J. Chem. Eng. Data*, 47:1116–1122, 2002.

[114] P. Deuflhard. Springer series in computational mathematics. In *Newton Methods for Nonlinear Problems*. Springer-Verlag, 2004.

[115] P. Deuflhard. Order and stepsize control in extrapolation methods. *Numerische Mathematik*, 41(3):399–422, 1983.

[116] P. Deuflhard, E. Hairer, and J. Zugck. One-step and extrapolation methods for differential-algebraic systems. *Numerische Mathematik*, 51(5):501–516, 1987.

[117] Kuznetsov Yu A Dhooge A, Govaerts W. *MATCONT and CL MATCONT: Continuation Toolboxes in Matlab*.

[118] Alexandre C. Dimian. *Integrated Design and Simulation of Chemical Processes*. Elsevier Science, 2003.

[119] M.C. McManus G.P. Hammond, S. Kallu. Development of biofuels for the uk automotive market. *Applied Energy*, 85(85):506–515, 2008.

[120] C. W. Gear. Differential algebraic equations, indices, and integral algebraic equations. *SIAM Journal on Numerical Analysis*, 27(6):1527–1534, 1990.

[121] C. W. Gear and L. R. Petzold. Ode methods for the solution of differential/algebraic systems. *SIAM Journal on Numerical Analysis*, 21(4):716–728, 1984.

[122] Rocha Loes V.L. Toledo Benavides J.V Gomes-Ruggiero, M.A. A modified descent direction for newton-gmres method.

[123] Willy J. F Govaerts. *Numerical Methods for the Bifurcation fo Dynamical Equilibrium*. SIAM, 2000.

[124] K. Gunvachai, M. G. Hassan, G. Shama, and K. Hellgardt. A new solubility model to describe biodiesel formation kinetics. *Process Safety and Environmental Protection*, 85(5):383–389, 2007.

[125] G. P. Hammond, S. Kallu, and M. C. McManus. Development of biofuels for the uk automotive market. *Applied Energy*, 85(6):506–515, 2008.

[126] Houfang Lu Hui Zhou and Bin Liang. Solubility of multicomponent systems in the biodiesel production by transesterification of jatropha curcas l. oil with methanol. *J. Chem. Eng. Data*, 51:1130–1135, 2006.

[127] Jack Dongarra Vicente Hernandez Marina Walden Jose M.L.M. Palma, A. Augusto Sousa. *High Performance Computing for Computational Science VECPAR 2002*, chapter A Parallel Newton-GMRES Algorithm for Solving Large Scale Nonlinear Systems, page 732. Springer Verlag, 2003.

[128] Taisei Fujimoto Yusuke Asakuma Keisuke Fukui Masahiro Osako Kazuo Nakamura Kouji Maeda, Hidetoshi Kuramochi and Shin ichi Sakai. Phase equilibrium of biodiesel compounds for the triolein + palmitic acid + methanol system with dimethyl ether as cosolvent. *J. Chem. Eng. Data*, 57:973–977, 2008.

[129] Gennady Kulikov and Alexandra Korneva. On efficient application of implicit runge-kutta methods to large-scale systems of index 1 differential-algebraic equations. In *Computational Science ICCS 2001*, pages 832–841. Springer-Verlag, 2001.

[130] Yuri A. Kustnetzov. Applied mathematical sciences. In *Elements of Applied Bifurcation*, number 112. Springer-Verlag, 1995.

[131] Per Lotstedt and Linda Petzold. Numerical solution of nonlinear differential equations with algebraic constraints i: Convergence results for backward differentiation formulas. *Mathematics of Computation*, 46(174):491 – 516, 1986.

[132] A. R. Champneys P. Kowalczyk M. Di Bernardo, C. J. Budd. Applied mathematical sciences. In *Piecewise-smooth Dynamical Systems*. Springer-Verlag, 2008.

[133] Conor M. McDonald and Christodoulos A. Floudas. Global optimization and analysis for the gibbs free energy function using the unifac, wilson, and asog equations. *Ind. Eng. Chem. Res.*, 34(5):1674–1687, 1995.

[134] Roswitha März. On initial value problems in differential-algebraic equations and their numerical treatment. *Computing*, 35(1):13–37, 1985.

[135] Linda Petzold and Per Lötstedt. Numerical solution of nonlinear differential equations with algebraic constraints ii: Practical implications. *SIAM Journal on Scientific and Statistical Computing*, 7(3):720–733, 1986.

[136] Jorge M. V. Prior and Jose M. Loureiro. Residual thermodynamic properties in reactor modeling. *Chemical Engineering Science*, 56:873–879, 2001.

[137] Prausnitz J M Renon H. Local composition in thermodynamic excess functions for liquid mixtures. *AICHE Journal*, 14:135–142, 1968.

[138] Juliana Rabelo Marcel Caruso Ana C. C. Cunha Flavio W. Cavaleri Eduardo A. C. Batista Roberta Ceriani, Cintia B. Gonçalves and Antonio J. A. Meirelles. Group contribution model for predicting viscosity of fatty compounds. *J. Chem. Eng. Data*, 52:956–972, 2007.

[139] Michel Roche. Implicit runge-kutta methods for differential algebraic equations. *SIAM Journal on Numerical Analysis*, 26(4):963–975, 1989.

[140] Youcef Saad and Martin H. Schultz. Gmres: A generalized minimal residual algorithm for solving nonsymmetric linear systems. *SIAM Journal on Scientific and Statistical Computing*, 7(3):856–869, 1986.

[141] Rüdiger Seydel. Interdisciplinary applied mathematics. In *Practical Bifurcation and Stability Analysis*, number 5. Springer-Verlag, 1994.

[142] Y. C. Sharma, B. Singh, and S. N. Upadhyay. Advancements in development and characterization of biodiesel: A review. *Fuel*, 87(12):2355–2373, 2008.

[143] Roland Bulirsch Josef Stoer. *Introduction to Numerical Analysis*. Springer-Verlag, 1980.

[144] Amy C. Sun and Warren D. Seider. Homotopy-continuation method for stability analysis in the global minimization of the gibbs free energy. *Fluid Phase Equilibria*, 103(2):213–249, 1995.

[145] W. T. Vetterling W. H. Press, Saul A. Teukolsky, Brian P. Flannery., and Numerical recipes in C. *Numerical recipes in C*. Cambridge University Press, 1992.

[146] S. K. Wasylkiewicz, M. F. Doherty, and M. F. Malone. Computing all homogeneous and heterogeneous azeotropes in multicomponent mixtures. *Ind. Eng. Chem. Res.*, 38(12):4901–4912, 1999.

[147] S. K. Wasylkiewicz, L. C. Kobylka, and F. J. L. Castillo. Pressure sensitivity analysis of azeotropes. *Ind. Eng. Chem. Res.*, 42(1):207–213, 2003.

[148] S. K. Wasylkiewicz, L. N. Sridhar, M. F. Doherty, and M. F. Malone. Global stability analysis and calculation of liquid-liquid equilibrium in multicomponent mixtures. *Ind. Eng. Chem. Res.*, 35(4):1395–1408, 1996.

[149] Stanislaw K. Wasylkiewicz and Sophie Ung. Global phase stability analysis for heterogeneous reactive mixtures and calculation of reactive liquid-liquid and vapor-liquid-liquid equilibria. *Fluid Phase Equilibria*, 175(1-2):253–272, 2000.

[150] Grant M. Wilson. Vapor-liquid equilibrium. xi. a new expression for the excess free energy of mixing. *Journal of the American Chemical Society*, 86(2):127–130, 1964.

Appendix A

Brief Review of the most used Activity Coefficient Models

As discussed in Chapter 2 in page 35, to predict the activity coefficient of a compound in a mixture, an excess Gibbs Free energy model must be formulated based on thermodynamical principles. Some of the most used models where studied, in order to select the best and most versatile theory to correctly model qualitatively phase behavior and reduce the quantitative error to the minimum possible.

The Activity coefficient is an excess property so it has to satisfy the Gibbs-Duhem Equation, therefore any excess model can be formulated meanwhile it satisfies it for N being the number of compounds in the liquid mixture:

$$\left(\sum_{i=1}^{N} x_i d\ln(\gamma_i)\right)_{P,T} \tag{A.1}$$

A.1 Wilson's Activity Coefficient Model

Wilson in 1964 [150], brought the first major contribution in the field of modem liquid activity models by developing the local composition concept. This is related to the segregation caused by different interaction energies between pairs of molecules. Thus, the probability of finding a species 1 surrounded by molecules of species 2, relative to the probability of being surrounded by the same species 1, is given by the expression:

$$\frac{x_{12}}{x_{11}} = \frac{x_2 \exp(\lambda_{12}/RT)}{x_1 \exp(\lambda_{11}/RT)} \tag{A.2}$$

The quantities λ_{12} and λ_{11} signify interaction energies between molecules. The quantity x_{12}

has the meaning of a local composition. Furthermore, a local volume fraction of the component 1 can be formulated as:

$$\zeta_1 = \frac{v_{1L}x_{11}}{v_{1L}x_{11} + v_{2L}x_{12}} \tag{A.3}$$

The quantities v_{lL} and v_{2L} are the molar liquid volumes of the two components. The following relation can describe the excess Gibbs free energy:

$$\frac{\overline{G}^E}{RT} = x_1 \ln \frac{\zeta_1}{x_1} + x_2 \ln \frac{\zeta_2}{x_2} \tag{A.4}$$

Binary interaction constants may be defined as:

$$\Lambda_{12} = \frac{v_{2L}}{v_{1L}} \exp\left[-\frac{\lambda_{12} - \lambda_{11}}{RT}\right] \tag{A.5}$$

$$\Lambda_{21} = \frac{v_{1L}}{v_{2L}} \exp\left[-\frac{\lambda_{21} - \lambda_{22}}{RT}\right] \tag{A.6}$$

The energies of interaction are $\lambda_{12} = \lambda_{21}$ but $\lambda_{11} \neq \lambda_{22}$ After substitution of equations A.5 and A.6 in A.4 the excess Gibbs energy becomes:

$$\frac{\overline{G}^E}{RT} = -x_1 \ln(x_1 + \Lambda_{12}x_2) - x_2 \ln(x_2 + \Lambda_{21}x_1) \tag{A.7}$$

Finally, the following equations for the activity coefficients are obtained:

$$\ln \gamma_i = -\ln(x_1 + x_2\Lambda_{12}) + x_2 \left(\frac{\lambda_{12}}{x_1 + x_2\Lambda_{12}} - \frac{\Lambda_{21}}{x_2 + x_1\Lambda_{21}}\right) \tag{A.8}$$

$$\ln \gamma_i = -\ln(x_2 + x_1\Lambda_{21}) + x_2 \left(\frac{\lambda_{12}}{x_1 + x_2\Lambda_{12}} - \frac{\Lambda_{21}}{x_2 + x_1\Lambda_{21}}\right) \tag{A.9}$$

Wilson model describes very accurately the VLE of strong non-ideal mixtures, but unfortunately is not convenient for liquid/liquid equilibrium [118].

A.2 NRTL Activity Coefficient Model

NRTL (non-random two-liquids) model developed by Renon and Prausnitz in 1968 [137] is an extension of the local composition concept that accounts for the non-randomness of interactions. The following expression for $\overline{G}^E$ is obtained:

$$\frac{\overline{G}^E}{RT} = x_1x_2 \left(\frac{\tau_{21}G_{21}}{x_1 + x_2G_{21}} + \frac{\tau_{12}G_{12}}{x_2 + x_1G_{12}}\right) \tag{A.10}$$

Quantities τ_{ij} express differences in interaction energies,$\tau_{ij} = (g_{ij} - g_{ji})/RT$ The parameters G_{ij} take into account the non-randomness of interactions such as $G_{ij} = \exp(-\alpha/RT)$. The parameter α can be treated as adjustable, although better it should be fixed. Some recommendations are:

- α=0.20 for saturated hydrocarbon with polar non-associated species
- α=0.30 for non-polar compounds, but also for water and non-associated species
- α=0.40 for saturated hydrocarbon and homologue per-fluorocarbons
- α=0.47 for alcohol and other self-associated non-polar species

Binary activity coefficients are given by the following equations:

$$\ln \gamma_1 = x_2^2 \left[\frac{\tau_{21} G_{21}^2}{(x_1 + x_2 G_{21})^2} + \frac{\tau_{12} G_{12}^2}{(x_2 + x_1 G_{12})^2} \right] \tag{A.11}$$

$$\ln \gamma_2 = x_1^2 \left[\frac{\tau_{12} G_{12}^2}{(x_2 + x_1 G_{21})^2} + \frac{\tau_{21} G_{21}^2}{(x_1 + x_2 G_{12})^2} \right] \tag{A.12}$$

NRTL model is somewhat sensitive in computation, but it can be used to describe very accurately both VLE, VLLE and LLE of high non-ideal mixtures [118].

A.3 UNIQUAC Activity Coefficient Model

UNIQUAC stands for UNiversal QUAsi-Chemical model, and has been developed by Abrams and Prausnitz 1978. Unlike Wilson and NRTL, where local volume fraction is used, in UNIQUAC the primary variable is the local surface area fraction θ_{ij}. Each molecule is characterised by two structural parameters: r the relative number of segments of the molecule (volume parameter) and q, the relative surface area (surface parameter). Values of these parameters have been obtained in some cases by statistical mechanics. In UNIQUAC the excess Gibbs free energy is computed from two contributions. The first called combinatorial part represents the influence of the structural parameters, as size (parameter r) and shape (area parameter q). The second called the residual part account for the energy of interactions between segments. for the UNIQUAC MODEL the expression for the excess Gibbs free energy is: For the combinatorial part:

$$\frac{\overline{G}_C^E}{RT} = \sum_i x_i \ln \frac{\Phi_i}{x_i} + 5 \sum_i q_i x_i \ln \frac{\theta_i}{\Phi_i} \tag{A.13}$$

For the residual part:

$$\frac{\overline{G}_C^E}{RT} = -\sum_i q_i x_i \ln\left(\sum_j \theta_j \tau_{ji}\right) \tag{A.14}$$

Where

$$\Phi_i = \frac{x_i r_i}{\sum_j x_j r_j} \tag{A.15}$$

$$\theta_i = \frac{x_i q_i}{\sum_j x_j q_j} \tag{A.16}$$

And the binary interaction energy is:

$$\tau_{ji} = \exp - \left(\frac{u_{ji} - u_{ii}}{RT}\right) \tag{A.17}$$

UNIQUAC is as accurate as Wilson's model, but it may be applied to liquid/liquid equilibrium. Despite its apparent complexity the UNIQUAC model is robust in computations [118].

A.4 UNIFAC Activity Coefficient Model

UNIFAC is an extension of UNIQUAC, in which the interaction parameters are estimated by means of contributions of groups. Firstly, the molecules are decomposed in characteristic structures, as functional groups and subgroups. Some small molecules are considered separately for more accuracy. Then the parameters involved in UNIQUAC-type equations are determined, as follows:

Molecular volume and area parameters in the combinatorial part are replaced by:

$$r_i = \sum_k v_k^{(i)} R_k \tag{A.18}$$

$$q_i = \sum_k v_k^{(i)} Q_k \tag{A.19}$$

$v_k^{(i)}$ is the number of functional group of type k in the molecule i, while R_k,Q_k are volume and area parameters of the functional group. Residual and combinatorial activity coefficients are calculated using the following expressions:

$$\ln \gamma_i^C = 1 - J_i + \ln J_i - 5 q_i \left(1 - \frac{J_i}{L_i} + \ln \frac{J_i}{L_i}\right) \tag{A.20}$$

$$\ln \gamma_i^R = q_i(1 - \ln L_i) - \sum_j \left(\theta \frac{s_{ji}}{\eta_j} - q_i \ln \frac{s_{ji}}{\eta_j}\right) \tag{A.21}$$

Where

$$J_i = \frac{r_i}{\sum_j r_j x_j} \tag{A.22}$$

$$L_i = \frac{q_i}{\sum_j q_j x_j} \tag{A.23}$$

$$G_{ki} = v_k^{(i)} Q_k \tag{A.24}$$

$$\theta_k = \sum_i G_{ki} x_i \tag{A.25}$$

$$s_{ki} = \sum_m G_{mi} \tau_{mk} \tag{A.26}$$

$$\eta_k = \sum_i s_{ki} x_i \tag{A.27}$$

And

$$\tau_{mk} = \exp \frac{-a_{mk}}{T} \tag{A.28}$$

UNIFAC is recommended only for exploratory purposes. A true liquid activity model should replace it when experimental data becomes available. Sometimes the predictions by UNIFAC are surprisingly good, when sufficient experimental data was available.

UNIFAC is not reliable for LLE, which is more difficult for modeling than VLE [118].

Since 1979 when the first UNIFAC revision and extension [70] was published, five more extensions were published [67–69, 71], a special UNIFAC for liquid-liquid equilibrium calculation [73] and other modifications of the method being UNIFAC Dortmund the more used [72].

Appendix B

ESIRK Butcher's Tableaus up to order 5

For the development of this thesis using the procedures in Dr. David Chen's PhD thesis [81], several Effective Order Singly Implicit Methods where obtained in order to select select an appropriate one for the implementation. As ESIRK are collocations methods, L-Stability was guaranteed using table B.1 which was obtained using Laguerre polinomials.

Table B.1: λ for L-stability with s-stage SIRK Methods

s	λ
2	$1 \pm \frac{\sqrt{2}}{2}$
3	0.43586652150845899942
4	0.57281606248213485541
5	0.27805384113645232493
6	0.33414236706805043595

B.1 Order 2 ESIRK

B.1.1 Starting Method

$$\begin{array}{c|cc} 0.171573 & 0.18934 & -0.017767 \\ 1 & 0.603553 & 0.396447 \\ \hline & 0.551777 & 0.362437 \end{array} \tag{B.1}$$

B.1.2 ESIRK Method

$$
\begin{array}{c|cc}
0 & 0.1286796564403574268 & -0.04289321881345247560 \\
1 & 0.6286796564403574268 & 0.45710678118654752440 \\
\hline
 & 0.58578643762690495120 & 0.41421356237309504880 \\
\hline
 & 0.62868 - 0.042893r^2 & 0.45711 - 0.085786r + 0.042893r^2
\end{array}
\tag{B.2}
$$

B.2 Order 3 ESIRK

B.2.1 Starting Method

$$
\begin{array}{c|ccc}
0.181222 & 0.208637 & -0.0308751 & 0.00346011 \\
1 & 0.574386 & 0.44267 & -0.0170564 \\
2.74158 & 0.154424 & 1.93086 & 0.656292 \\
\hline
 & 0.530301 & -0.347665 & 0.00976398
\end{array}
\tag{B.3}
$$

B.2.2 ESIRK Method

$$
\begin{array}{c|ccc}
0 & 0.95243 & -0.12405 & -0.020783 \\
\frac{1}{2} & 1.1608 & 0.20929 & -0.062449 \\
1 & 1.1191 & 0.54262 & 0.14588 \\
\hline
 & 1.3055 & 0.0042206 & -0.30971 \\
\hline
 & b_1(r) & b_2(r) & b_3(r)
\end{array}
\tag{B.4}
$$

Where,

$$b_1(r) = 1.1191 + 0.082806r^2 + 0.10359r^3 \tag{B.5}$$

$$b_2(r) = 0.54262 - 0.33122r^2 - 0.20718r^3 \tag{B.6}$$

$$b_3(r) = 0.14588 - 0.80760r + 0.24842r^2 + 0.10359r^3 \tag{B.7}$$

B.3 Order 4 ESIRK

B.3.1 Starting Method

0.18476	0.217813	−0.0403479	0.00793744	−0.00064175
1.	0.561829	0.468287	−0.0323334	0.00221716
2.59865	0.323308	1.59757	0.692906	−0.0151317
5.38165	1.37366	−0.79636	3.89209	0.912258
	−0.164054	−0.873452	0.266426	−0.0201843

(B.8)

B.3.2 ESIRK Method

0	7.2564	−8.4408	3.3998	−0.42420
$\frac{1}{3}$	7.3814	−8.1769	3.3304	−0.41031
$\frac{2}{3}$	7.3675	−7.9963	3.5110	−0.42420
1	7.3814	−8.0658	3.7748	−0.29920
	8.2980	−10.029	2.0382	0.69302
	$b_1(r)$	$b_2(r)$	$b_3(r)$	$b_4(r)$

(B.9)

Where,

$$b_1(r) = 7.3814 - 0.97123r^2 + 0.67041r^3 + 1.2174r^4 \quad \text{(B.10)}$$

$$b_2(r) = -8.0658 + 4.3705r^2 - 2.6816r^3 - 3.6523r^4 \quad \text{(B.11)}$$

$$b_3(r) = 3.7748 - 8.7410r^2 + 3.3521r^3 + 3.6523r^4 \quad \text{(B.12)}$$

$$b_4(r) = -0.29920 - 1.7913r + 5.3417r^2 - 1.3408r^3 - 1.2174r^4 \quad \text{(B.13)}$$

B.4 Order 5 ESIRK

B.4.1 Starting Method

0.073284	0.0877152	−0.0186247	0.00490082	−0.000752492	0.0000450816
0.393002	0.217993	0.19057	−0.0177425	0.00231088	−0.000129449
1	0.148462	0.579999	0.283114	−0.0121375	0.000563101
1.97024	0.319203	0.130998	1.15509	0.370183	−0.00523269
3.51482	−1.01861	3.19715	−1.7046	2.5822	0.458687
	0.345336	0.0221253	−0.316524	0.062002	−0.0032084

(B.14)

B.4.2 ESIRK Method

0	2.0135	−1.1885	−0.18870	0.32454	−0.070572
$\frac{1}{4}$	2.1006	−0.96417	−0.28036	0.36135	−0.077169
$\frac{1}{2}$	2.0940	−0.84403	−0.12203	0.33566	−0.073349
$\frac{3}{4}$	2.0978	−0.86972	0.036303	0.45579	−0.079947
1	2.0912	−0.83292	−0.055364	0.68010	0.0072061
	1.8250	0.12265	−0.81183	−0.48337	0.34751
	$b_1(r)$	$b_2(r)$	$b_3(r)$	$b_4(r)$	$b_5(r)$

(B.15)

Where,

$$b_1(r) = 2.0912 + 0.21863r^2 + 0.069440r^3 - 0.38702r^4 - 0.16726r^5 \quad \text{(B.16)}$$

$$b_2(r) = -0.83292 - 1.1660r^2 - 0.35351r^3 + 1.8061r^4 + 0.66902r^5 \quad \text{(B.17)}$$

$$b_3(r) = -0.055364 + 2.6236r^2 + 0.71965r^3 - 3.0961r^4 - 1.0035r^5 \quad \text{(B.18)}$$

$$b_4(r) = 0.68010 - 3.4981r^2 - 0.65652r^3 + 2.3221r^4 + 0.66902r^5 \quad \text{(B.19)}$$

$$b_5(r) = 0.0072061 - 0.89027r + 1.8219r^2 + 0.22095r^3 - 0.64503r^4 \quad \text{(B.20)}$$

$$-0.16726r^5 \quad \text{(B.21)}$$

Appendix C

Globaly Stable Liquid-Liquid Equilibrium Calculations

Equilibrium calculations are common in process modeling and simulation, sometimes heterogeneous liquid systems are encountered in many processes like distillation and they are necessary in others like liquid extraction. In Processes presenting this, the number of liquid phases is not fixed and can vary for different parts of the process or over time in case of a dynamical simulation, although a simulation based on a wrong prediction of the number of phases or even with the right number of phases converging to thermodynamically unstable or metastable solutions of phase equilibrium may lead to results far away from the real behavior of the modeled phenomena, misleading the designer into a wrong equipment sizing. Conceptual design is based on intelligently simplified equipment models that sacrificing precision intends to qualitatively and quantitatively serve as a first design model to determine the most relevant design parameters to be fixed. This kind of design approach relies on equilibrium models and on its capability to accurately predict the behavior of a physical and/or chemical phenomena happening into steady state equipment. For this reason is really important for modelers, simulators and designers to attain the correct number of phases and globally stable results in order to make its work correctly.

C.1 Stability test

In 1876, Gibbs showed that the necessary and sufficient condition for absolute stability of a mixture at fixed temperature, pressure and overall composition is that the Gibbs energy surface be at no point below the plane tangent to the surface at the given overall composition [148].

Let the overall composition of a mixture be z, temperature T, and pressure P, let the chemical potential of the $i-th$ component of the mixture be μ at this conditions. The stability condition can be stated quantitatively as follows:

$$F(x) \equiv g(x) - L(x,z) = \sum_{i=1}^{c} x_i \left[\mu_i(x) - \mu_i(z)\right] \tag{C.1}$$

Where $g(x)$ is the Gibbs energy at $\mathbf{x}$ and $L(x,z)$ is the tangent plane to the Gibbs energy surface at composition z. $F(x)$ is the tangent plane distant function, which represents the displacement from the tangent plane to the Gibbs energy surface at composition $\mathbf{x}$.
The necessary and sufficient condition for Global stability is:

$$F(x) \geq 0 \tag{C.2}$$

All the minimums of $F(x)$ are located in the permissible region. Consequently $F(x)$ will be nonnegative at all stationary points where it derivatives with respect to the independent variables vanish.
For liquid mixtures at low moderate pressures it is common to write the chemical potentials in terms of activity coefficients then (C.1) can be rewritten as:

$$\frac{F(x)}{RT} = \sum_{i=1}^{c} x_i \left[\ln x_i + \ln \gamma_i(x) - \ln z_i - \ln \gamma_i(z)\right] \geq 0 \tag{C.3}$$

Where $\gamma_i(x)$ and $\gamma_i(z)$ are the activity coefficients of the ith component evaluated at $\mathbf{x}$ and $\mathbf{z}$, $\mathbf{z}$ is the fixed overall composition, and any term related to it is constant.
To locate all the $F(x)$ special points (minimums, maximums and saddles), is necessary to solve $\nabla F(x) = 0$ finding all its roots, or Minimize $F(x)$ with a numerical algorithm to find the global minimum. This approaches seem easy but they are not, most numerical method are based on local convergence, specially Newton method and all Gradient and hessian based numerical optimization methods [146, 148, 149]. In fact there are several approaches to global optimization and Global Newton Methods such like homotopy based techniques, interval algebra, tunneling and Artificial intelligence, all of them proved to be successful in some cases, but none of them infallible.
The main idea of solving material stability problems by tangent plane approach is to obtain real results, but solving the optimization or the Newton problem is time consuming, and most of the

simulations are complicated enough to be slowed down by time consuming internal algorithms. A way to solve this problem is leaving behind the traditional LL and LLV flash algorithms that are extremely time consuming (and why not, obsolete) and use hybrid algorithms whom use globally convergent methods that guarantee material stability.

C.2 Liquid-Liquid Equilibrium Calculation by Homotopy

For a given liquid composition z, pressure P and temperature T, the number and composition of liquid phases has to be calculated. To perform the phase stability test, the LLE flash equations $F(\mathbf{u}) = 0$ defined by

$$F_i(\mathbf{u}) = (1-\phi)x_i^{II} + \phi x_i^I - z_i, \quad i = 1, \ldots, C \tag{C.4}$$

$$F_{C+i}(\mathbf{u}) = \gamma_i(\mathbf{x^I}, P, T)x_i^I - \gamma_i(\mathbf{x^{II}}, P, T)x_i^{II}, \quad i = 1, \ldots, C \tag{C.5}$$

$$F_{2C+1}(\mathbf{u}) = \sum_{k=1}^{C}(x_k^I - x_k^{II}) \tag{C.6}$$

are solved for $\mathbf{u} = [\mathbf{x^{IT}}, \mathbf{x^{IIT}}, \phi]^T$, comprising the composition of both liquid phases x^I and $x^I I$ and the phase fraction ϕ. A lack of convergence of equations (C.4)-(C.6) does not reliably indicate, that no phase split exists, since convergence strongly depends on the initialization of the solver. Thus, the idea of the algorithm presented here is to always provide good initial values to the solver by means of a homotopy continuation algorithm. In order to solve the difficult problem $F(\mathbf{u}) = 0$, we start with an easy problem $G(\mathbf{u}) = 0$ that has the same number of variables and a similar structure.The homotopy is defined as

$$H(\mathbf{u}, \lambda) = \lambda F(\mathbf{u}) + (1-\lambda)G(\mathbf{u}) \tag{C.7}$$

involving both problems and the additional parameter λ. The solution of $H(\mathbf{u}, \lambda) = 0$ for $0 \leq \lambda \leq 1$ is calculated starting at the easy problem $H(\mathbf{u}, \lambda = 0) = G(\mathbf{u})$ and ending up at the difficult problem $H(\mathbf{u}, \lambda = 1) = F(\mathbf{u})$. For the LLE flash problem, $G(\mathbf{u})$ is defined by equations (C.5) and (C.6) and

$$G_i(u) = (1-\phi)x_i^I + \phi x_i^{II} - z_{0,i}, \quad i = 1, \ldots, C \tag{C.8}$$

where $\mathbf{z_0}$ is a composition inside the heterogeneus region stored in the preprocessing step. The resulting Homotopy comprises equations (C.5) and (C.6) and

$$H_i(\mathbf{u}, \lambda) = (1 - \phi)x_i^I + \phi x_i^{II} - [\lambda z_i + (1 - \lambda)z_{o,i}], \quad i = 1, \ldots, C \tag{C.9}$$

Due to the choice of $\mathbf{z_0}$, the homotpy is solved by $\lambda = 0$ and $\mathbf{u} = [\mathbf{x_0^{IT}}, \mathbf{x_0^{IIT}}, \phi_0]^T$. To obtain results at $\lambda = 1$ a predictor/corrector continuation algorithm is used [97, 117, 123, 141].

C.2.1 Preprocessing Step

Wasylkiewicz et al. [146, 148, 149] , developed a global stability analysis for liquid-liquid equilibrium based on topology, this approach uses idea from differential geometry and ODE theory, the differential equation

$$\frac{dx}{d\tau} = \nabla F(x) \tag{C.10}$$

is a gradient system of the tangent plane distant function, a gradient system has the following properties [148]:

1. The singular points of equation (C.10) occur at stationary points in $F(x)$ and vice versa.
2. The Jacobian is a symmetric matrix and have all real eigenvalues
3. Inspection of Eigenvalues of $J[\nabla F(x)]$ reveals the following:
   - Unstable Nodes Occur at maximums of $F(x)$
   - Stable Nodes Occur at Minimums of $F(x)$
   - Saddle points occur at saddles of $F(x)$
4. Ridges in $F(x)$ correspond to unstable invariant manifolds of equation (C.10), and valleys correspond to the stable invariant manifolds.
5. The flow trajectories are always downhill
6. The flow trajectories are always into the permissible region $\sum x_i = 1, x_i \geq 0$

All properties are common to all gradient systems but number six is a special property of the tangent plane function, this property combined with the first four allows the application of the following topological criterion based on index theory for n dimensions:

$$N_{max} + (-1)^n N_{min} + N_{saddle}^{even} - N_{saddle}^{odd} = (-1)^n \tag{C.11}$$

Where N_{max} is the number of maximums of $F(x)$, N_{min} is the number of minimums of $F(x)$, N_{saddle}^{even} is the number of saddles with even number negatives of eigenvalues, N_{saddle}^{odd} is the number of saddles with odd number negatives of eigenvalues of the jacobian of the matrix $J[\nabla F(x)]$.

By integrating equation (C.10) along the direction of its stationary points' eigenvectors (invariant manifolds), it is possible to track all the ridges and valleys of $F(x)$ searching for other stationary points. This enables a systematic exploration of the domain rather than repeated calculations starting from various points generated from heuristics.

Using a binary system equation (C.10) and (C.11) get reduced, and the calculation of initialization $\mathbf{z_0}$ gets easier due to the lack of saddles, so preprocessing step is done for binary systems tracking its valley and ridges in a two dimensional space.

C.3 Trilinolein + Methanol + MethylLinoleate + Glycerol LLE

Using the numerical techniques described above, Trilinolein + Methanol + MethylLinoleate + Glycerol LLE was calculated.

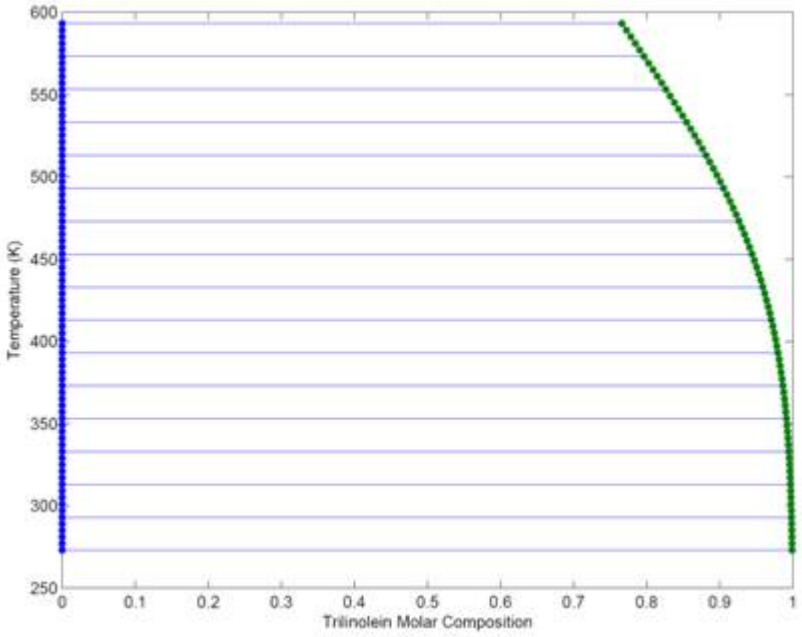

Figure C.1: Trilinolein + Gycerol LLE at Different Temperatures

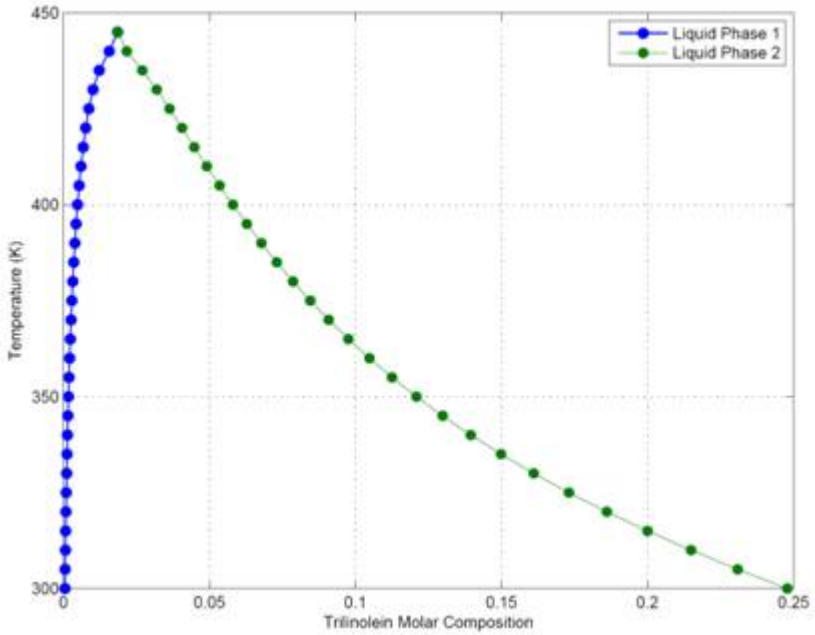

Figure C.2: Trilinolein + Methanol LLE at Different Temperatures

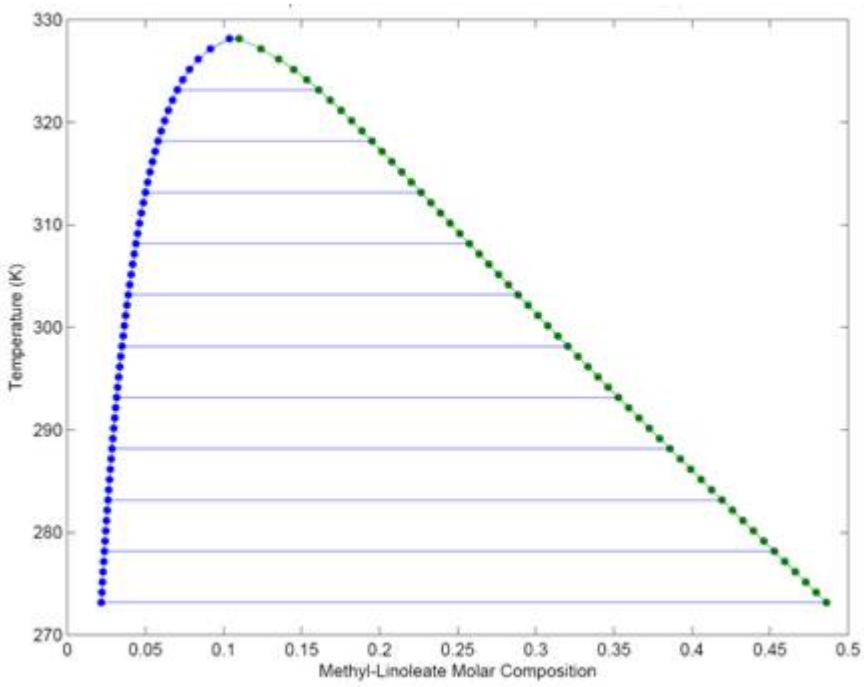

Figure C.3: Methyl Linoleate + Methanol LLE at Different Temperatures

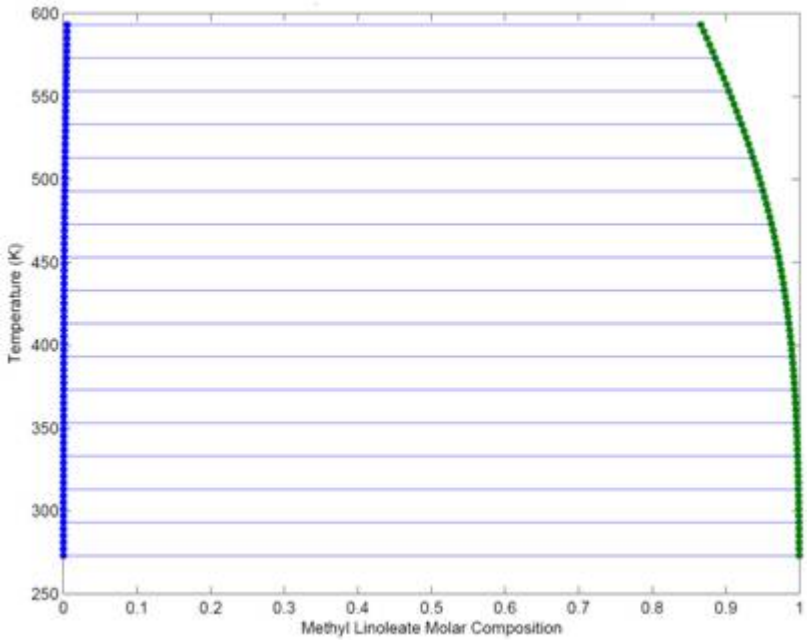

Figure C.4: Methyl Linoleate + Glycerol LLE at Different Temperatures

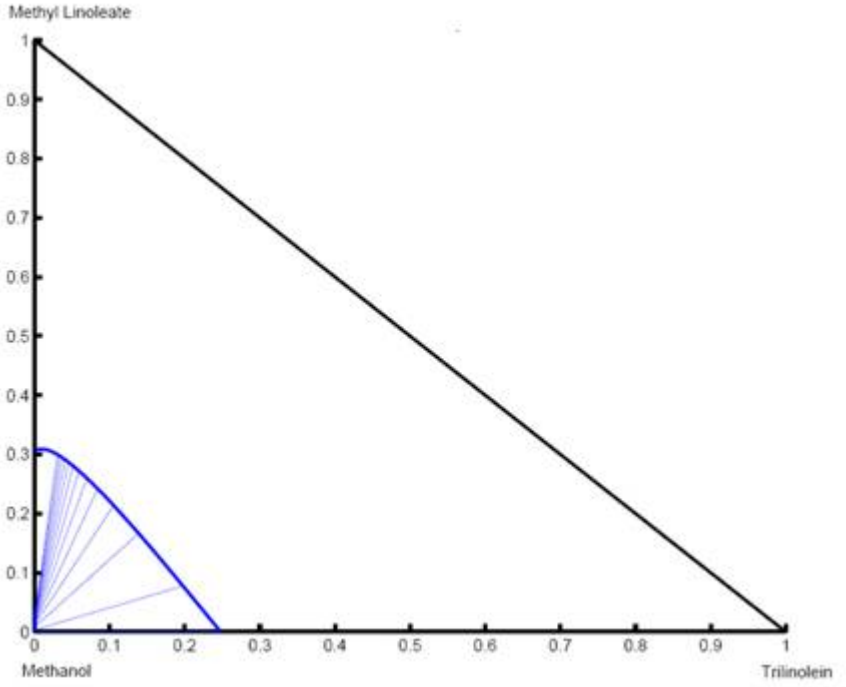

Figure C.5: Trilinolein + Methyl Linoleatre + Methanol LLE at 300K

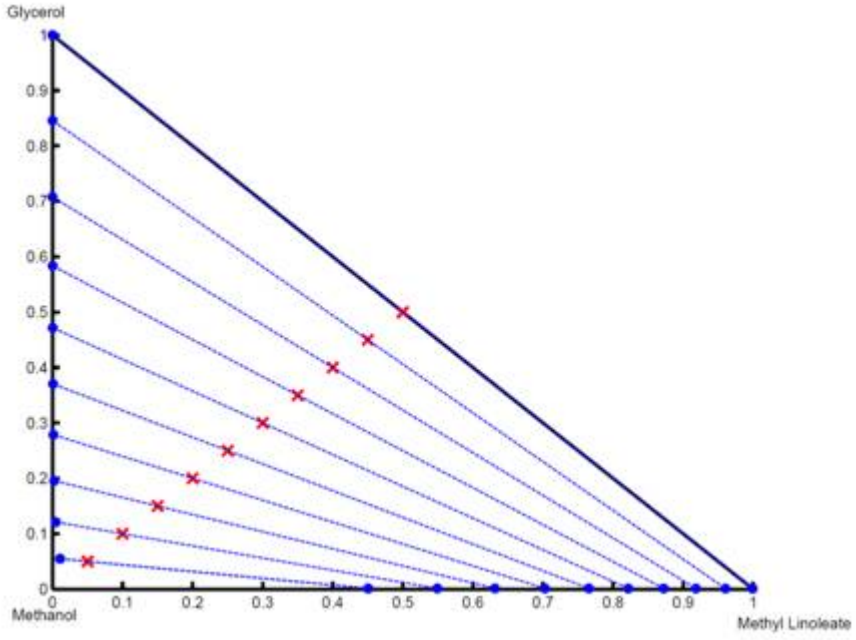

Figure C.6: Glycerol + Methyl Linoleatre + Methanol LLE at 300K

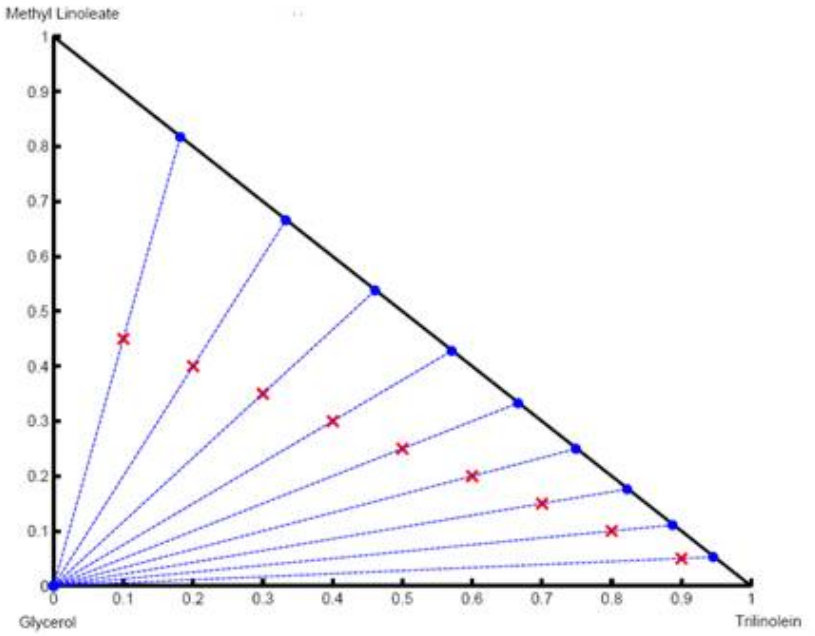

Figure C.7: Trilinolein + Methyl Linoleatre + Glycerol LLE at 300K

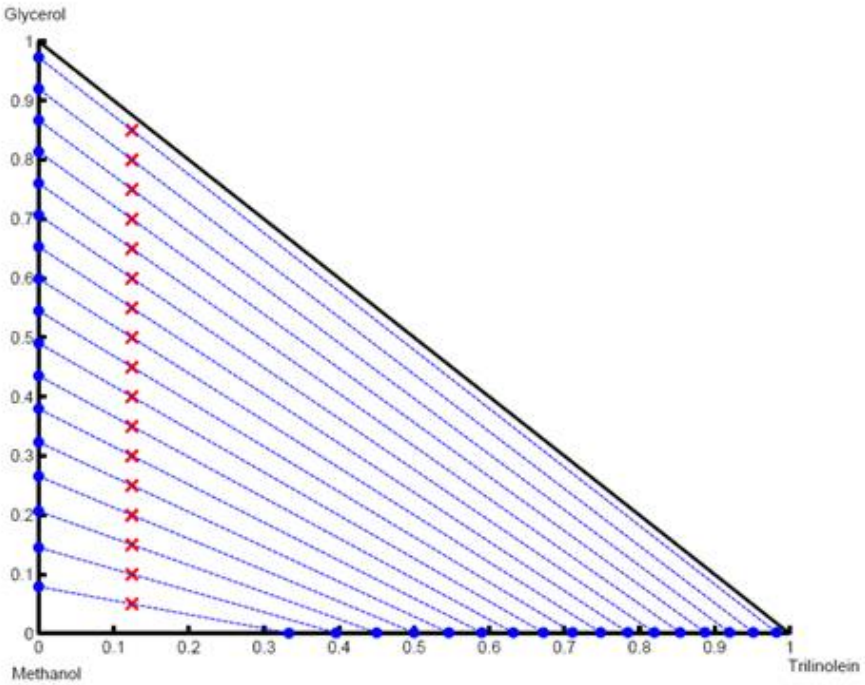

Figure C.8: Trilinolein + Glycerol + Methanol LLE at 300K

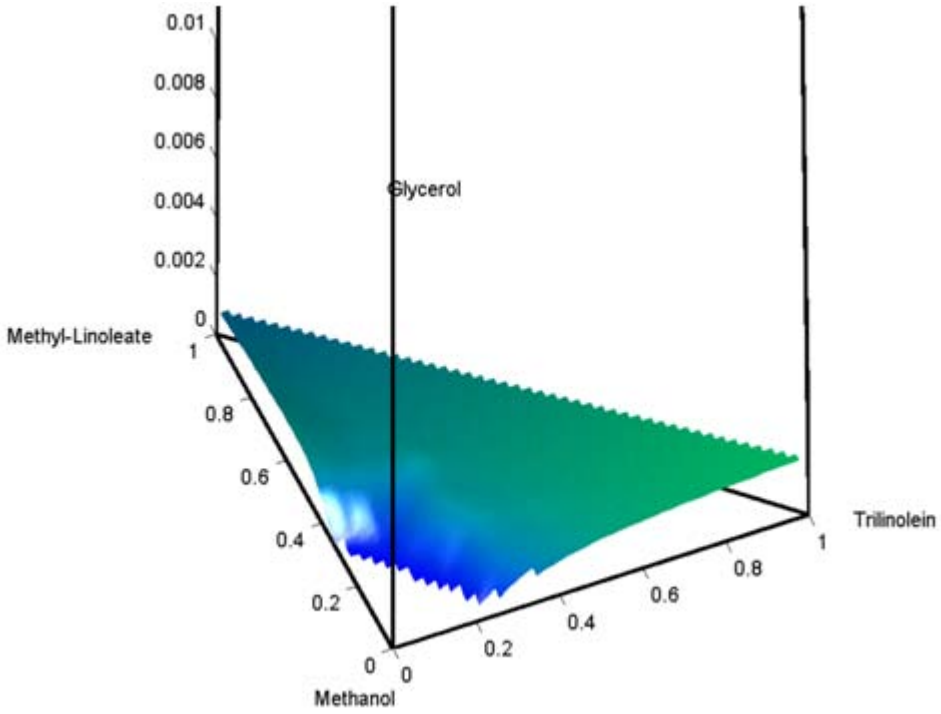

Figure C.9: Quaternanry LLE Phase II surface